Tropical Seminar: Nickel-Catalyzed Cross-Coupling

Reggie Mills

Apr. 12, 2022

Nickel Catalysis

Today's topics in nickel cross-coupling:

Directions in Precatalyst Synthesis

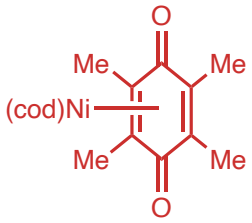

"Inert"/"Nonclassical" $C(sp^2)$–X Electrophiles Ni(0)/Ni(II)

Benzylic $C(sp^3)$–X Electrophiles Ni(0)/Ni(II)

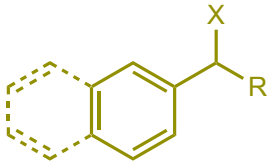

X = OR, NR_3X

"Unactivated" $C(sp^3)$–X Electrophiles Ni(I)/Ni(III)

Cross-Electrophile Coupling Ni(0)/Ni(I)/Ni(II)/Ni(III)

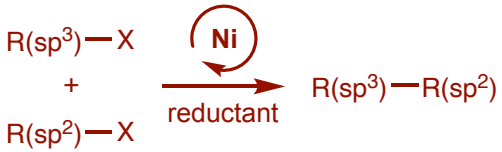

Conjunctive Cross-Coupling (Short)

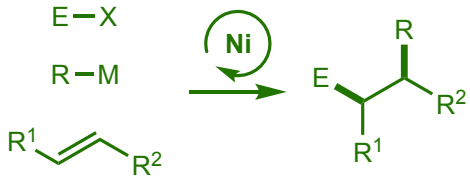

Nickel Catalysis

Things not covered:

1. Ancient history (Kochi, etc.)

2. Multimetallic chemistry

3. Metallophotoredox (“lazy nickel”)

Nickel Catalysis

Properties of nickel vs. palladium (Diao):

(i) Access to many oxidation states

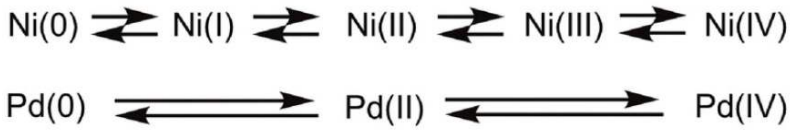

(ii) One- and two-electron pathways are accessible

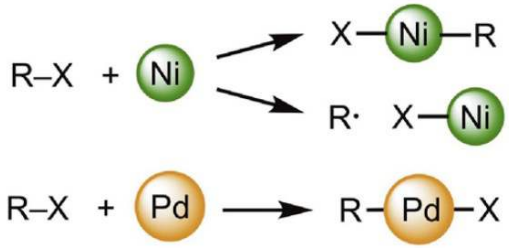

(iii) Low reduction potential

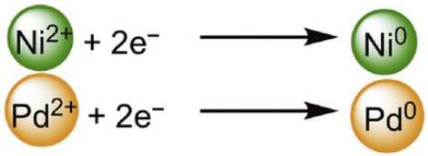

	E^0/V (SHE)
$Ni^{2+} + 2e^- \rightarrow Ni^0$	−0.257
$Pd^{2+} + 2e^- \rightarrow Pd^0$	0.951

(iv) Smaller and less electronegative

	Ni	Pd
Van der Waals radius:	1.92 Å	2.05 Å
Electronegativity:	1.91	2.20
HSAB:	hard	soft

(v) Slow β-hydride elimination

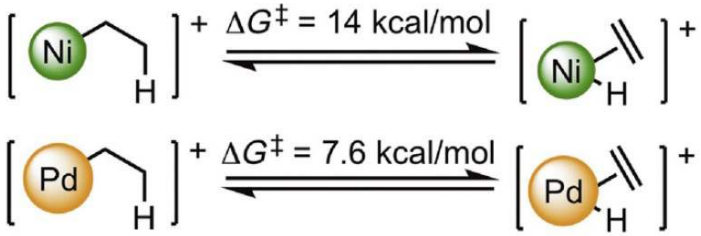

Diccianni, J. B.; Diao, T. *Trends Chem.* **2019**, *9*, 830–844.

Nickel Catalysis

Topics in nickel cross-coupling:

Directions in Precatalyst Synthesis

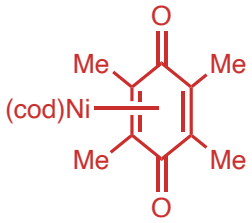

"Inert"/"Nonclassical" $C(sp^2)$–X Electrophiles Ni(0)/Ni(II)

Benzylic $C(sp^3)$–X Electrophiles Ni(0)/Ni(II)

X = OR, NR_3X

"Unactivated" $C(sp^3)$–X Electrophiles Ni(I)/Ni(III)

Cross-Electrophile Coupling Ni(0)/Ni(I)/Ni(II)/Ni(III)

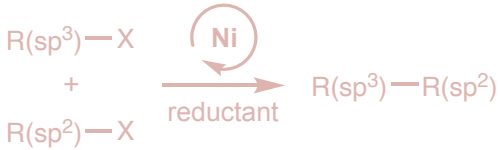

Conjunctive Cross-Coupling (Short)

Nickel Catalysis

Jamison: Early report of air-stable Ni(II) precatalysts (2014)

Scheme 1. Synthesis of Precatalysts[a]

Monodentate Phosphines

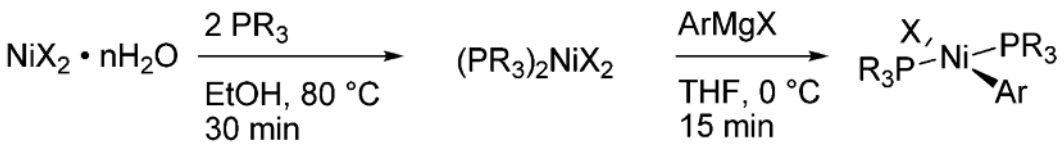

Bidentate Phosphines

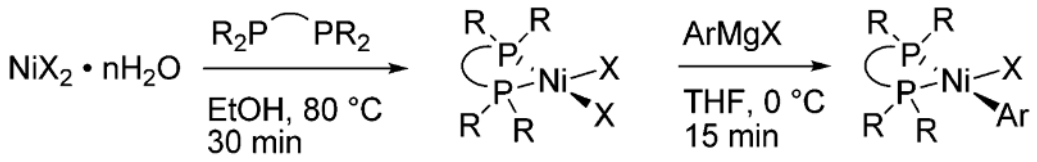

[a]X = Cl, Br. R = alkyl, aryl.

(a) Standley, E. A.; Smith, S. J.; Müller, P.; Jamison, T. F. *Organometallics* **2014**, *33*, 2012–2018; (b) Chatt, J.; Shaw, B. L. *J. Chem. Soc.* **1960**, 1718–1729.

Nickel Catalysis

Jamison: Early report of air-stable Ni(II) precatalysts (2014)

Table 1. Nickel Phosphine Complexes Synthesized[a]

compd	ligand	geometry	R	X	isolated yield (%)		
					L_nNiX_2	$L_nNi(R)X$	overall
Monodentate Ligands							
1	PPh_3	*trans*	*o*-tolyl	Cl	91	89	81
2	$PCyPh_2$	*trans*	*o*-tolyl	Cl	92	81	75
3	PCy_2Ph	*trans*	*o*-tolyl	Cl	95	88	84
4	PCy_3	*trans*	*o*-tolyl	Cl	97	87	84
5	$PCyp_3$	*trans*	*o*-tolyl	Cl	99	90	89
6	PBn_3	*trans*	*o*-tolyl	Cl	96	90	86
7	PPh_2Me	*trans*	*o*-tolyl	Cl	99	81	80
8	PMe_2Ph	*trans*	2,4,6-triisopropylphenyl	Cl	95	83	79
9	PMe_2Ph	*trans*	2,6-dimethoxyphenyl	Br	95	87	83
10	PEt_3	*trans*	2-mesityl	Br	95	88	84
11	$P(n\text{-}Bu)_3$	*trans*	2-mesityl	Br	89	90	80
Bidentate Ligands							
12	dppe	*cis*	*o*-tolyl	Cl	98	84	82
13	dppp	*cis*	2-mesityl	Br	89	85	76
14	dppb	*trans*	2-mesityl	Br	96	86	83
15	(*S*)-BINAP	*cis*	*o*-tolyl	Cl	94	97	91
16	dppf	*cis*	*o*-tolyl	Cl	97	95	92
17	dcpf	*trans*	*o*-tolyl	Cl	98	83	81
18	Xantphos	*trans*	*o*-tolyl	Cl	86	92	79
19	pyphos	*cis*	*o*-tolyl	Cl	90	82	74

[a]Abbreviations: dppe, 1,2-bis(diphenylphosphino)ethane; dppp, 1,3-bis(diphenylphosphino)propane; dppb, 1,4-bis(diphenylphosphino)butane; BINAP, 2,2′-bis(diphenylphosphino)-1,1′-binaphthyl; dppf, 1,1′-bis(diphenylphosphino)ferrocene; dcpf, 1,1′-bis(dicyclohexylphosphino)ferrocene; Xantphos, 9,9-dimethyl-4,5-bis(diphenylphosphino)xanthene; pyphos, 2-[2-(diphenylphosphino)ethyl]pyridine.

(a) Standley, E. A.; Smith, S. J.; Müller, P.; Jamison, T. F. *Organometallics* **2014**, *33*, 2012–2018; (b) Chatt, J.; Shaw, B. L. *J. Chem. Soc.* **1960**, 1718–1729.

Nickel Catalysis

Jamison: Early report of air-stable Ni(II) precatalysts (2014)

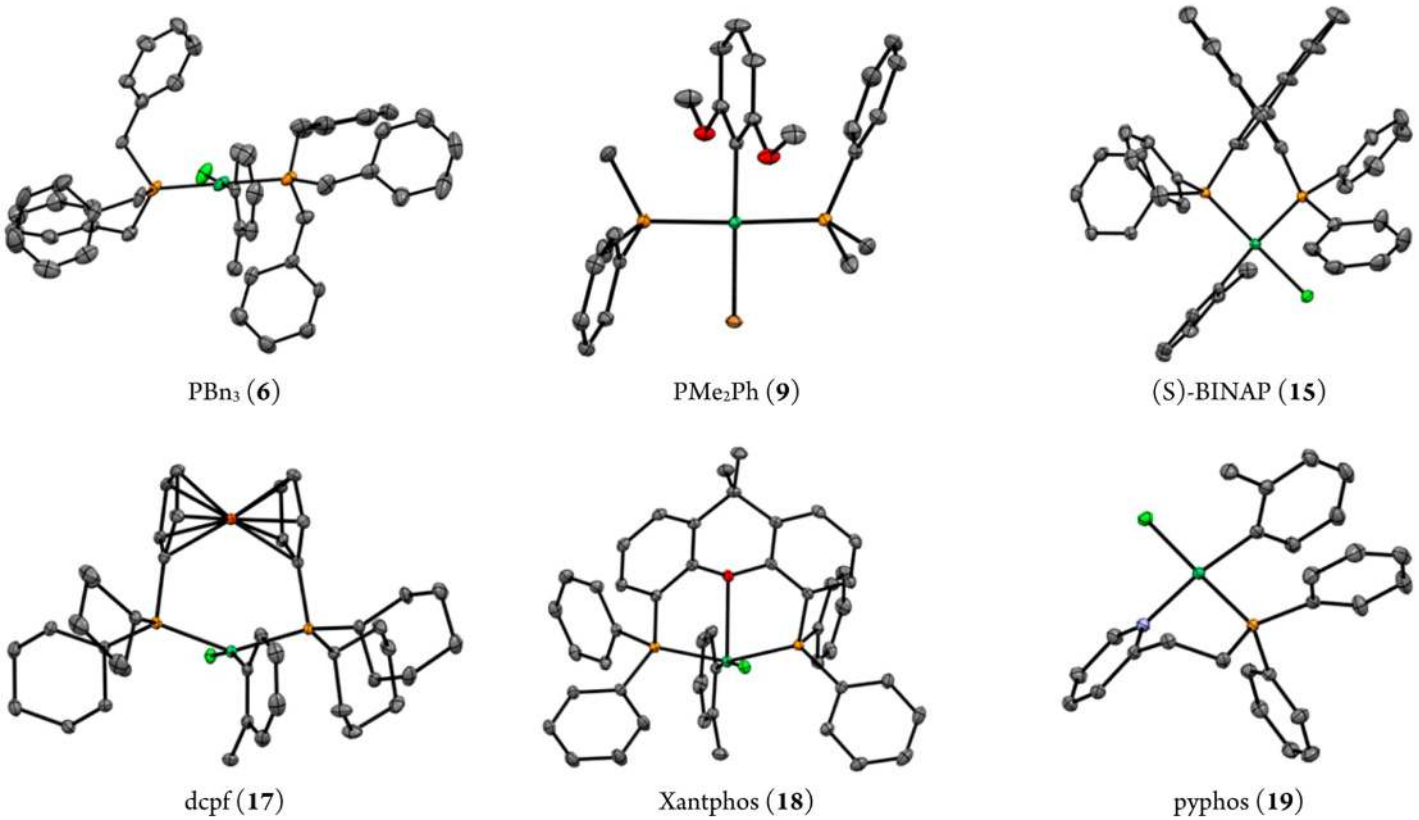

Figure 1. Complexes analyzed by single-crystal X-ray diffraction. Thermal ellipsoids are drawn at the 50% probability level, and hydrogen atoms are not included. Disorder of the *o*-tolyl ligand (**6**, **15**, **18**, **19**) and solvent molecules of crystallization (**6**, **15**, **17**, **18**) are not shown.

Useful for entry into Ni(0)/Ni(II) chemistry
Not modular: Need to know ideal ligand

(a) Standley, E. A.; Smith, S. J.; Müller, P.; Jamison, T. F. *Organometallics* **2014**, *33*, 2012–2018; (b) Chatt, J.; Shaw, B. L. *J. Chem. Soc.* **1960**, 1718–1729.

Nickel Catalysis

Doyle: Air-stable, modular precatalyst (2015)

Scheme 1. Synthesis of Nickel Precatalyst 1

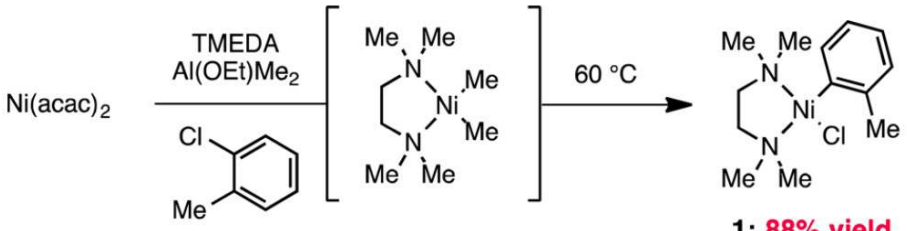

- one-pot synthesis w/o purification
- commercial starting materials
- air-stable, crystalline solid

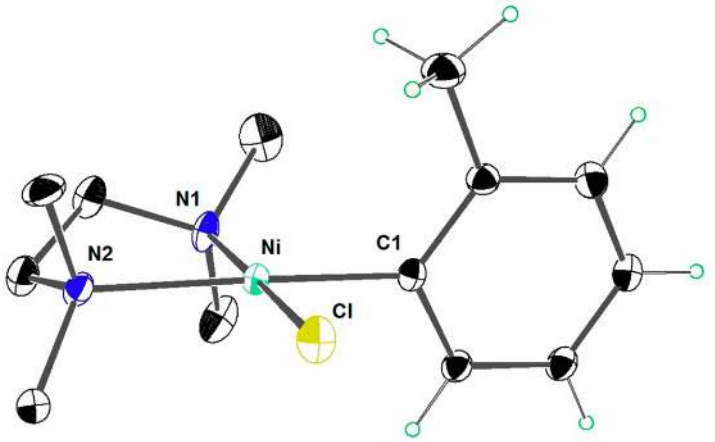

Figure 2. X-ray crystal structure of complex **1**. Ellipsoids are set to 30% probability. Hydrogen atoms on the TMEDA ligand have been removed for clarity.

Scheme 2. Mechanisms for Precatalyst Activation

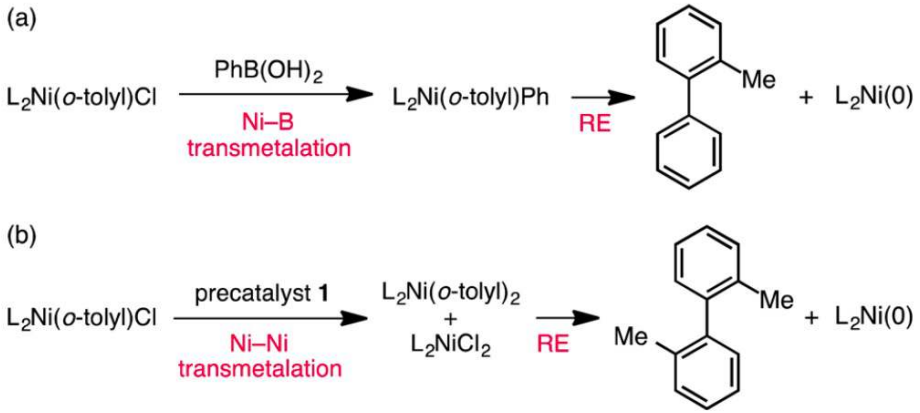

Shields, J. D.; Gray, E. E.; Doyle, A. G. *Org. Lett.* **2015**, *17*, 2166–2169.

Nickel Catalysis

Garg: $Ni(cod)_2$ paraffin capsules (2016)

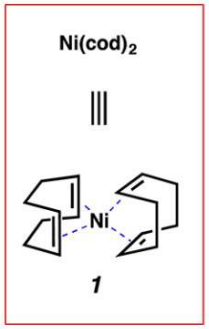

- *Most commonly used Ni(0) precatalyst*
- *Employed in >800 transformations over the last three decades*
- *Glove box handling limits general usage*

Present Study: First Benchtop Delivery of $Ni(cod)_2$

Paraffin Capsules

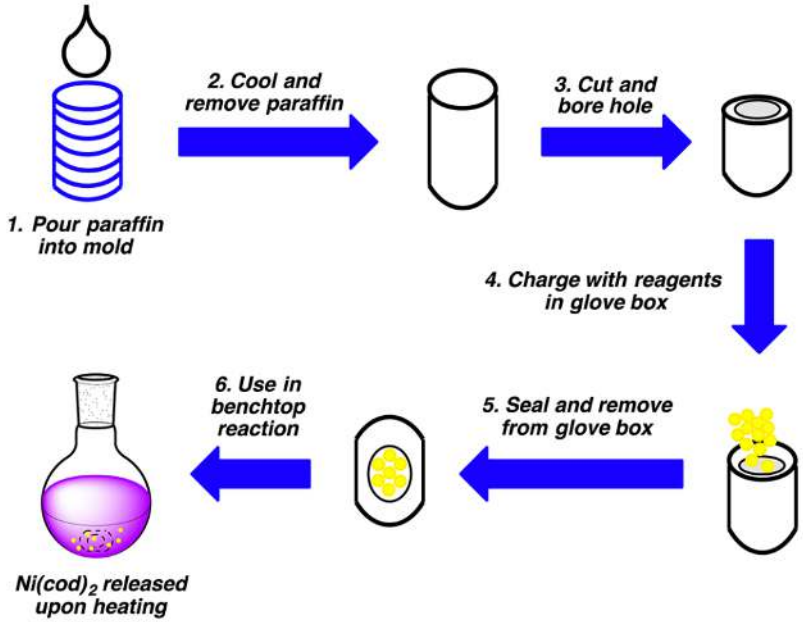

open capsule

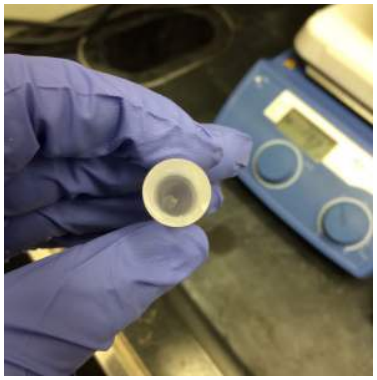

sealed capsule

Dander, J. E.; Weires, N. A.; Garg, N. K. *Org. Lett.* **2016**, *18*, 3934–3936.

Nickel Catalysis

Cornella: “Kinetic” air stability—$Ni(stb)_3$ (2020)

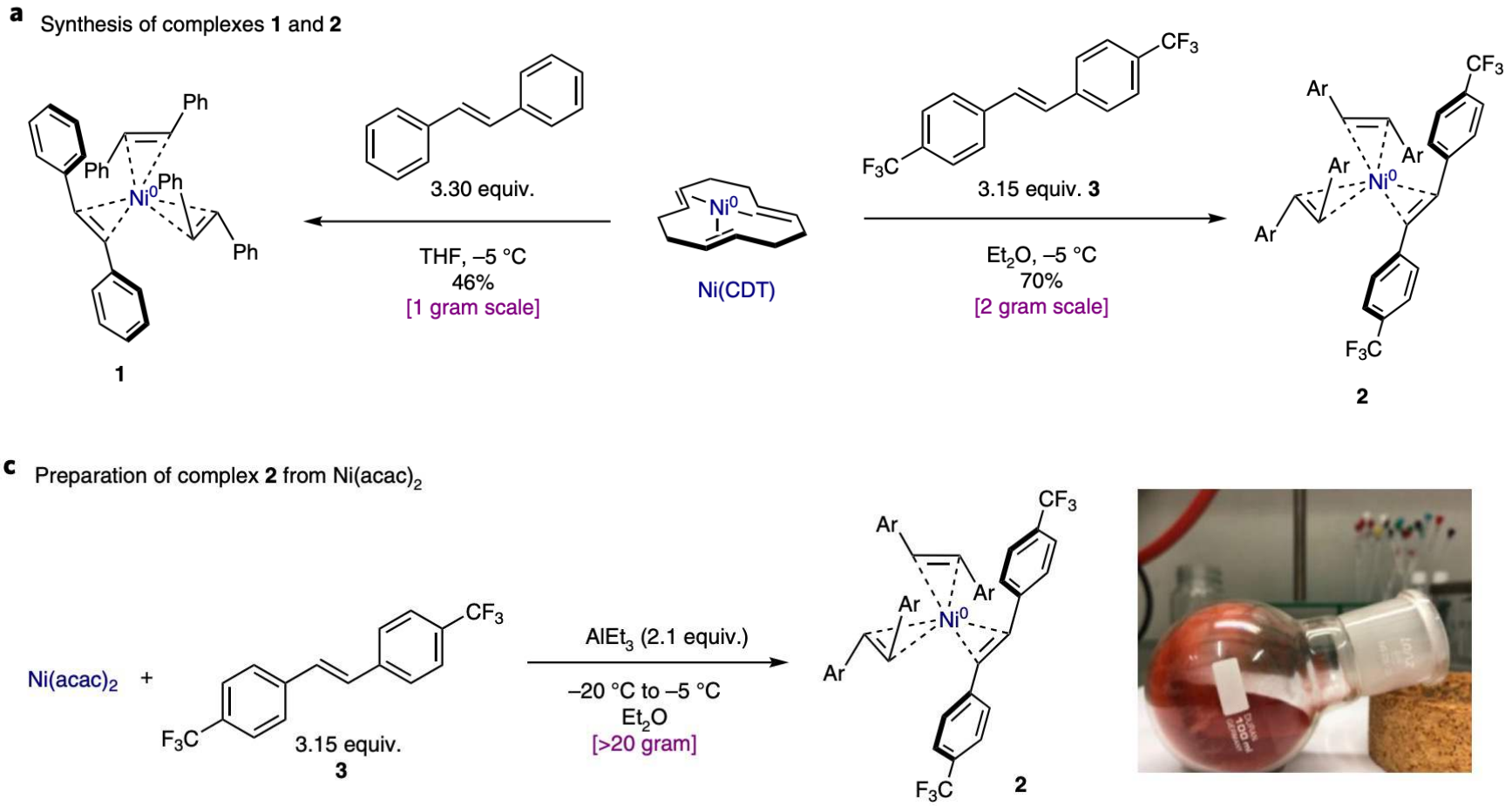

Nattmann, L.; Saeb, R.; Nöthling, N.; Cornella, J. *Nat. Catal.* **2020**, *3*, 6–13.

Nickel Catalysis

Cornella: “Kinetic” air stability—$Ni(stb)_3$ (2020)

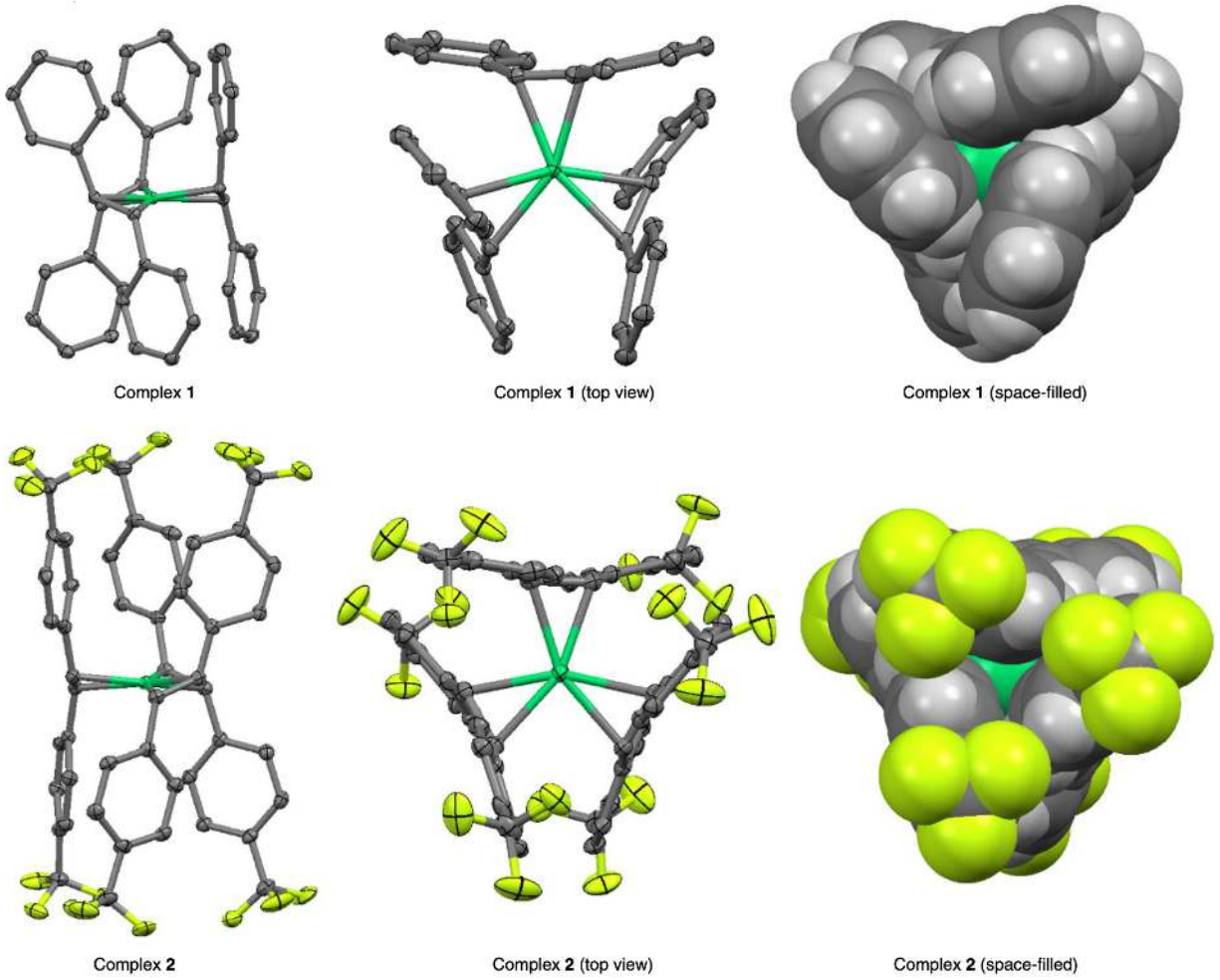

space-filling: Ni(0) atom inaccessible to O_2 in solid-state (kinetic stability)

Nattmann, L.; Saeb, R.; Nöthling, N.; Cornella, J. *Nat. Catal.* **2020**, *3*, 6–13.

Nickel Catalysis

Cornella: “Kinetic” air stability—Ni(stb)$_3$ (2020)

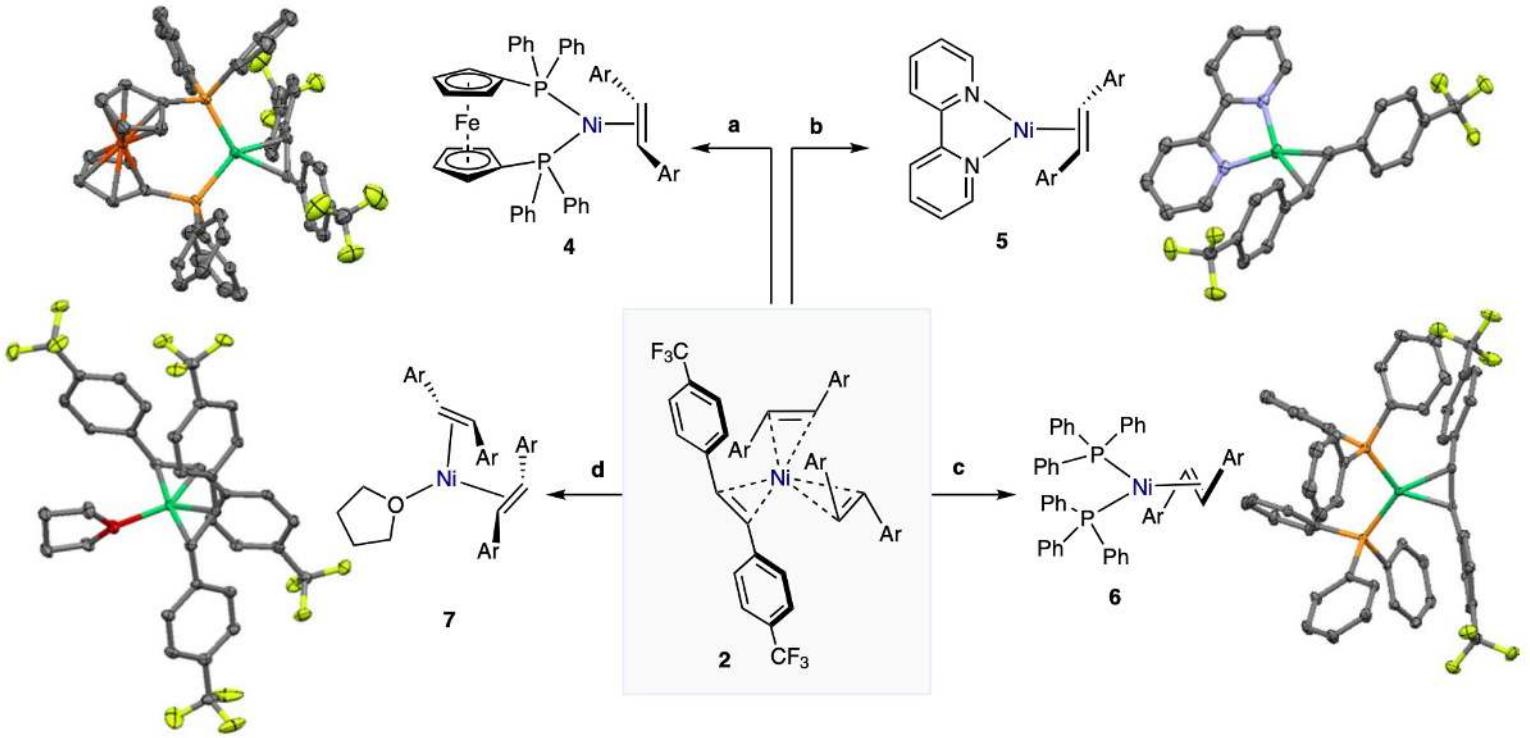

Fig. 3 | Ligand exchange of complex 2 with different ligands. a, Complex **2** (1 equiv.) and dppf (1 equiv.) in d_8-THF at 25 °C. One molecule of PhMe was present in the solid state and is omitted for clarity. **b**, Complex **2** (1 equiv.) and bipy (1 equiv.) in d_8-THF at 25 °C. One molecule of **3** crystallizes in the unit cell and is omitted for clarity. **c**, Complex **2** (1 equiv.) and PPh_3 (2 equiv.) in d_8-THF at 25 °C. **d**, Slow crystallization of **2** in THF from –20 °C to –78 °C. Ar, *p*-CF_3-C_6H_4; green, Ni; black, C; yellow, F; orange, P; deep orange, Fe; red, O; hydrogen atoms omitted for clarity (see the Supplementary Information for procedures).

solution-state substitution viable for a number of ligands (even bpy, THF, MeCN!)

Nattmann, L.; Saeb, R.; Nöthling, N.; Cornella, J. *Nat. Catal.* **2020**, *3*, 6–13.

Nickel Catalysis

Cornella follow-up: Ni($^{t\text{-Bu}}$stb)$_3$

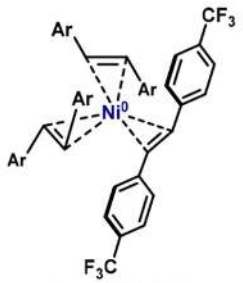

Ar = 4-CF_3-C_6H_4
2, 95% (Ni($^{4\text{-CF3}}$stb)$_3$)
air-stable:
at -18 °C: > 3 months
at 25 °C: (<1 week)

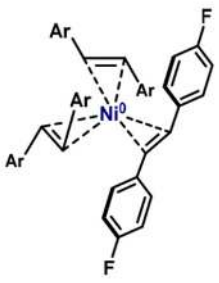

Ar = 4-F-C_6H_4
3, 67% (Ni($^{4\text{-F}}$stb)$_3$)
air-stable:
at -18 °C: > 3 months
at 25 °C: (<1 week)

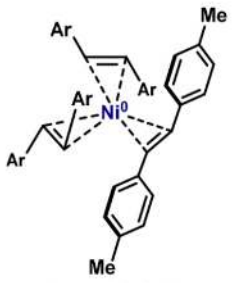

Ar = 4-Me-C_6H_4
4, 74% (Ni($^{4\text{-Me}}$stb)$_3$)
air-stable:
at -18 °C: > 3 months
at 25 °C: (<1 week)

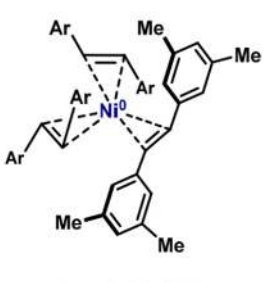

Ar = 3,5-Me-C_6H_4
5, 77% (Ni($^{3,5\text{-Me}}$stb)$_3$)
air-stable:
at -18 °C: 1 month
at 25 °C: (<1 week)

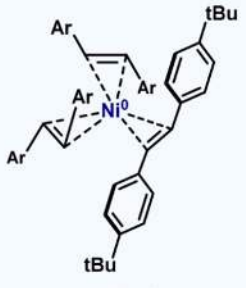

Ar = 4-tBu-C_6H_4
6, 95%, (Ni($^{4\text{-tBu}}$stb)$_3$)
air-stable:
at -18 °C: > 3 months
at 25 °C: 1 month

Nattmann, L.; Cornella, J. *Organometallics* **2020**, *39*, 3295–3300.

Nickel Catalysis

Cornella follow-up: Ni($^{t\text{-Bu}}$stb)$_3$

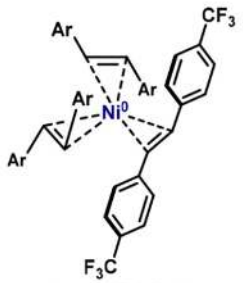

Ar = 4-CF_3-C_6H_4
2, 95% (Ni($^{4\text{-CF3}}$stb)$_3$)
air-stable:
at -18 °C: > 3 months
at 25 °C: (<1 week)

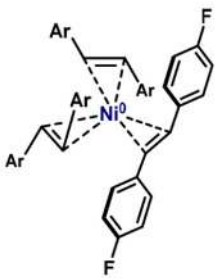

Ar = 4-F-C_6H_4
3, 67% (Ni($^{4\text{-F}}$stb)$_3$)
air-stable:
at -18 °C: > 3 months
at 25 °C: (<1 week)

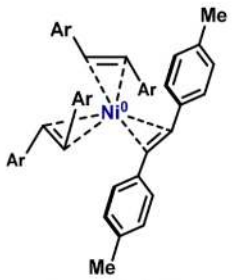

Ar = 4-Me-C_6H_4
4, 74% (Ni($^{4\text{-Me}}$stb)$_3$)
air-stable:
at -18 °C: > 3 months
at 25 °C: (<1 week)

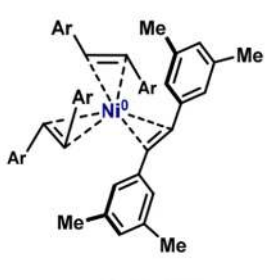

Ar = 3,5-Me-C_6H_4
5, 77% (Ni($^{3,5\text{-Me}}$stb)$_3$)
air-stable:
at -18 °C: 1 month
at 25 °C: (<1 week)

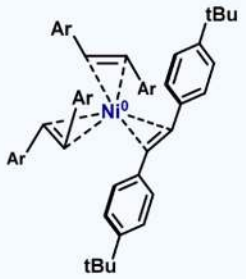

Ar = 4-tBu-C_6H_4
6, 95%, (Ni($^{4\text{-tBu}}$stb)$_3$)
air-stable:
at -18 °C: > 3 months
at 25 °C: 1 month

A. Ni(0)-catalyzed amination of aryl chlorides: a kinetic analysis

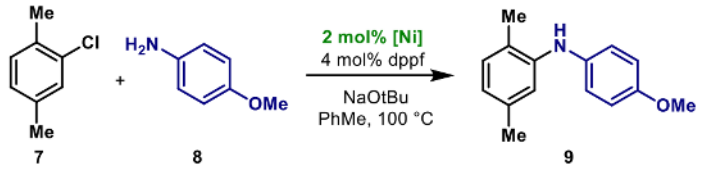

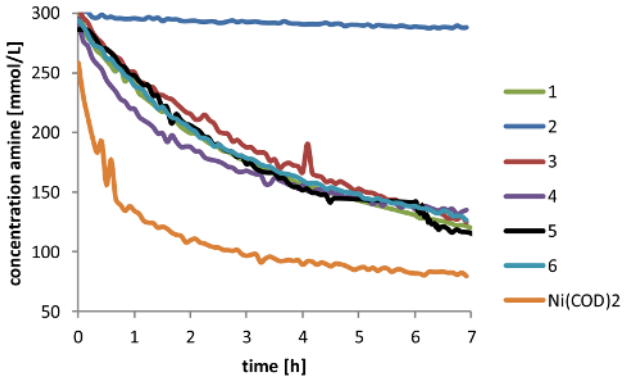

Nattmann, L.; Cornella, J. *Organometallics* **2020**, *39*, 3295–3300.

Nickel Catalysis

Cornella follow-up: Ni($^{t\text{-Bu}}$stb)$_3$

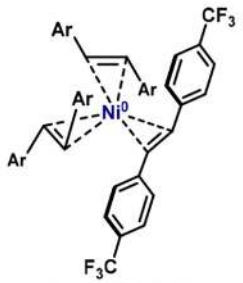

Ar = 4-CF_3-C_6H_4
2, 95% (Ni($^{4\text{-CF3}}$stb)$_3$)
air-stable:
at -18 °C: > 3 months
at 25 °C: (<1 week)

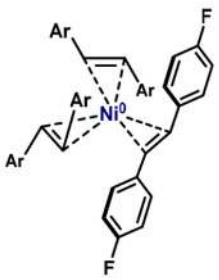

Ar = 4-F-C_6H_4
3, 67% (Ni($^{4\text{-F}}$stb)$_3$)
air-stable:
at -18 °C: > 3 months
at 25 °C: (<1 week)

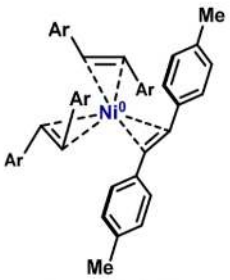

Ar = 4-Me-C_6H_4
4, 74% (Ni($^{4\text{-Me}}$stb)$_3$)
air-stable:
at -18 °C: > 3 months
at 25 °C: (<1 week)

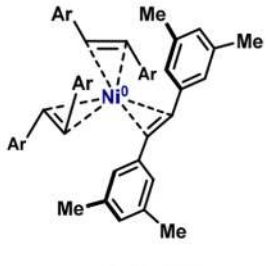

Ar = 3,5-Me-C_6H_4
5, 77% (Ni($^{3,5\text{-Me}}$stb)$_3$)
air-stable:
at -18 °C: 1 month
at 25 °C: (<1 week)

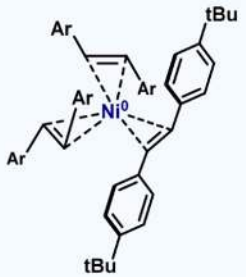

Ar = 4-tBu-C_6H_4
6, 95%, (Ni($^{4\text{-tBu}}$stb)$_3$)
air-stable:
at -18 °C: > 3 months
at 25 °C: 1 month

organic transformations

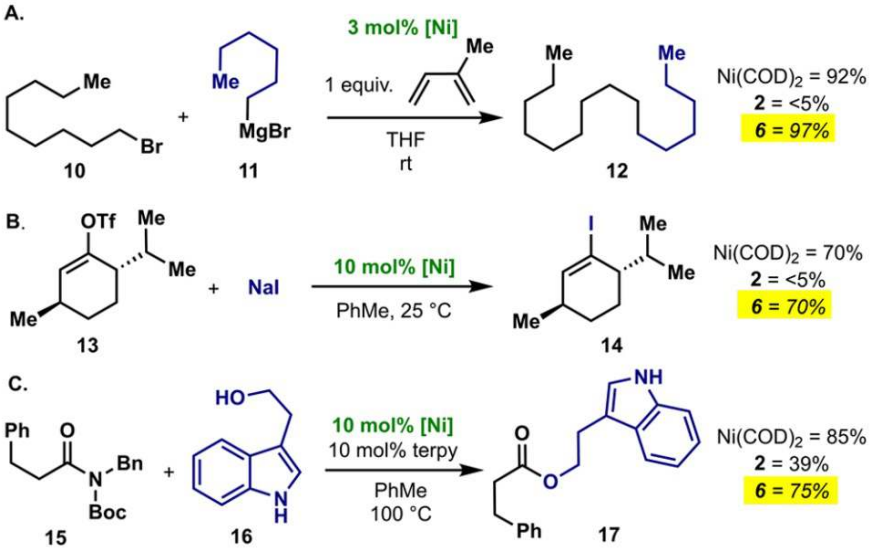

Nattmann, L.; Cornella, J. *Organometallics* **2020**, *39*, 3295–3300.

Nickel Catalysis

Engle: Ni(cod)(DQ) (2020)—“thermodynamic” stability

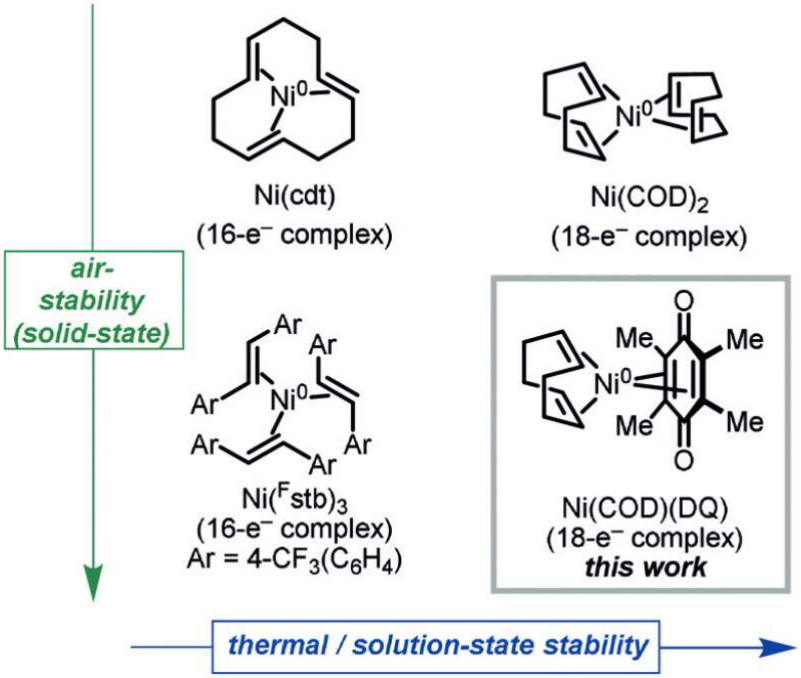

Tran, V. T.; Li, Z.-Q.; Apolinar, O.; Derosa, J.; Joannou, M. V.; Wisniewski, S. R.; Eastgate, M. D.; Engle, K. M. *Angew. Chem. Int. Ed.* **2020**, *59*, 7409–7413.

Nickel Catalysis

Engle: Ni(cod)(DQ) (2020)—“thermodynamic” stability

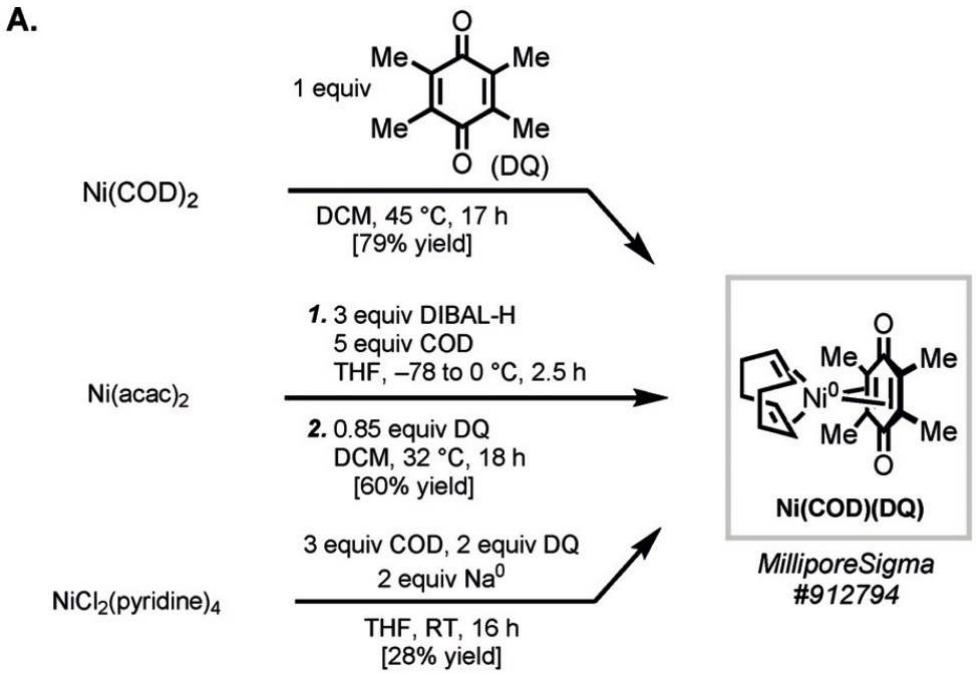

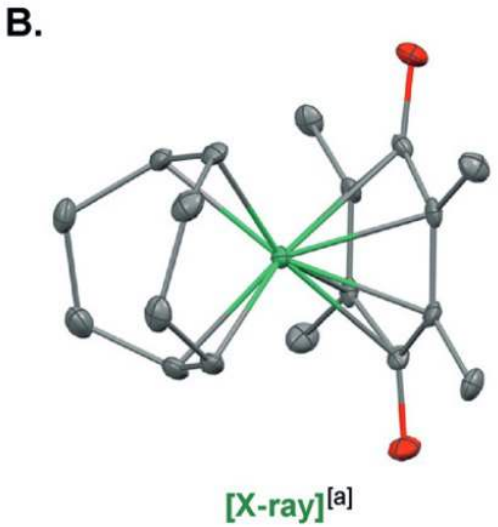

Tran, V. T.; Li, Z.-Q.; Apolinar, O.; Derosa, J.; Joannou, M. V.; Wisniewski, S. R.; Eastgate, M. D.; Engle, K. M. *Angew. Chem. Int. Ed.* **2020**, *59*, 7409–7413.

Nickel Catalysis

Engle: Ni(cod)(DQ) (2020)—“thermodynamic” stability

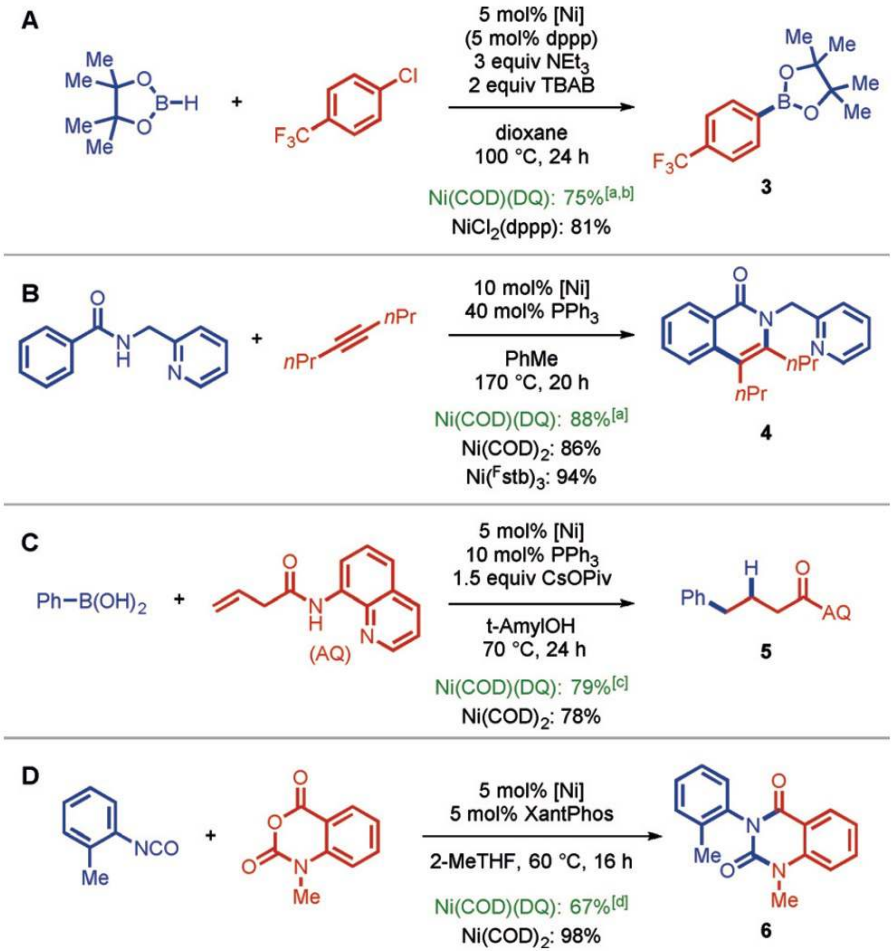

Table 2: Photographs of a representative stress test (Table 1, Entry 4).

note: viable transformations require in situ catalyst to be more thermodynamically stable

Tran, V. T.; Li, Z.-Q.; Apolinar, O.; Derosa, J.; Joannou, M. V.; Wisniewski, S. R.; Eastgate, M. D.; Engle, K. M. *Angew. Chem. Int. Ed.* **2020**, *59*, 7409–7413.

Nickel Catalysis

Topics in nickel cross-coupling:

Directions in Precatalyst Synthesis

"Inert"/"Nonclassical" $C(sp^2)$–X Electrophiles Ni(0)/Ni(II)

Benzylic $C(sp^3)$–X Electrophiles Ni(0)/Ni(II)

X = OR, NR_3X

"Unactivated" $C(sp^3)$–X Electrophiles Ni(I)/Ni(III)

Cross-Electrophile Coupling Ni(0)/Ni(I)/Ni(II)/Ni(III)

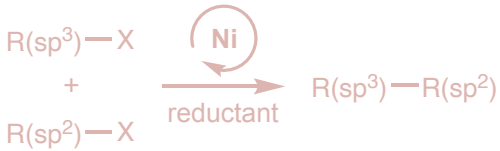

Conjunctive Cross-Coupling (Short)

Nickel Catalysis

C–CN oxidative addition to nickel(0), 1983:

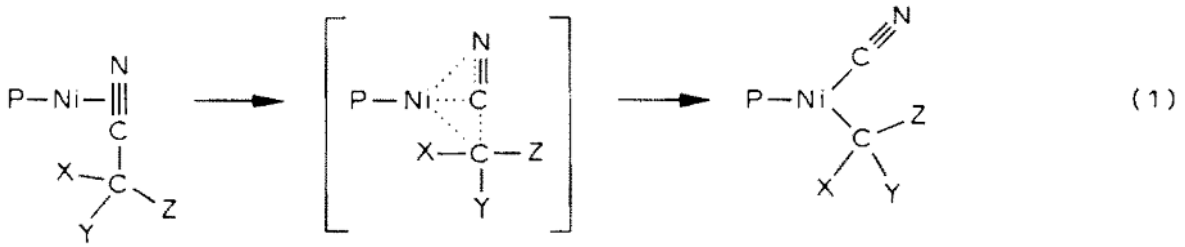

(1)

Compounds confirmed by IR, though slowly decompose

Favero, G.; Morvillo, A.; Turco, A. *J. Organomet. Chem.* **1983**, *241*, 251–257.
Tolman, C. A.; Seidel, W. C.; Druliner, J. D.; Domaille, P. J. *Organometallics* **1984**, *3*, 33–38.
Miller, J. A. *Tetrahedron Lett.* **2001**, *42*, 6991–6993.
Miller, J. A.; Dankwardt, J. W.; Penney, J. M. *Synthesis* **2003**, 1643–1648.

Nickel Catalysis

Oxidative addition of benzonitriles (Jones, 2002):

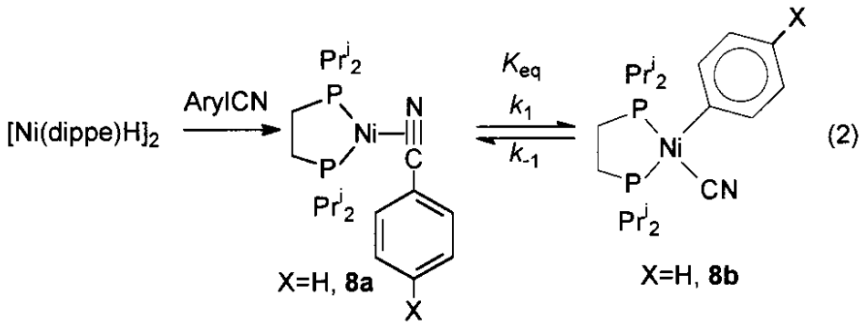

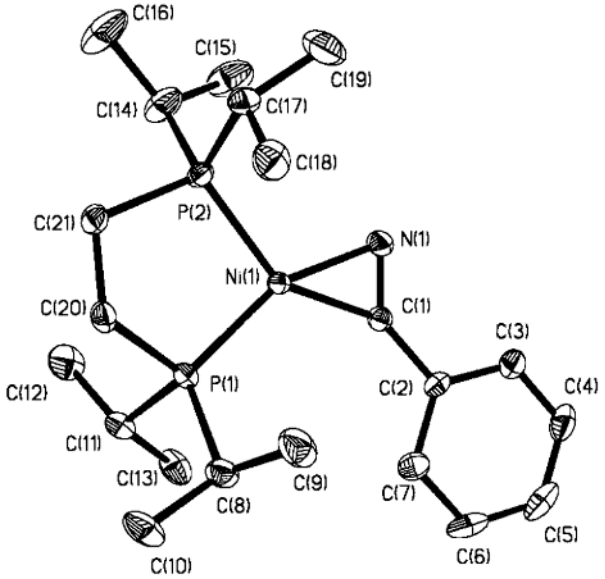

Figure 7. ORTEP drawing of (dippe)Ni(η^2-benzonitrile), **8a**. Ellipsoids are shown at the 30% probability level. Selected distances (Å) and angles (deg): Ni(1)−N(1), 1.908(3); Ni(1)−C(1), 1.867(4), C(1)−N(1), 1.225-(6); N(1)−C(1)−C(2), 136.1(4); P(1)−Ni(1)−P(2), 91.54(5).

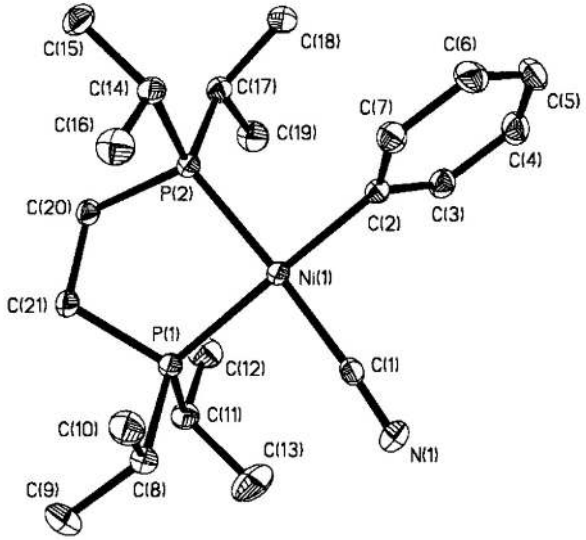

Figure 8. ORTEP drawing of (dippe)Ni(Ph)(CN), **8b**. Ellipsoids are shown at the 30% probability level. Selected distances (Å) and angles (deg): Ni-(1)−C(2), 1.935(2); Ni(1)−C(1), 1.877(3); C(1)−N(1), 1.148(3), P(1)−Ni(1)−P(2), 88.56(3).

Garcia, J. J.; Brunkan, N. M.; Jones, W. D. *J. Am. Chem. Soc.* **2002**, *124*, 9547–9555.

Nickel Catalysis

Oxidative addition of benzonitriles (Jones, 2002):

Scheme 3

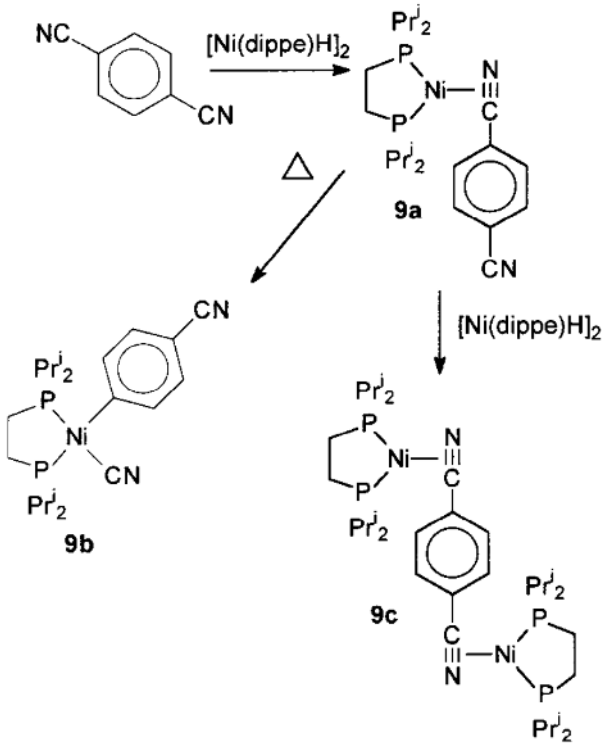

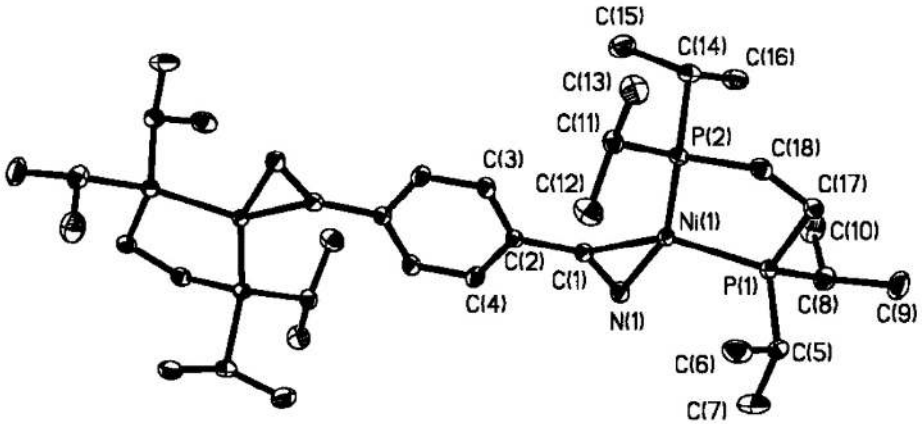

Figure 13. ORTEP drawing of [(dippe)Ni]$_2$(η^2,η^2-1,4-dicyanobenzene), **9c**. Ellipsoids are shown at the 30% probability level. Ni(1)−N(1), 1.918(3); Ni(1)−C(1), 1.853(3), C(1)−N(1), 1.225(4); N(2)−C(8), 1.148(3); N(1)−C(1)−C(2), 136.4(3); P(1)−Ni(1)−P(2), 91.70(4).

Garcia, J. J.; Brunkan, N. M.; Jones, W. D. *J. Am. Chem. Soc.* **2002**, *124*, 9547–9555.

Nickel Catalysis

Kumada coupling using nitriles (Miller, 2001):

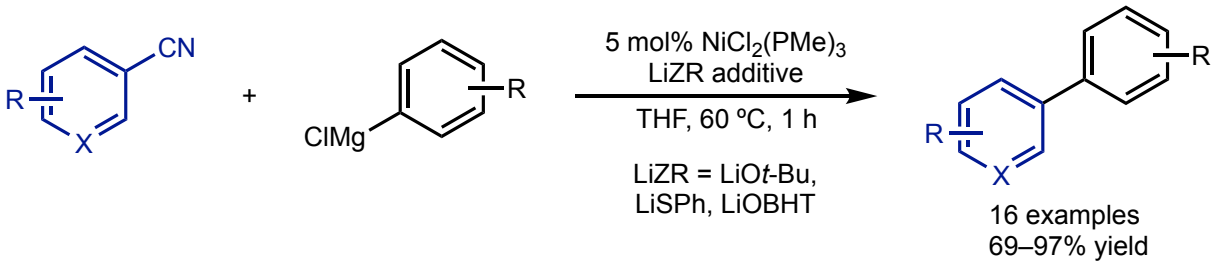

Role of bulky base additive: form modified ArMgZR (prevents nitrile addition)

For amination, see Miller et al., 2003.

Favero, G.; Morvillo, A.; Turco, A. *J. Organomet. Chem.* **1983**, *241*, 251–257.
Tolman, C. A.; Seidel, W. C.; Druliner, J. D.; Domaille, P. J. *Organometallics* **1984**, *3*, 33–38.
Miller, J. A. *Tetrahedron Lett.* **2001**, *42*, 6991–6993.
Miller, J. A.; Dankwardt, J. W.; Penney, J. M. *Synthesis* **2003**, 1643–1648.

Nickel Catalysis

Cross-coupling using aryl ethers (Wenkert and Dankwardt)

Wenkert, 1979:

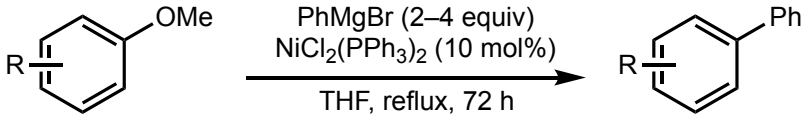

Table II. The Reactions of Aryl Ethers with Phenylmagnesium Bromide[a]

ether	products	% yield
1-methoxynaphthalene	1-phenylnaphthalene	70
2-methoxynaphthalene	2-phenylnaphthalene	77[b]
2,3-dimethoxynaphthalene	2,3-diphenylnaphthalene[c]	45
m-dimethoxybenzene	*m*-methoxybiphenyl	23 (79)
p-dimethoxybenzene	*p*-methoxybiphenyl,	33 (37)
	p-terphenyl	24 (27)
p-methoxybiphenyl	*p*-terphenyl	30 (55)
m-cresyl methyl ether	*m*-methylbiphenyl	16 (74)
p-cresyl methyl ether	*p*-methylbiphenyl	20 (60)

[a] A benzene solution of 2–4 mol of Grignard reagent and 0.1 mol of bis(triphenylphosphine)nickel dichloride/mol of aryl ether was refluxed for 72 h. Isolated product yields are based on the initial ether quantity, whereas those listed in parentheses take into account recovered ether. [b] Reaction time 24 h. [c] H. M. Crawford, *J. Am. Chem. Soc.*, **61**, 608 (1939).

Dankwardt, 2004:

Table 3: Ni-catalyzed cross-coupling of **1**: Optimization of the phosphane.[a]

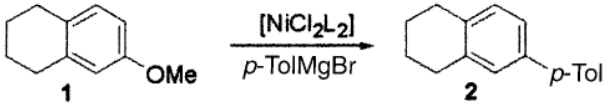

Entry	L	Recovd. **1** [%]	Conv. **2** [%]
1	PMe_3	33	33
2	PEt_3	75	7
3	$PiBu_3$	32	42
4	$PiPr_3$	<1	82
5	PCy_3	0	93
6	$PhPCy_2$	<1	92
7	Ph_2PCy	7	81
8	Ph_3P	74	15

[a] Reactions were carried out at 60 °C in iPr_2O for 15 h with 5 mol% nickel catalyst. Conversions were determined by GC analysis with tridecane as an internal standard.

(a) Wenkert, E.; Michelotti, E. L.; Swindell, C. S. *J. Am. Chem. Soc.* **1979**, *101*, 2246–2247; (b) Dankwardt, J. W. *Angew. Chem. Int. Ed.* **2004**, *43*, 2428–2432.

Nickel Catalysis

Evidence for C–O oxidative addition: Tobisu and Chatani, 2015

Scheme 20. Experimental Implication of Oxidative Addition of a C(aryl)–OMe Bond to Ni(0)

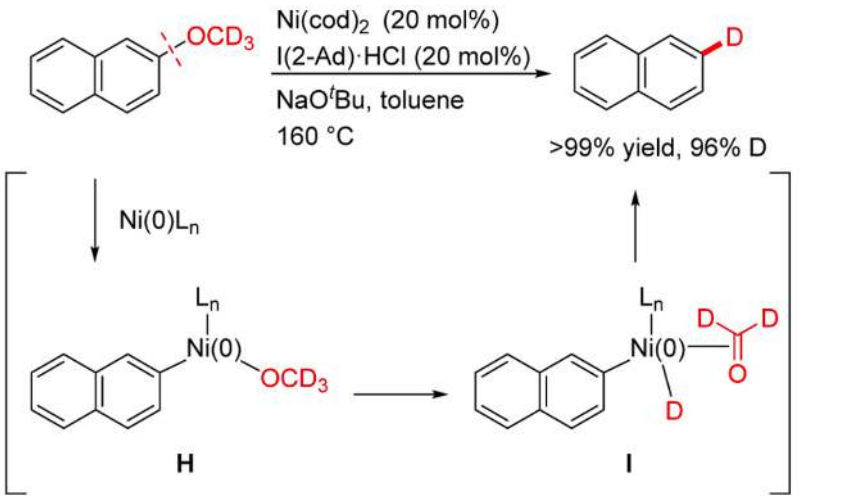

(a) Tobisu, M.; Morioka, T.; Ohtsuki, A.; Chatani, N. *Chem. Sci.* **2015**, *6*, 3410–3414; (b) Tobisu, M.; Chatani, N. *Acc. Chem. Res.* **2015**, *48*, 1717–1726.

Nickel Catalysis

Shi: Iterative cross-coupling of ethers and nitriles (2009)

Scheme 2. Sequential Cross-Coupling to Construct Polysubstituted Benzene

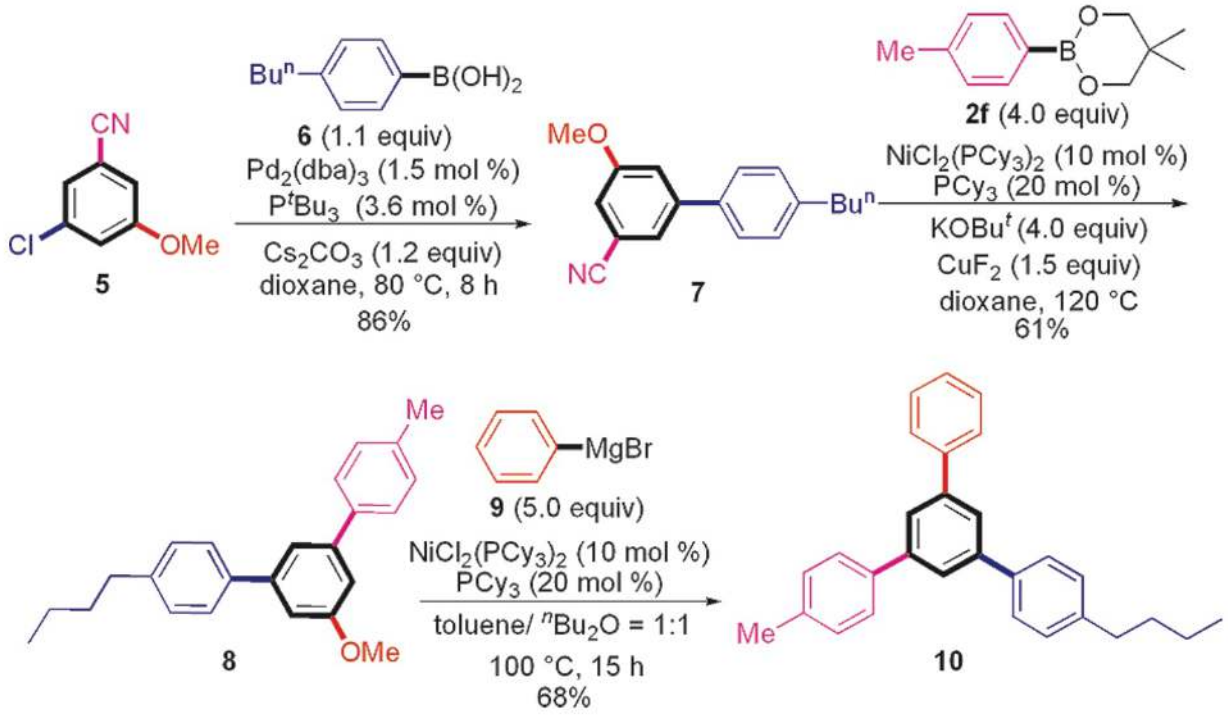

Yu, D.-G.; Yu, M.; Guan, B.-T.; Li, B.-J.; Zheng, Y.; Wu, Z.-H.; Shi, Z.-J. *Org. Lett.* **2009**, *11*, 3374–3377.

Nickel Catalysis

Table 1 Nickel-catalyzed Suzuki-Miyaura type cross-coupling of aryl esters, carbamates and carbonates

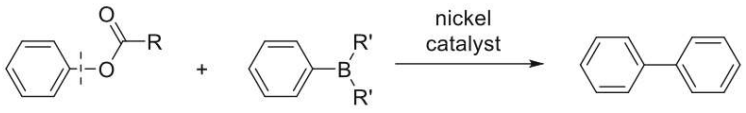

Year	Author	Phenolic substrate	Boron source	Catalyst system	Reference
2008	Garg	Ar–OCO^{t}Bu	Ar'B(OH)$_2$	$NiCl_2(PCy_3)_2$ K_3PO_4	42
2008	Shi	Ar–OCOR (R = Me, ^{t}Bu, Ph)	(Ar'BO)$_3$ + 0.88 H_2O	$NiCl_2(PCy_3)_2$ K_3PO_4	43
2009	Garg	Ar–OCONEt$_2$ Ar–OCO$_2$^{t}Bu	Ar'B(OH)$_2$	$NiCl_2(PCy_3)_2$ K_3PO_4	44
2009	Snieckus	Ar–OCONEt$_2$	Ar'B(OH)$_2$ + 0.1 (Ar'BO)$_3$	$NiCl_2(PCy_3)_2$ PCy_3•HBF_4 K_3PO_4	46
2010	Shi	Ar–OCONMe$_2$	(Ar'BO)$_3$ + 1.0 H_2O	$NiCl_2(PCy_3)_2$ PCy_3 K_2CO_3	45
2010	Molander	Ar–OCO^{t}Bu Ar–OCONEt$_2$	$ArBF_3K$ + H_2O	$Ni(cod)_2$[a] PCy_3•HBF_4 K_3PO_4	49
2011	Kuwano	Ar–OCO$_2$Me	Ar'B(OH)$_2$	$Ni(cod)_2$ DCyPF[b] K_2CO_3	51

[a] cod = 1,5-cyclooctadiene

[b] 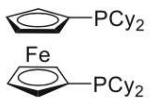

Tobisu, M.; Chatani, N. *Top. Curr. Chem.* **2016**, *374*, 41.

Nickel Catalysis

Activation of alternate aryl C–O electrophiles

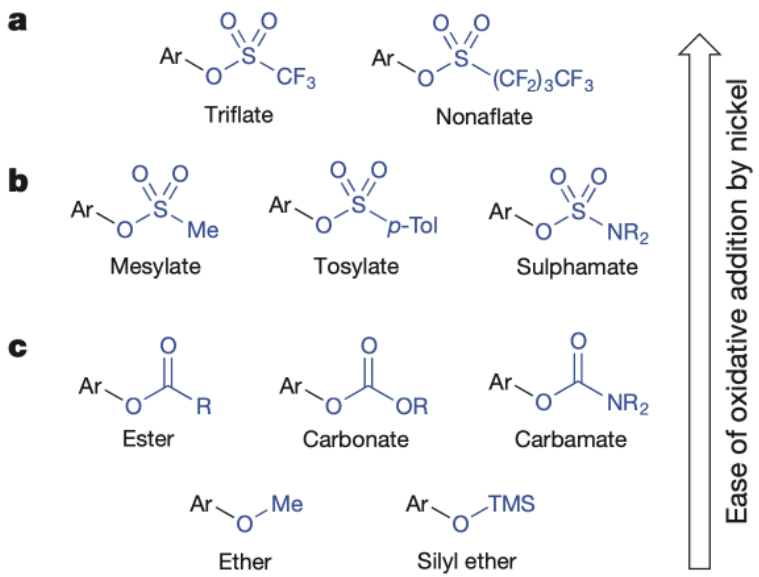

Figure 3 | Halogen alternatives used in cross-coupling reactions. **a**, Aryl triflates have long been used as replacements for halogens in cross-coupling reactions. Aryl nonaflates were developed later to address some of the issues encountered when working with aryl triflates, but their use is less widespread. **b**, The use of aryl mesylates, tosylates and sulphamates presents many advantages over triflates and related fluorinated sulphonates owing to their increased stability. **c**, Like sulphonate derivatives, the use of carboxylic esters, carbonates, carbamates, ethers and silyl ethers can be advantageous in many situations. *p*-Tol, *para*-tolyl (4-methylphenyl); TMS, trimethylsilyl.

Tasker, S. Z.; Standley, E. A.; Jamison, T. F. *Nature* **2014**, *509*, 299–309.

Nickel Catalysis

Iterative cross-coupling of ”unreactive” electrophiles (Reuping):

Scheme 2. Programmed Selective C–O Bond Activation

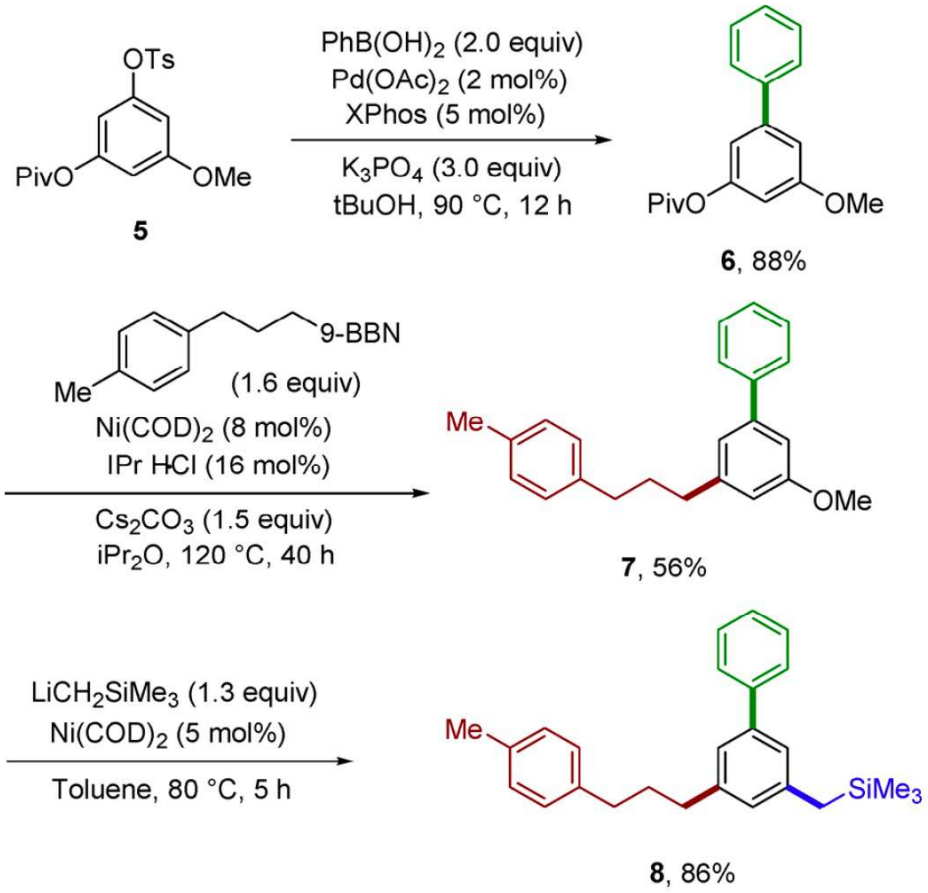

Guo, L.; Hsiao, C.-C.; Yue, H.; Liu, X.; Rueping, M. *ACS Catal.* **2016**, *6*, 4438–4442.

Nickel Catalysis

Neufeldt: Cl vs. OTs iterative cross-couping (2020)

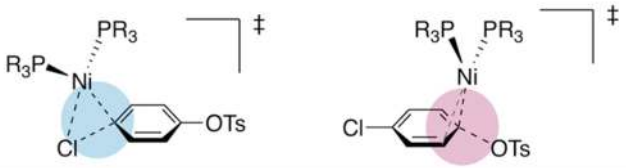

R	reaction at chloride ΔG‡ (kcal mol^{-1})	reaction at tosylate ΔG‡ (kcal mol^{-1})	$\Delta\Delta G^{\ddagger}_{OTs-Cl}$
Me	16.1	13.1	-3.0
Ph	12.6	14.6	2.0
Cy	10.2	9.0	-1.2

Figure 2. Calculated free energies of activation (in kcal mol^{-1}) for oxidative addition with PMe_3, PPh_3, and PCy_3, measured from the preceding π complex.

Table 1. Ligand Effect on Selectivity of Oxidative Addition

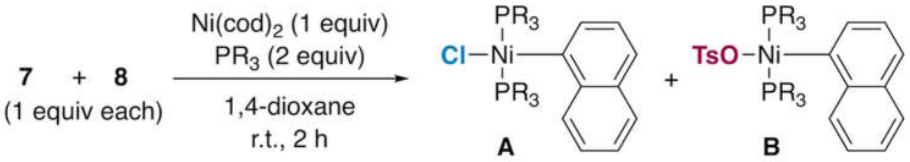

entry	ligand	A : B	entry	ligand	A : B
1	PPh_3	>99 : 1	7	PCy_3	1.5 : 1
2	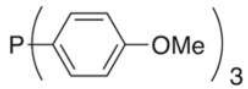	>99 : 1	8	$P(n\text{-}Bu)_3$	1.1 : 1
			9	$P(i\text{-}Bu)_3$	2.9 : 1
3	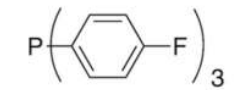	>99 : 1	10[a]	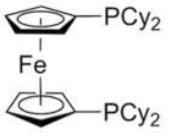	>99 : 1
4	$PPhMe_2$	1 : 5.7			
5	$PPhEt_2$	2.2 : 1	11	PEt_3	1.8 : 1
6	PPh_2Me	1 : 1	12	PMe_3	1 : 6.3

[a]With 1 equiv of bisphosphine relative to nickel.

Entz, E. D.; Russel, J. E. A.; Hooker, L. V.; Neufeldt, S. R. *J. Am. Chem. Soc.* **2020**, *142*, 15454–15463.

Nickel Catalysis

Cl vs. OTs iterative cross-couping (Neufeldt):

Scheme 2. Chemoselective Oxidative Addition with PMe_3

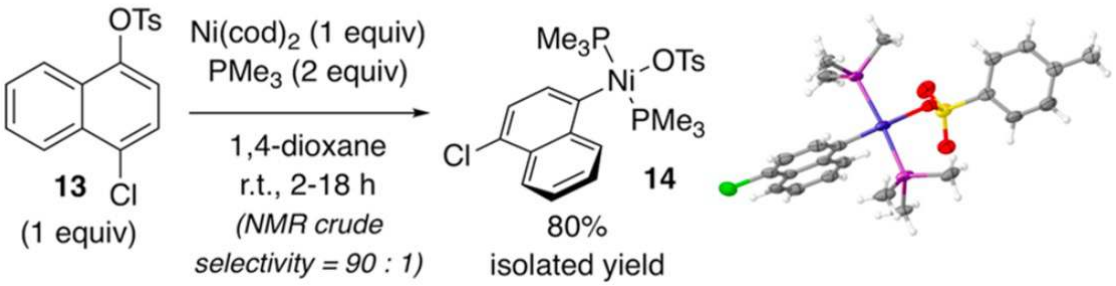

Entz, E. D.; Russel, J. E. A.; Hooker, L. V.; Neufeldt, S. R. *J. Am. Chem. Soc.* **2020**, *142*, 15454–15463.

Nickel Catalysis

Cl vs. OTs iterative cross-couping (Neufeldt):

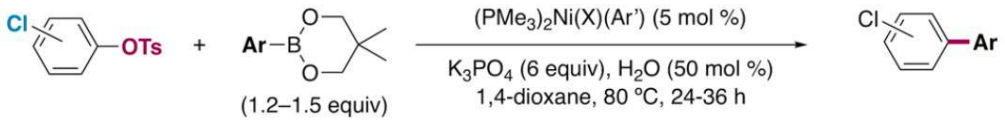

entry	substrate	major product	% GC yield (selectivity)[b]	isolated yield (%)
1[c]	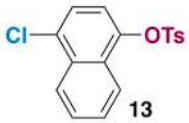	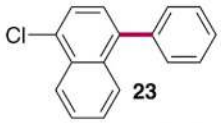 **23**	80 (>50:1)	72
2	**13**	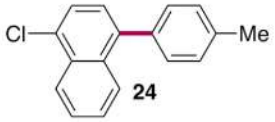 **24**	80 (>50:1)	61
3	**13**	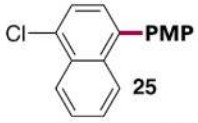 **25**	95 (>50:1)	78
4	**13**	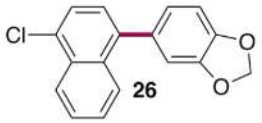 **26**	86 (>50:1)	75
5	**13**	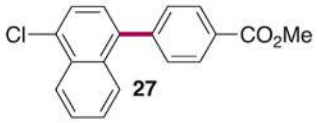 **27**	86 (>50:1)	62
6[c]	**13**	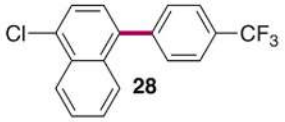 **28**	87 (>50:1)	64

entry	substrate	major product	% GC yield (selectivity)[b]	isolated yield (%)
7[d]	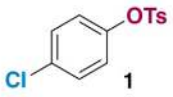 **1**	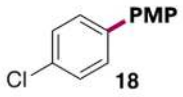 **18**	88 (44:1)	72
8[d]	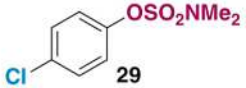 **29**	**18**	55 (8:1)	39
9[d]	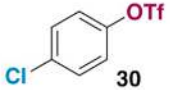 **30**	**18**	49 (>50:1)	48
10	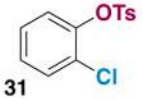 **31**	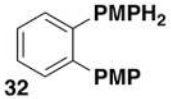 **32**	48	35
11	 **33**	 **34**	73 (>50:1)	35
12	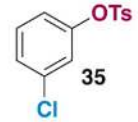 **35**	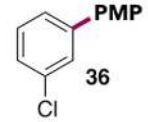 **36**	89 (30:1)	67

Entz, E. D.; Russel, J. E. A.; Hooker, L. V.; Neufeldt, S. R. *J. Am. Chem. Soc.* **2020**, *142*, 15454–15463.

Nickel Catalysis

Cl vs. OTs iterative cross-couping (Neufeldt):

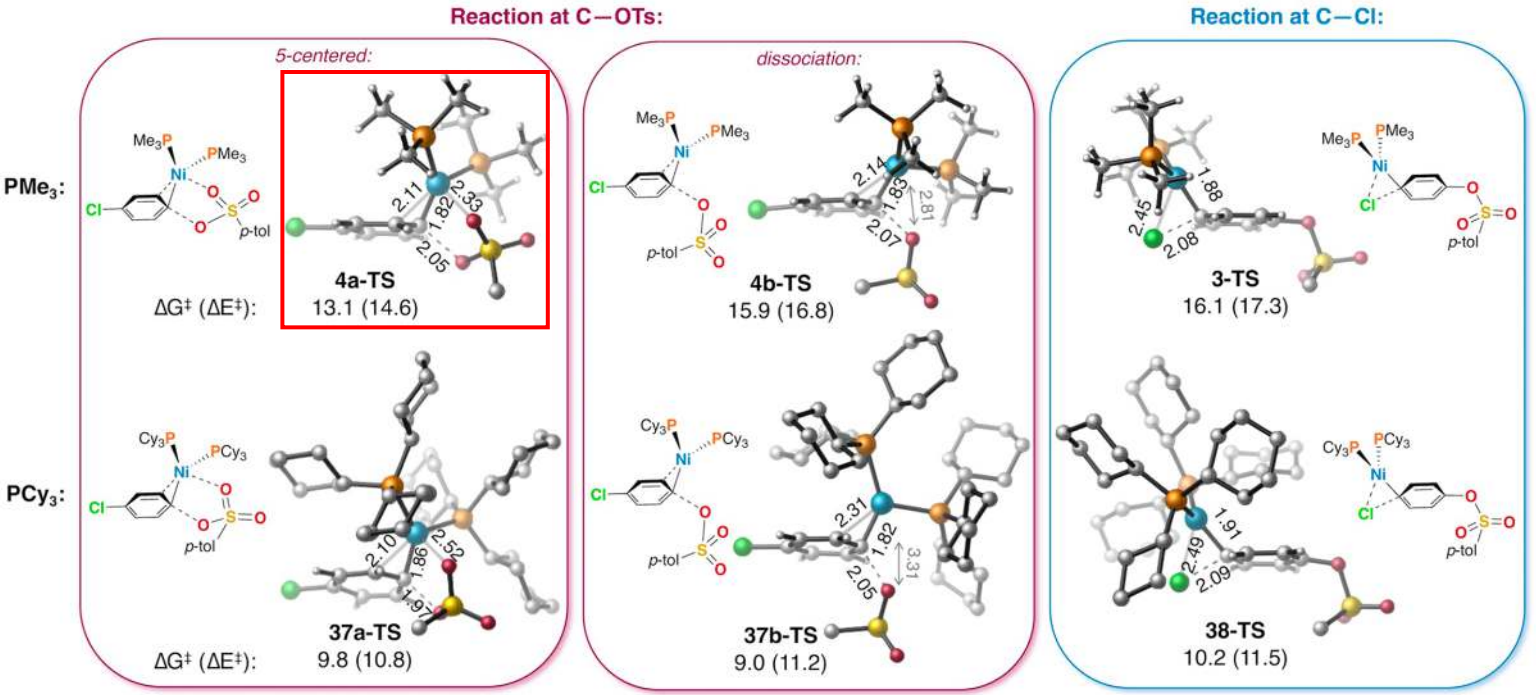

Figure 7. Oxidative addition transition structures using $Ni(PMe)_3$ and $Ni(PCy_3)_2$. Most of the carbons and hydrogens of tosylate, as well as the hydrogens on PCy_3, are hidden for clarity (see SI for complete structures).

Steric feature: More stabilizing Ni–O=S interaction in TS using PMe_3

Entz, E. D.; Russel, J. E. A.; Hooker, L. V.; Neufeldt, S. R. *J. Am. Chem. Soc.* **2020**, *142*, 15454–15463.

Nickel Catalysis

Topics in nickel cross-coupling:

Directions in Precatalyst Synthesis

"Inert"/"Nonclassical" $C(sp^2)$–X Electrophiles Ni(0)/Ni(II)

Benzylic $C(sp^3)$–X Electrophiles Ni(0)/Ni(II)

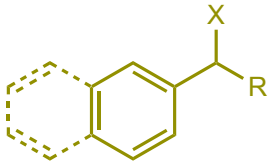

X = OR, NR_3X

"Unactivated" $C(sp^3)$–X Electrophiles Ni(I)/Ni(III)

Cross-Electrophile Coupling Ni(0)/Ni(I)/Ni(II)/Ni(III)

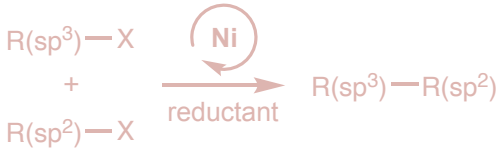

Conjunctive Cross-Coupling (Short)

Nickel Catalysis

Methylation of benzylic C–OMe electrophiles (Shi, 2008)

Table 3. Benzylic Methylation with Different Substractes via Ni-Catalyzation[a]

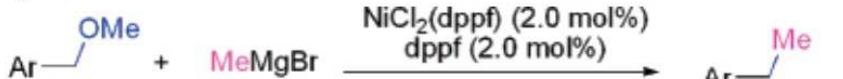

1 2

entry	Ar	1	2 (%)[b]
1[c]	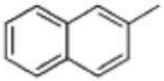	**1a**	**2a** (80)
2[c]	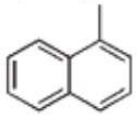	**1k**	**2g** (75)
3	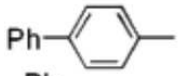	**1l**	**2h** (99)
4	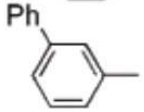	**1m**	**2i** (91)
5	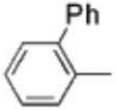	**1n**	**2j** (86)
6[d]		X = F **1o**	**2k** (92)
7	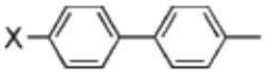	X = OMe **1p**	**2l** (89)
8		X = Me **1q**	**2k** (95)
9[e]		X = OH **1r**	**2m** (70)
10[f]	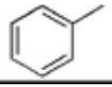	**1s**	**2n** (> 99)

Guan, B.-T.; Xiang, S.-K.; Wang, B.-Q.; Sun, Z.-P.; Wang, Y.; Zhao, K.-Q.; Shi, Z.-J. *J. Am. Chem. Soc.* **2008**, *130*, 3268–3269.

Nickel Catalysis

Methylation of benzylic C–OMe electrophiles (Shi, 2008)

Scheme 1. High Chemoselective C−O Activation of Both sp^3 and sp^2 C−OMe

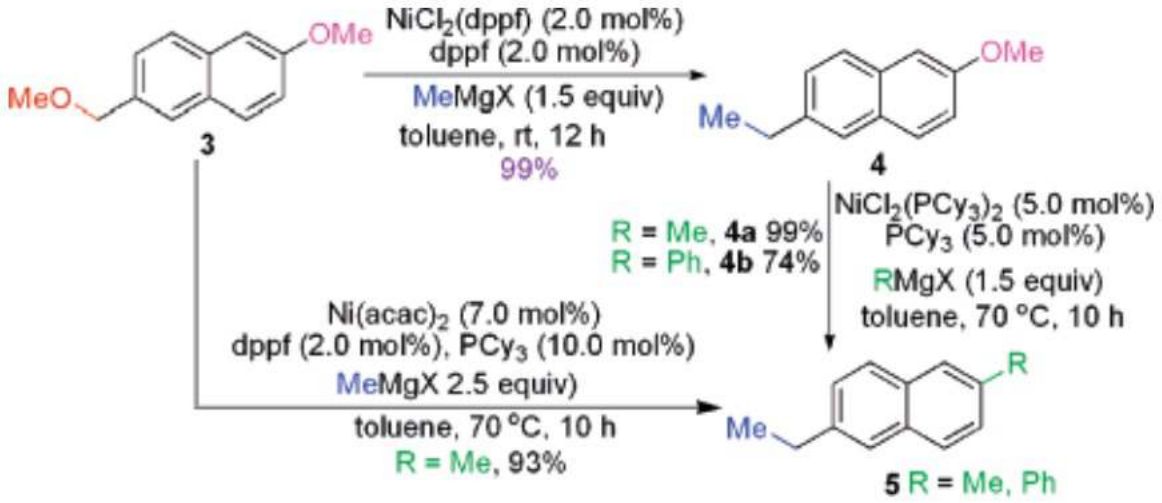

Guan, B.-T.; Xiang, S.-K.; Wang, B.-Q.; Sun, Z.-P.; Wang, Y.; Zhao, K.-Q.; Shi, Z.-J. *J. Am. Chem. Soc.* **2008**, *130*, 3268–3269.

Nickel Catalysis

Jarvo (2011): Enantiospecific methylation of α-aryl ethers

Table 2. Stereospecific Cross-Coupling Reactions

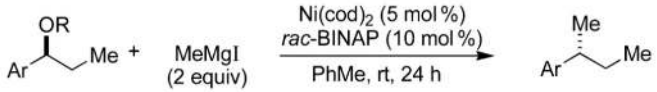

entry	substrate, (ee (%))[a]	product	yield (%)[b]	ee (%)[a]
	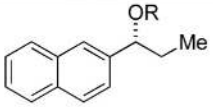	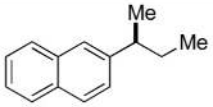		
1	**1** R = Me (96)	**2**	72	94
2[c]	**4** R = Bn (95)	**2**	72	96
3	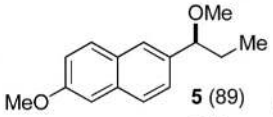 **5** (89)	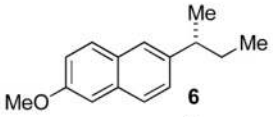 **6**	70	85
4[d]	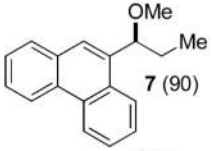 **7** (90)	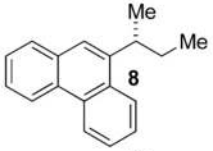 **8**	71	90
5[d]	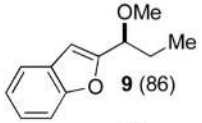 **9** (86)	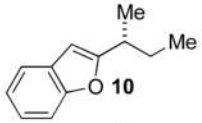 **10**	82	87
6[d]	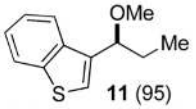 **11** (95)	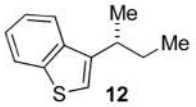 **12**	87	95

[a] %ee determined by SFC. [b] Isolated yield after column chromatography. [c] Reaction run at 35 °C instead of rt. [d] DPEphos used instead of *rac*-BINAP.

Taylor, B. L.; Swift, E. C.; Waetzig, J. D.; Jarvo, E. R. *J. Am. Chem. Soc.* **2011**, *133*, 389–391.

Nickel Catalysis

Jarvo (2012): Enantiospecific arylation of α-aryl ethers

Table 1: Effect of chelating leaving groups.

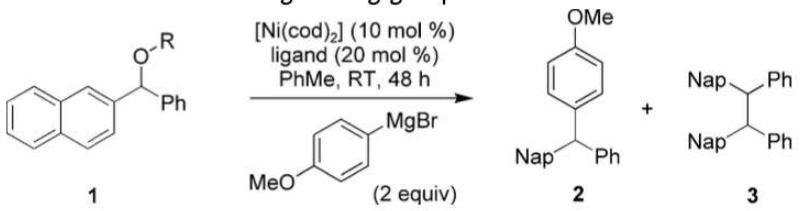

1 2 3

Entry	Ether	R	Ligand	Yield **2** [%][a]	*es* **2** [%][b]	Yield **3** [%][a]
1[c,d]	(*S*)-**1a**	Me	DPEphos	56[e]	33	18[e,f]
2[d]	(±)-**1a**		*rac*-BINAP	<2	–	26
3[d]	(±)-**1a**		dppf	3	–	10
4[d]	(*S*)-**1a**		dppb	14	93	<2
5	(±)-**1b**	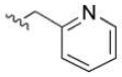	DPEphos	<2	–	<2
6[g]	(±)-**1c**	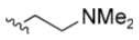	DPEphos	67	–	16
7	(*S*)-**1d**		DPEphos	69[e]	46	17[e,f]
8[d]	(*S*)-**1d**		dppb	67	93	3
9[h]	(*S*)-**1d**		dpppent	73	>99	<2
10[h]	(*S*)-**1d**		dpph	>95	>99	<2
11[h]	(*S*)-**1d**		dppo	84	>99	<2
12[h,i]	(±)-**1d**		$MePh_2P$	12	–	<2
13[h,i]	(*S*)-**1d**		Ph_3P	90	94	5

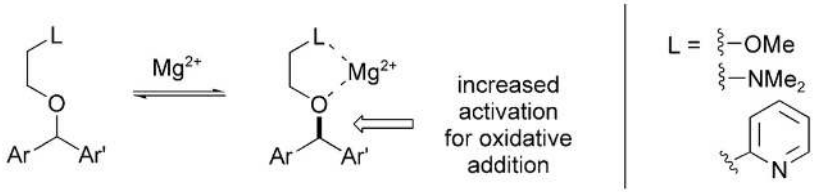

Scheme 2. Design of a chelating leaving group to activate C–O bonds toward oxidative addition

Taylor, B. L. H.; Harris, M. R.; Jarvo, E. R. *Angew. Chem. Int. Ed.* **2012**, *51*, 7790–7793.

Nickel Catalysis

Watson (2013): Enantiospecific Suzuki–Miyaura arylation of α-aryl pivalates

Scheme 2. Scope of Boroxines[a]

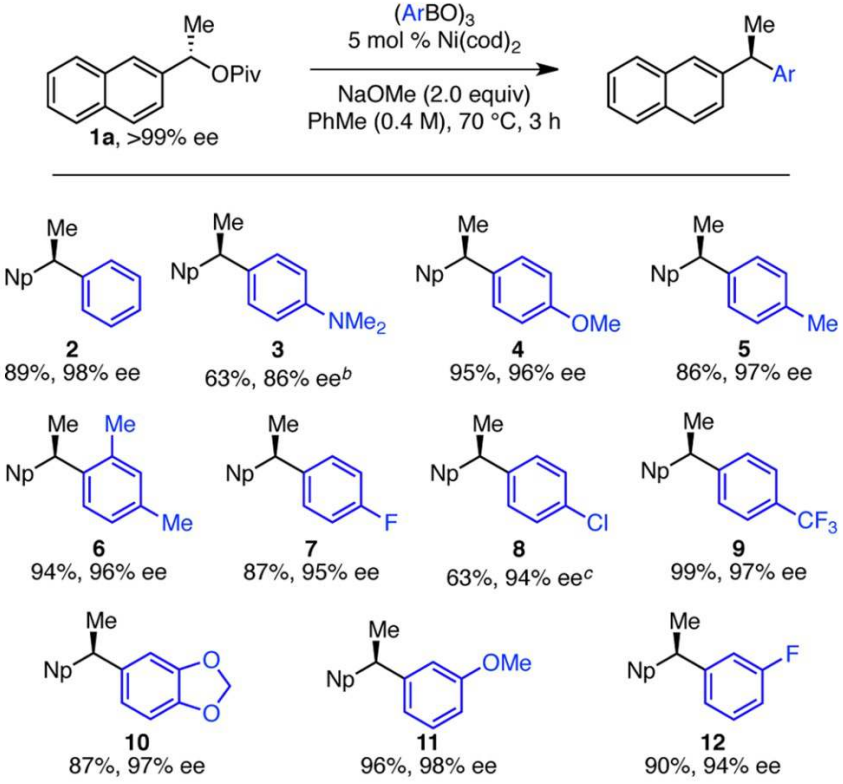

[a]Conditions: pivalate **1a** (0.20 mmol, 1.0 equiv), boroxine (0.83 equiv), $Ni(cod)_2$ (5 mol %), and NaOMe (2.0 equiv) in PhMe (0.4 M) at 70 °C for 3 h, unless otherwise noted. Average isolated yields of duplicate experiments (±0–2%) and average ee's of duplicate experiments (±0–1%) as determined by chiral HPLC are reported. [b]10 mol % $Ni(cod)_2$, 90 °C, 12 h. [c]40 °C, 24 h.

Zhou, Q.; Srinivas, H.; Dasgupta, S.; Watson, M. P. *J. Am. Chem. Soc.* **2013**, *135*, 3307–3310.

Nickel Catalysis

Watson (2013): Enantiospecific Suzuki–Miyaura arylation of α-aryl pivalates

Table 2. Scope of Pivalates[a]

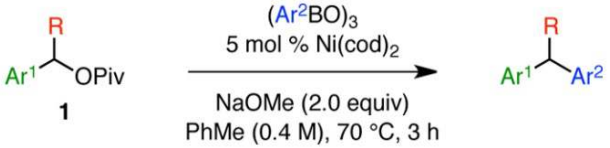

entry	1 (% ee)[b]	Product	yield (%)[c]	ee (%)[d]	es (%)[e]
7[k]	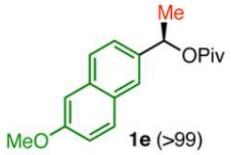 1e (>99)	 19	87	93	≥93
8	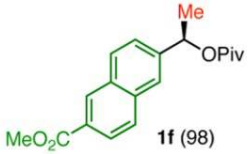 1f (98)	 20	84	94	96
9	 1g (95)	 21	45	89	94
10	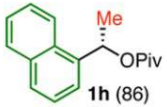 1h (86)	 22	73	73	85
11	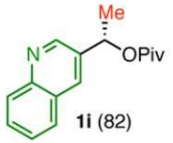 1i (82)	 23	94	58	71
12[l,m]	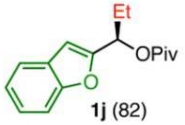 1j (82)	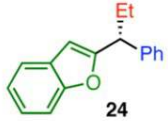 24	49	72	88
13[f,m,n]	 1k (93)	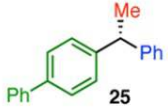 25	33	84	90

Note: all **electrophiles** are π-extended or conjugated π

Zhou, Q.; Srinivas, H.; Dasgupta, S.; Watson, M. P. *J. Am. Chem. Soc.* **2013**, *135*, 3307–3310.

Nickel Catalysis

Watson (2016): Application to quaternary acetates

Scheme 3. Scope of Tertiary Acetates[a]

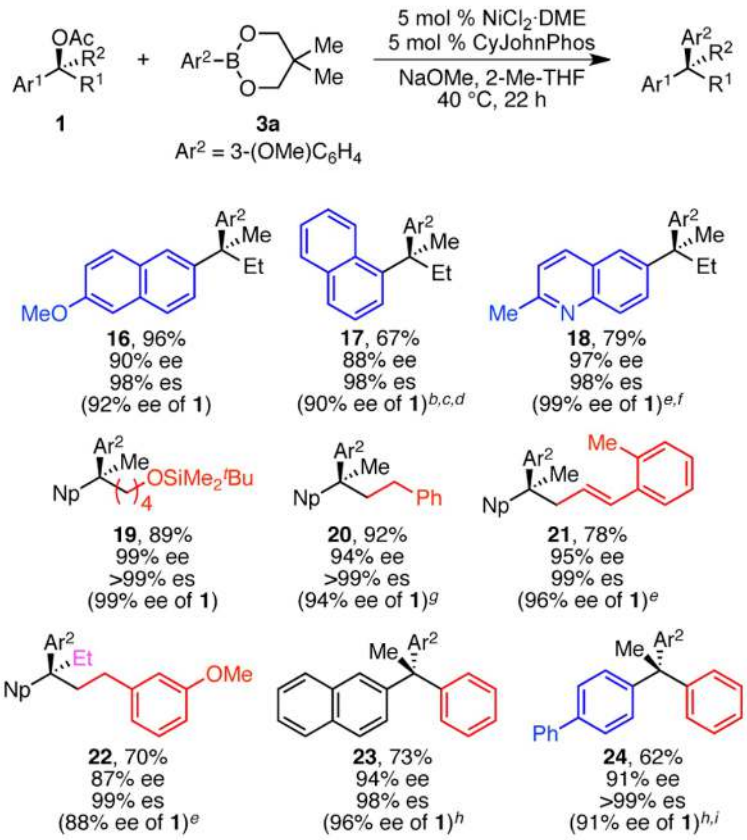

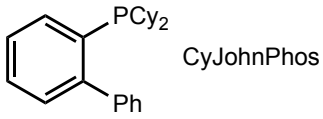

CyJohnPhos

Again: all electrophiles are π-extended or conjugated π

Scheme 4. Putative Catalytic Cycle

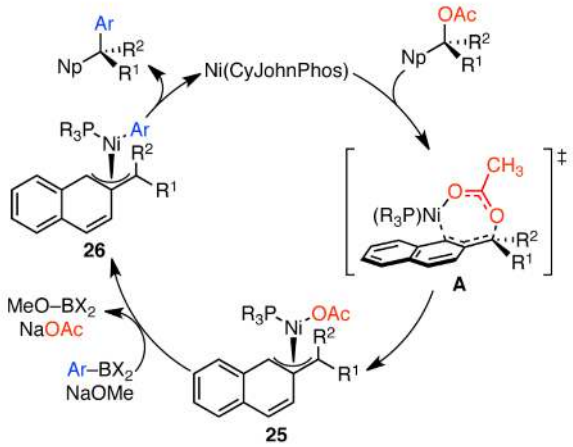

Zhou, Q.; Cobb, K. M.; Tan, T.; Watson, M. P. *J. Am. Chem. Soc.* **2016**, *138*, 12057–12060.

Nickel Catalysis

Carmona (1989): Isolation of benzylic Ni(II) compounds

$$[Ni(cod)_2] + C_6H_5CH_2Cl + 2PMe_3 \longrightarrow [Ni(\eta^1\text{-}CH_2C_6H_5)Cl(PMe_3)_2] + 2cod \quad (1) \quad 60\%$$

$$[Ni(cod)_2] + C_6H_5CH_2Cl + PMe_3 \longrightarrow [Ni(\eta^3\text{-}CH_2C_6H_5)Cl(PMe_3)] + 2cod. \quad (2) \quad 50\%$$

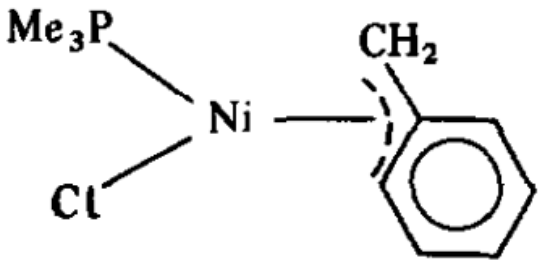

C

Benzylic CH_2 (^{1}H NMR):
η^1 (eq. 1): 1.71 (s, 2H) ppm
η^3 (eq. 2): 1.00 (br s, 2H) ppm

Carmona, E.; Paneque, M.; Poveda, M. L. *Polyhedron* **1989**, *8*, 285–291.

Nickel Catalysis

Martin (2013): Isolation of benzylic Ni(II) compounds

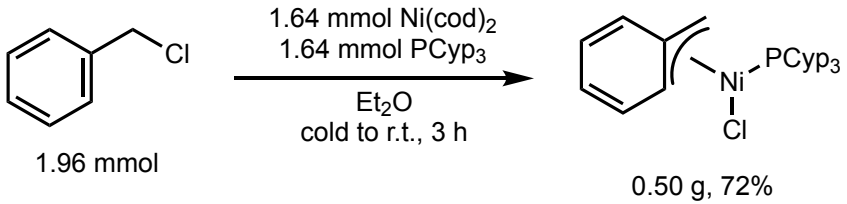

1.96 mmol

0.50 g, 72%

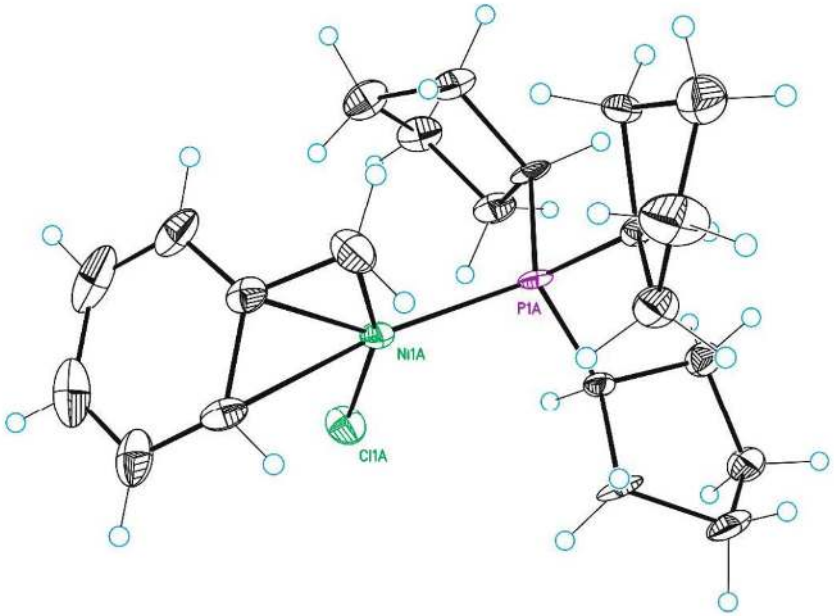

León, T.; Correa, A.; Martin, R. *J. Am. Chem. Soc.* **2013**, *135*, 1221–1224.
See also: Matsubara, R.; Gutierrez, A. C.; Jamison, T. F. *J. Am. Chem. Soc.* **2011**, *133*, 19020–19023.

Nickel Catalysis

Watson (2016): Application to quaternary acetates

Scheme 3. Scope of Tertiary Acetates[a]

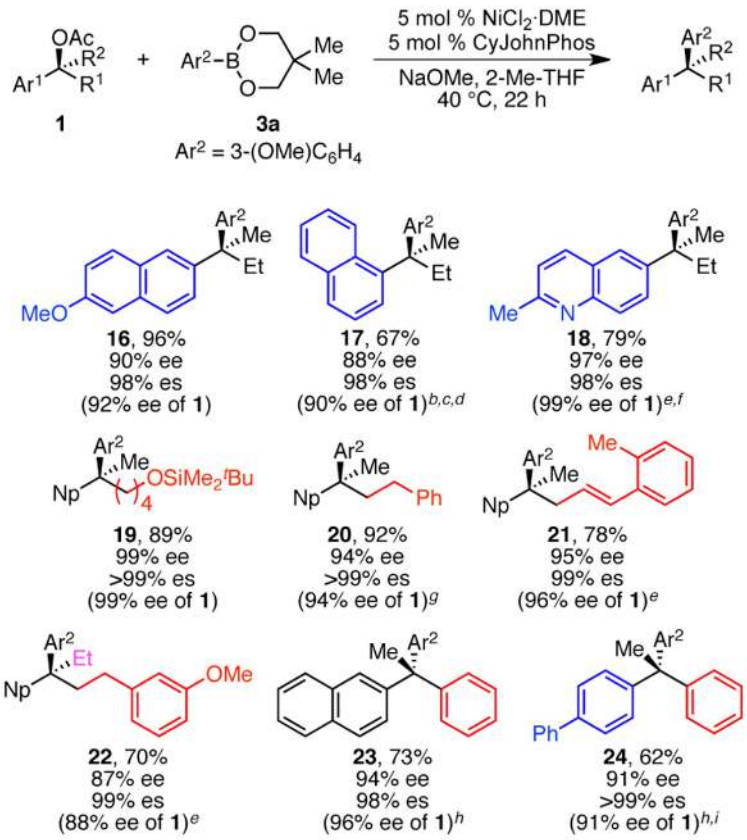

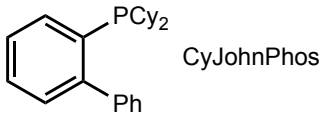

CyJohnPhos

Again: all electrophiles are π-extended or conjugated π

Scheme 4. Putative Catalytic Cycle

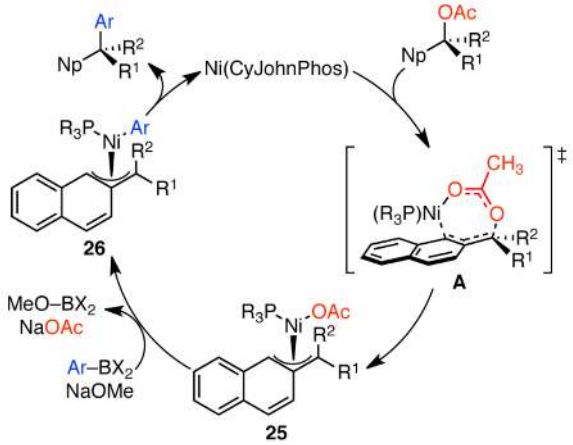

Zhou, Q.; Cobb, K. M.; Tan, T.; Watson, M. P. *J. Am. Chem. Soc.* **2016**, *138*, 12057–12060.

Nickel Catalysis

Jarvo (2013): Enantiospecific Suzuki–Miyaura arylation of α-aryl pivalates (retention or inversion)

Table 1. Optimization of the Reaction Conditions

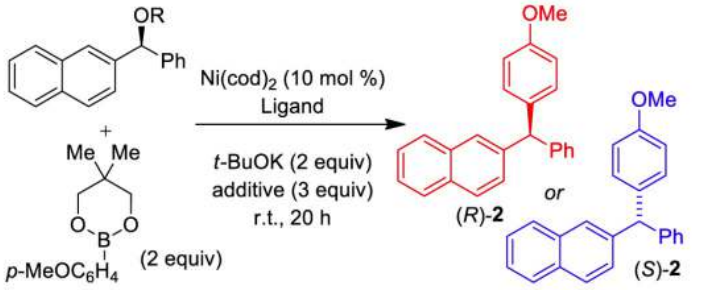

Entry	R	ligand[a]	solvent	additive	% yield[b]	es[c]	retention/ inversion
1	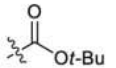 (S)-3	PCy_3	PhMe	none	46	7	retention
2		PCy_3	THF	none	53	43	retention
3		PCy_3	THF	H_2O	74	10	retention
4		PCy_3	THF	*n*-BuOH	76	87	retention
5		PCy_3	THF	*i*-PrOH	46	78	retention
6		PCy_3	THF	*t*-BuOH	55	43	retention
7		PCy_3	THF	F_3CCH_2OH	< 5	na	retention
8	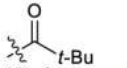 (S)-4	PCy_3	THF	*n*-BuOH	53	76	retention
9		SIMes	THF	*n*-BuOH	60	77	inversion
10	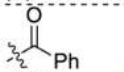 (S)-5	PCy_3	THF	*n*-BuOH	57	91	retention
11		SIMes	THF	*n*-BuOH	83	>99	inversion
12	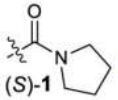 (S)-1	PCy_3	THF	*n*-BuOH	62	95	retention
13		PCy_3	THF/PhMe	none	67	35	retention
14		SIMes	THF/PhMe	none	82	92	inversion
15		**PCy_3**	**THF/PhMe**	***n*-BuOH**	**88**	**99**	**retention**
16		**SIMes**	**THF/PhMe**	***n*-BuOH**	**84**	**99**	**inversion**

[a] PCy_3 (20 mol %); SIMes (11 mol %). [b] Isolated yields after column chromatography. [c] Enantiospecificity (es) = $(ee_{product}/ee_{starting\ material}) \times 100\%$.

Harris, M. R.; Hanna, L. E.; Greene, M. A.; Moore, C. E.; Jarvo, E. R. *J. Am. Chem. Soc.* **2013**, *135*, 3303–3306.

Nickel Catalysis

Jarvo, Houk, Hong (2017): Computational study of retention/inversion mechanism

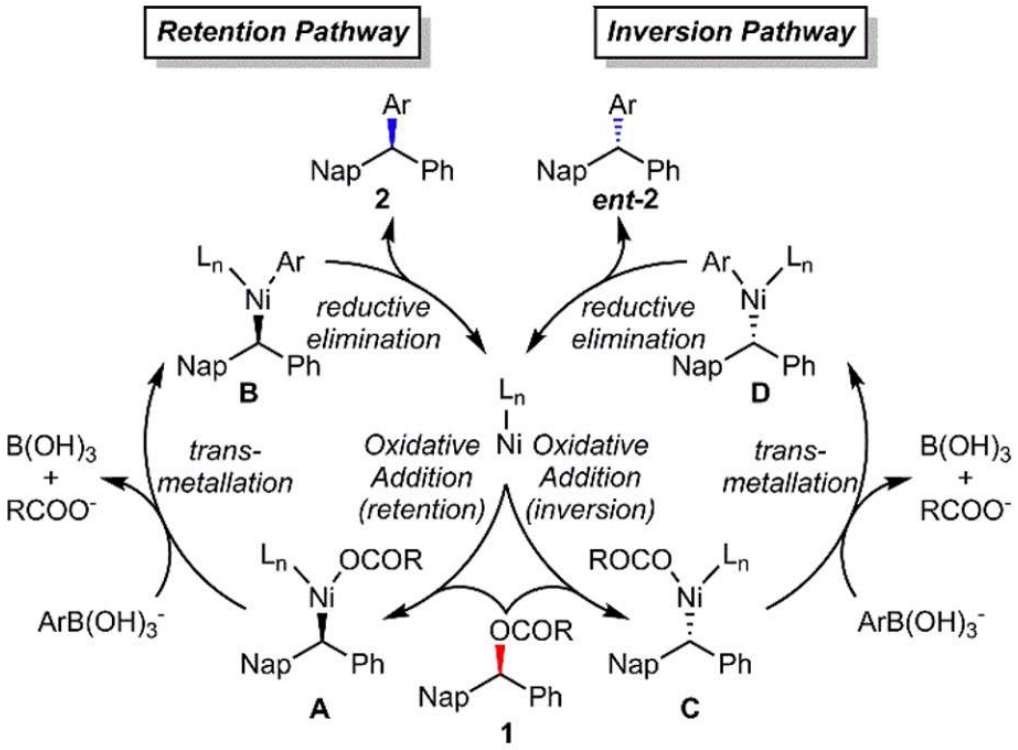

Zhang, S.-Q.; Taylor, B. L. H.; Ji, C.-L.; Gao, Y.; Harris, M. R.; Hanna, L. E.; Jarvo, E. R.; Houk, K. N.; Hong, X. *J. Am. Chem. Soc.* **2017**, *139*, 12994–13005.

Nickel Catalysis

Jarvo, Houk, Hong (2017): Computational study of retention/inversion mechanism

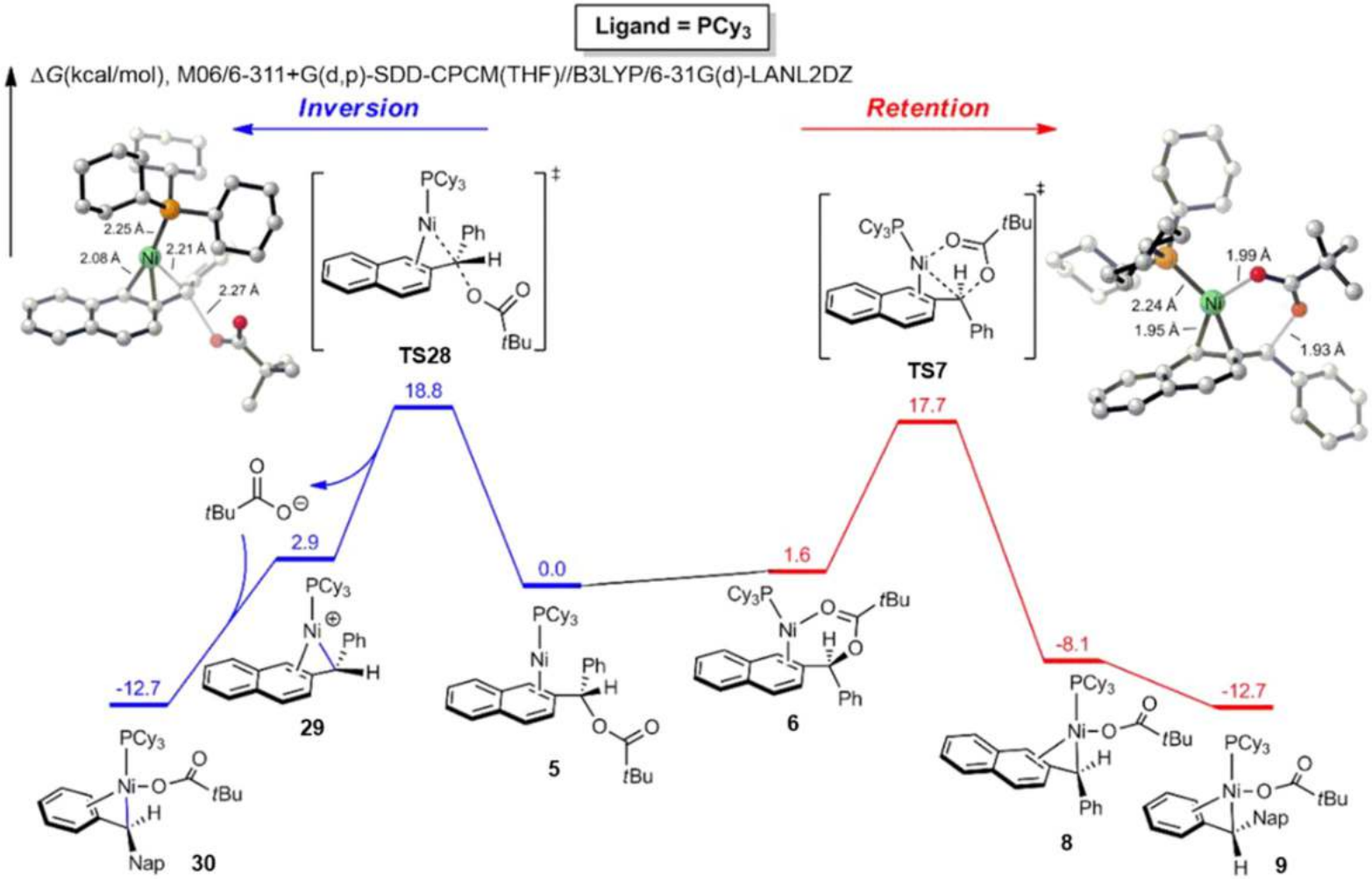

PCy_3: Curtin–Hammett scenario operational

Zhang, S.-Q.; Taylor, B. L. H.; Ji, C.-L.; Gao, Y.; Harris, M. R.; Hanna, L. E.; Jarvo, E. R.; Houk, K. N.; Hong, X. *J. Am. Chem. Soc.* **2017**, *139*, 12994–13005.

Nickel Catalysis

Jarvo, Houk, Hong (2017): Computational study of retention/inversion mechanism

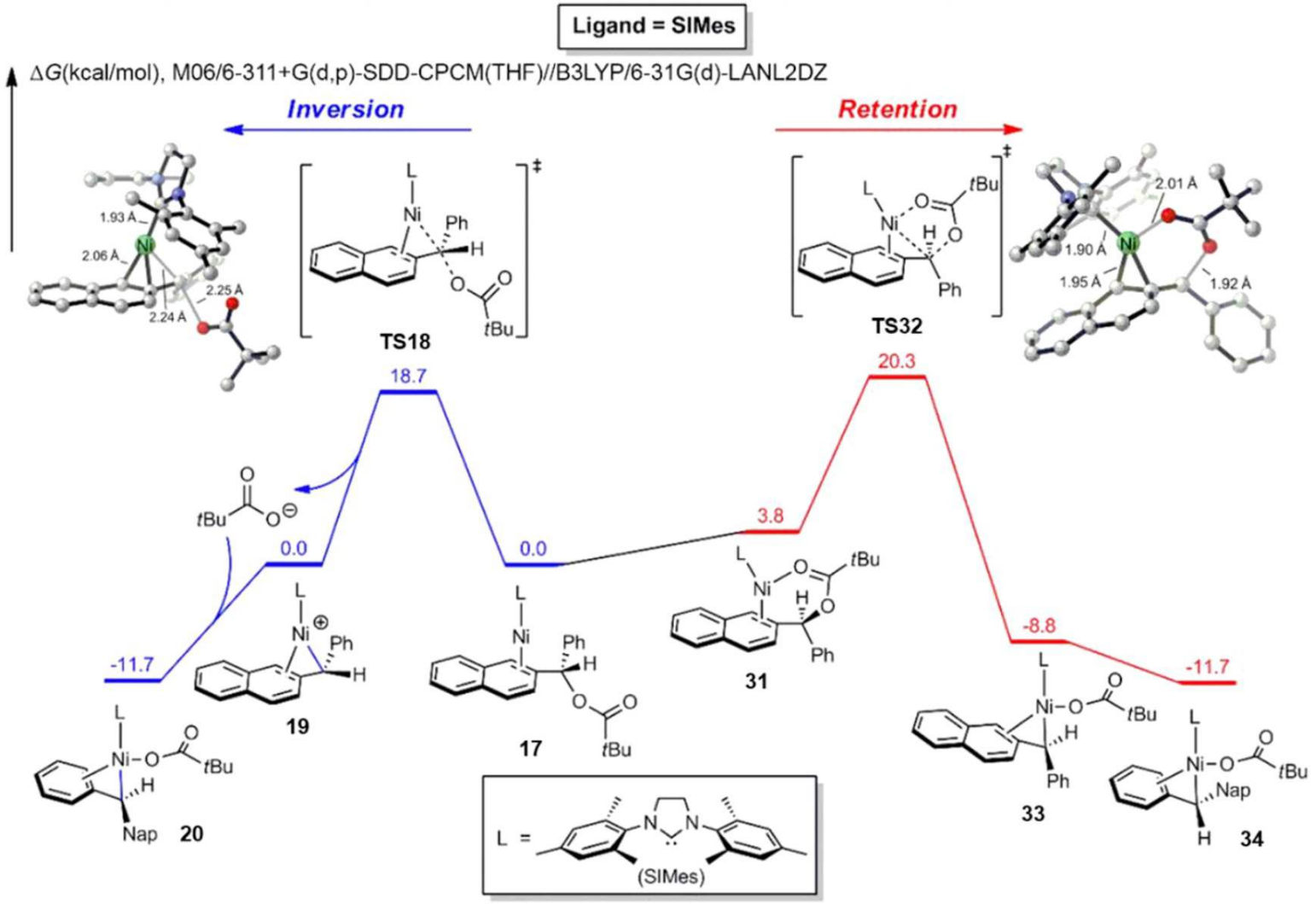

SIMes: Curtin–Hammett scenario *not* operational

Zhang, S.-Q.; Taylor, B. L. H.; Ji, C.-L.; Gao, Y.; Harris, M. R.; Hanna, L. E.; Jarvo, E. R.; Houk, K. N.; Hong, X. *J. Am. Chem. Soc.* **2017**, *139*, 12994–13005.

Nickel Catalysis

Jarvo, Houk, Hong (2017): Computational study of retention/inversion mechanism

**Ground-state analysis*—but early TS in both cases*

PCy_3: Retention occurs

SIMes: Inversion occurs

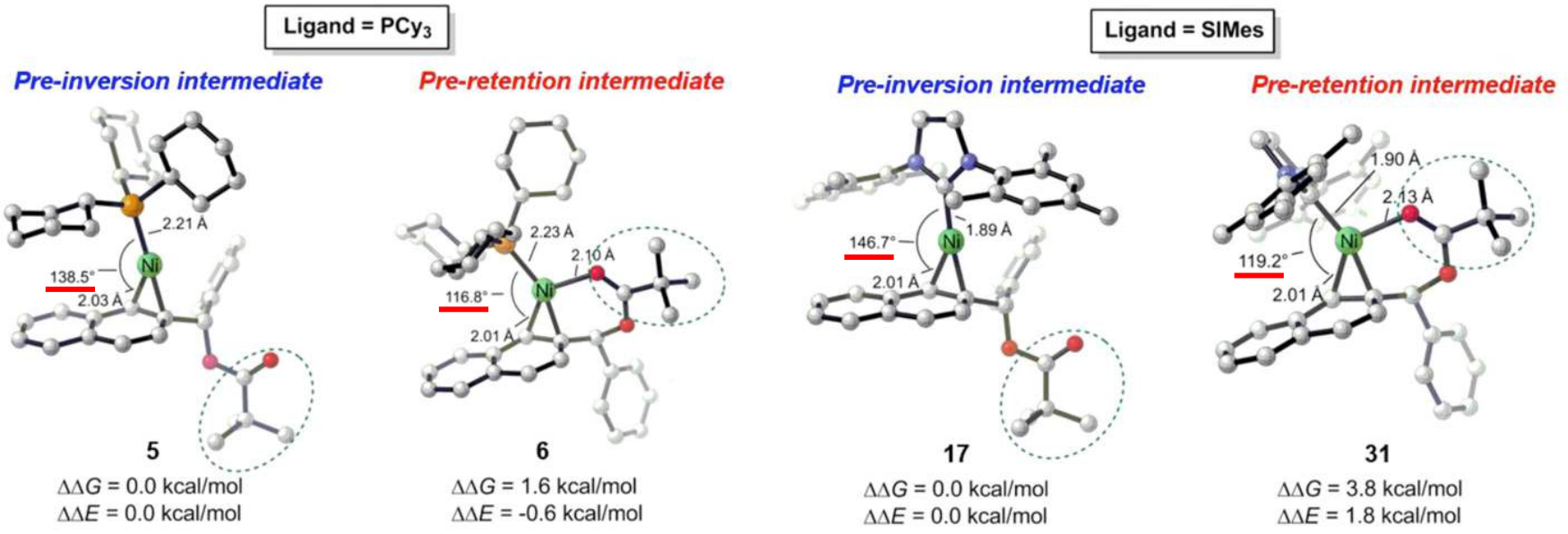

Retention pathway:
Key distortion of (η^2–Ni–L angle)

Zhang, S.-Q.; Taylor, B. L. H.; Ji, C.-L.; Gao, Y.; Harris, M. R.; Hanna, L. E.; Jarvo, E. R.; Houk, K. N.; Hong, X. *J. Am. Chem. Soc.* **2017**, *139*, 12994–13005.

Nickel Catalysis

Jarvo, Houk, Hong (2017): Computational study of retention/inversion mechanism

PCy_3: Retention occurs

SIMes: Inversion occurs

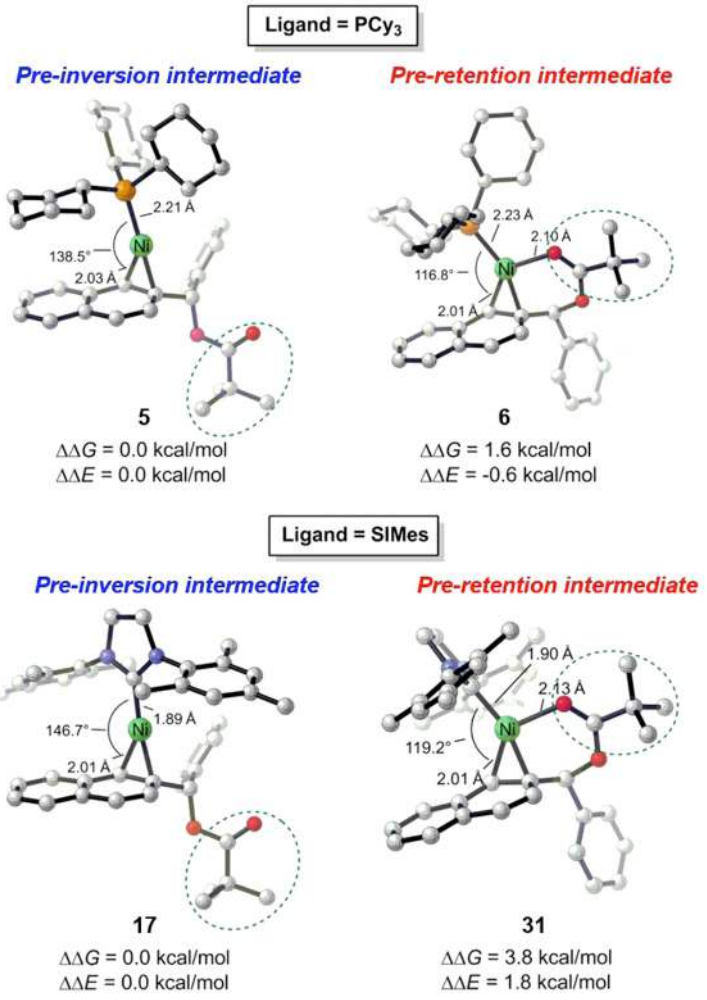

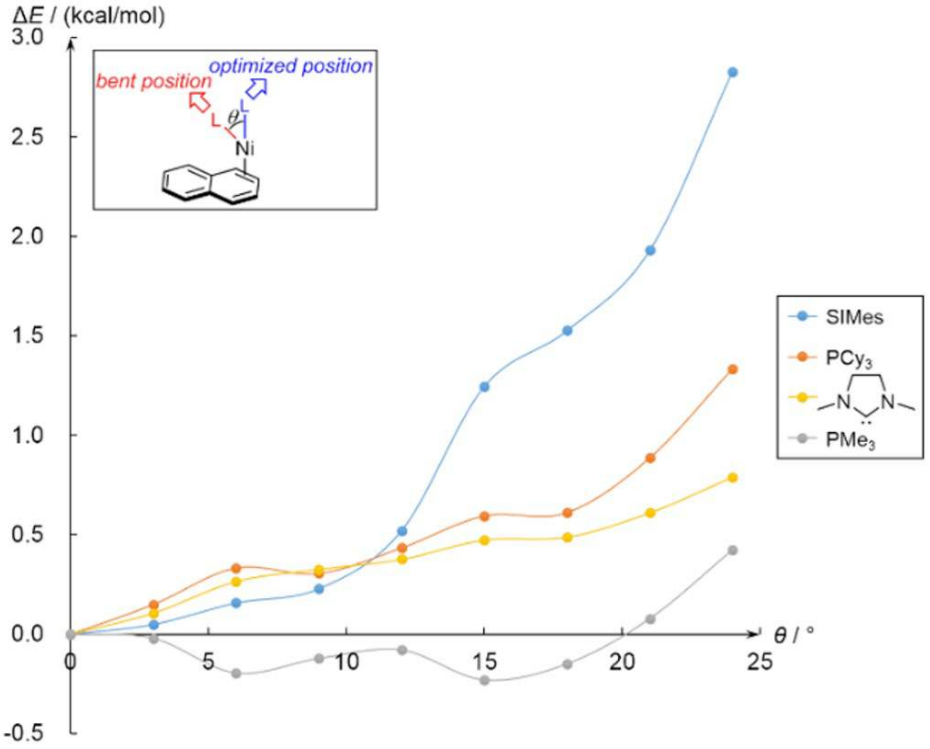

Figure 8. Relative gas phase electronic energies of [LNi(naphthalene)] complexes with different substrate–nickel–ligand angles. θ is the bending angle of ligand from the optimized position to the bent position.

Zhang, S.-Q.; Taylor, B. L. H.; Ji, C.-L.; Gao, Y.; Harris, M. R.; Hanna, L. E.; Jarvo, E. R.; Houk, K. N.; Hong, X. *J. Am. Chem. Soc.* **2017**, *139*, 12994–13005.

Nickel Catalysis

Jarvo, Houk, Hong (2017): Computational study of retention/inversion mechanism

PCy_3: Retention occurs

SIMes: Inversion occurs

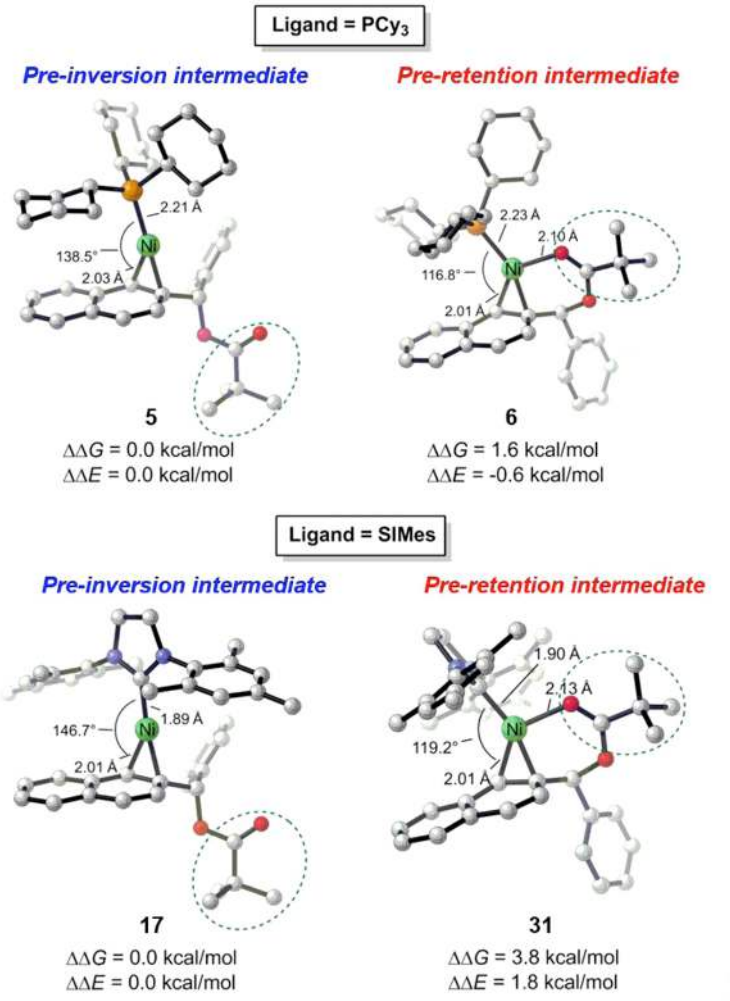

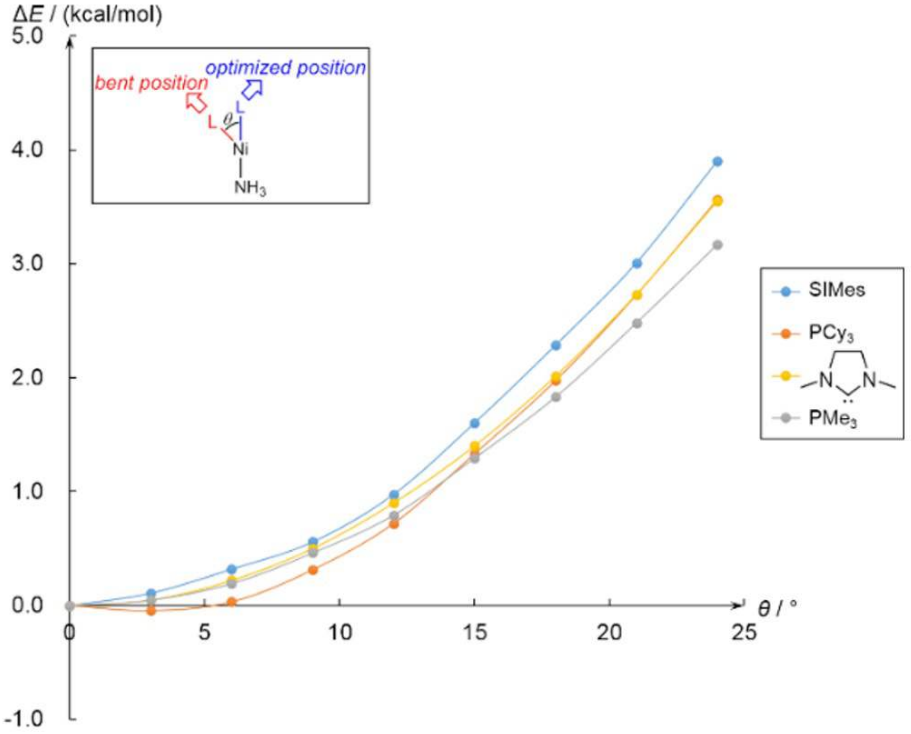

Figure 9. Relative gas phase electronic energies of $[LNi(NH_3)]$ complexes with different substrate–nickel–ligand angles. θ is the bending angle, defined in Figure 8.

Zhang, S.-Q.; Taylor, B. L. H.; Ji, C.-L.; Gao, Y.; Harris, M. R.; Hanna, L. E.; Jarvo, E. R.; Houk, K. N.; Hong, X. *J. Am. Chem. Soc.* **2017**, *139*, 12994–13005.

Nickel Catalysis

Jarvo, Houk, Hong (2017): Computational study of retention/inversion mechanism

PCy_3: Retention occurs

SIMes: Inversion occurs

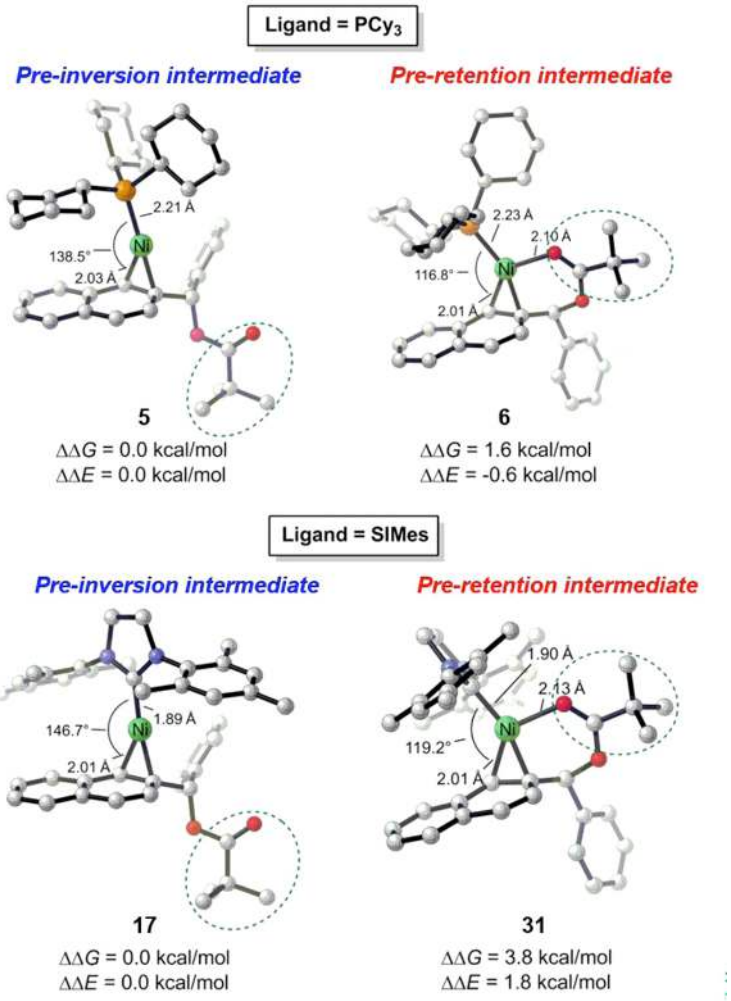

B. Steric effects of ligand

Substrate	$\Delta\Delta G^{\ddagger}$ (PCy_3)	$\Delta\Delta G^{\ddagger}$ ($PtBu_3$)	$\Delta\Delta G^{\ddagger}$ (SIMes)	$\Delta\Delta G^{\ddagger}$ (SIPr)
3	1.1	−3.8	−1.6	−6.2

[a] The computed stereoselectivities are listed as $\Delta\Delta G^{\ddagger} = \Delta G^{\ddagger}(\text{inversion}) - \Delta G^{\ddagger}(\text{retention})$ in kcal/mol.

Zhang, S.-Q.; Taylor, B. L. H.; Ji, C.-L.; Gao, Y.; Harris, M. R.; Hanna, L. E.; Jarvo, E. R.; Houk, K. N.; Hong, X. *J. Am. Chem. Soc.* **2017**, *139*, 12994–13005.

Nickel Catalysis

Watson (2013): Coupling of benzylic ammonium compounds

Table 2. Optimization of Branched Ammonium Salt[a]

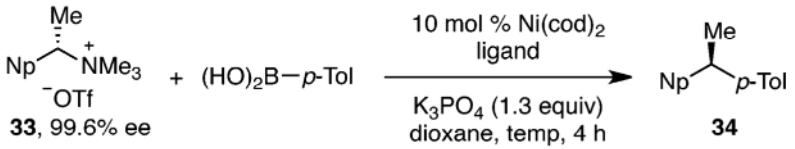

entry	ligand (mol %)	temp (°C)	yield (%)[b]	ee (%)[c]
1	PPh_2Cy (22)	100	84	81
2	$PPhCy_2$ (22)	100	97	79
3	PPh_3 (22)	100	83	81
4	*t*-Bu-XantPhos (12)	100	(91)	98
5	XantPhos (12)	100	15	40
6	P(*o*-Tol)$_3$ (22)	100	71	98
7	P(*o*-Tol)$_3$ (22)	70	94	98
8[d]	P(*o*-Tol)$_3$ (22)	70	95	98
9[e]	none	70	0	n.d.[f]
10[e]	none	100	0	n.d.[f]

[a]Conditions: ammonium triflate **33** (0.10 mmol, 1.0 equiv), boronic acid (1.2 equiv), $Ni(cod)_2$ (10 mol %), ligand, K_3PO_4 (1.3 equiv), dioxane (0.4 M), 4 h, unless noted otherwise. [b]Determined by ^1H NMR analysis using 1,3,5-trimethoxybenzene as internal standard. [c]Determined by chiral HPLC. [d]PhMe replaced dioxane as solvent. [e]No $Ni(cod)_2$ used. [f]n.d. = not determined.

Maity, P.; Shacklady-McAtrr, D. M.; Yap, G. P. A.; Sirianni, E. R.; Watson, M. P. *J. Am. Chem. Soc.* **2013**, *135*, 280–285.

Nickel Catalysis

Watson (2013): Coupling of benzylic ammonium compounds

Table 3. Formation of Enantioenriched Diarylethanes[a]

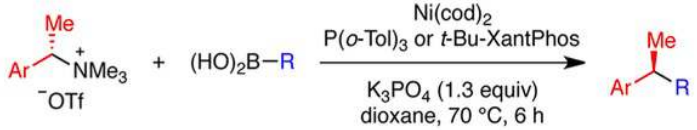

entry	product	mol % Ni	ligand (mol %)	yield (%)[b]	prod ee (%)[c]
1	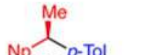 34	3	P(*o*-Tol)$_3$ (7)	60	99
2[d,e]		10	P(*o*-Tol)$_3$ (22)	72	97
3	 35	3	P(*o*-Tol)$_3$ (7)	82	99
4	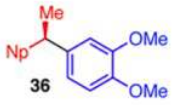 36	3	P(*o*-Tol)$_3$ (7)	51	95
5	 37	3	P(*o*-Tol)$_3$ (7)	68	98
6	 (*S*)-38	10	P(*o*-Tol)$_3$ (22)	(15)	n.d.[f]
7[d,g]		10	P(*o*-Tol)$_3$ (22)	94	98
8[g]	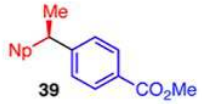 39	10	P(*o*-Tol)$_3$ (22)	71	98
9[d,h]	 40	1	P(*o*-Tol)$_3$ (3)	76	95
10	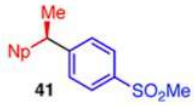 41	3	P(*o*-Tol)$_3$ (7)	94	97
11[d,i]	 42	10	P(*o*-Tol)$_3$ (22)	53	52
12[j]	 43	2	P(*o*-Tol)$_3$ (5)	96	99
13[d,i]		10	P(*o*-Tol)$_3$ (22)	(91)	77
14[d,e,k]	 44	10	*t*-Bu-XantPhos (12)	46	98
15[e]	 (*R*)-38	10	*t*-Bu-XantPhos (12)	37	95
16[e]	 45	15	P(*o*-Tol)$_3$ (32)	56	98
17[e]	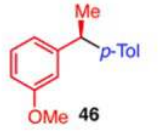 46	15	P(*o*-Tol)$_3$ (32)	54	91

Maity, P.; Shacklady-McAtrr, D. M.; Yap, G. P. A.; Sirianni, E. R.; Watson, M. P. *J. Am. Chem. Soc.* **2013**, *135*, 280–285.

Nickel Catalysis

Watson (2013): Coupling of benzylic ammonium compounds

Scheme 4. Synthesis and Crystal Structure of Oxidative Addition Complex 48[a]

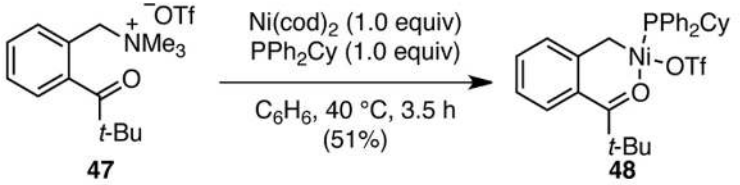

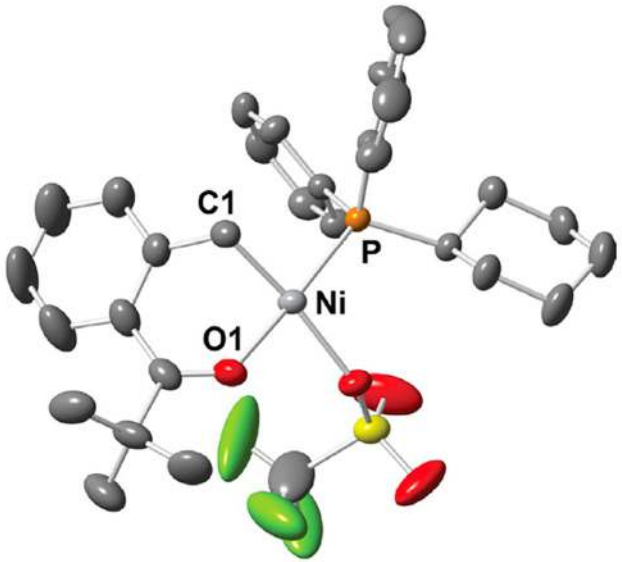

[a]Molecular diagram of **48** with ellipsoids at 30% probability. H-atoms omitted for clarity.

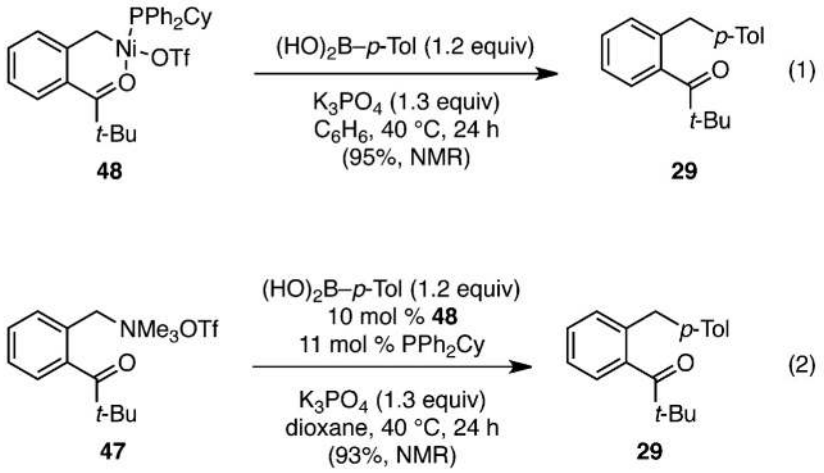

Maity, P.; Shacklady-McAtrr, D. M.; Yap, G. P. A.; Sirianni, E. R.; Watson, M. P. *J. Am. Chem. Soc.* **2013**, *135*, 280–285.

Nickel Catalysis

Watson (2018): Loss of aromaticity according to sterically accessible positions

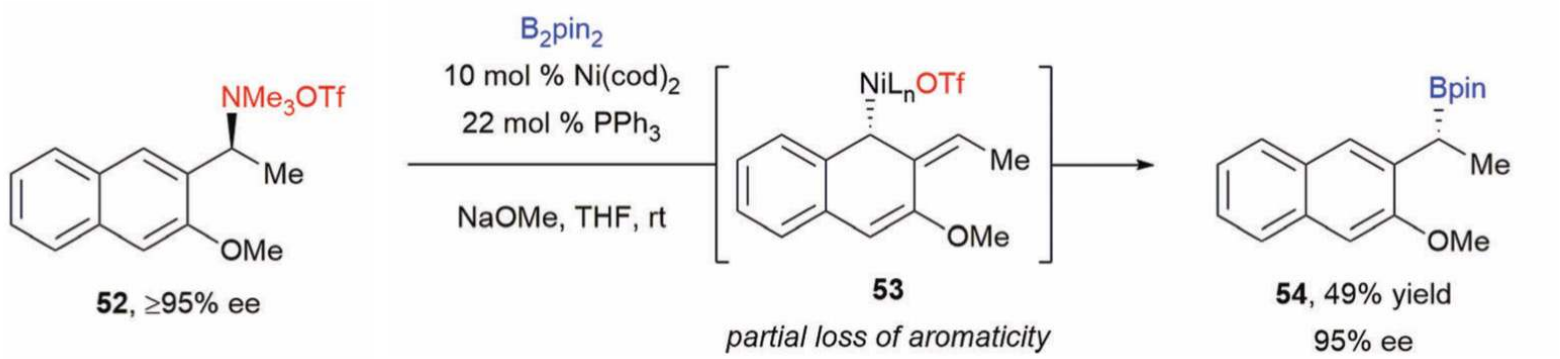

Pound, S. M.; Watson, M. P. *Chem. Commun.* **2018**, *54*, 12286–12301.

Nickel Catalysis

Nambo and Crudden (2018): Coupling of benzylic sulfones

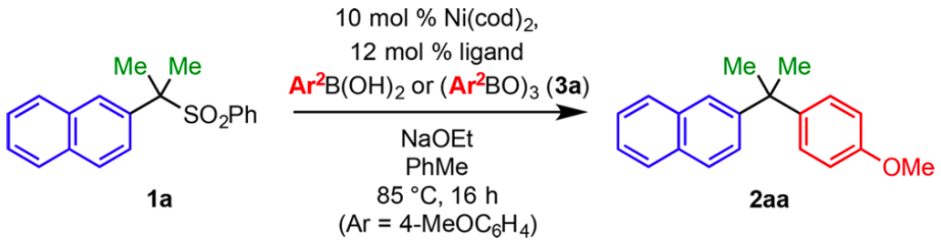

entry	arylboron (equiv)	ligand	NaOEt (equiv)	yield[b]
1	$ArB(OH)_2$ (2.0)	RuPhos (**L1**)	1.5	40%
2	$(ArBO)_3$ (**3a**) (1.0)	**L1**	2.25	86%
3	**3a** (0.7)	BrettPhos (**L2**)	2.2	91%
4[c]	**3a** (0.7)	Doyle (**L3**)	2.2	98%[d]

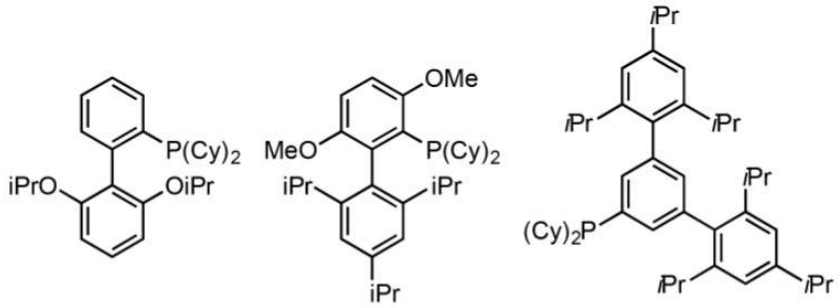

Ariki, Z. T.; Maekawa, Y.; Nambo, M.; Crudden, C. M. *J. Am. Chem. Soc.* **2018**, *140*, 78–81.

Nickel Catalysis

Fu: Halide exchange for benzylic substrates (2013)

Table 1. Influence of Reaction Parameters on the Catalytic Asymmetric Synthesis of a 1,1-Diarylalkane[a]

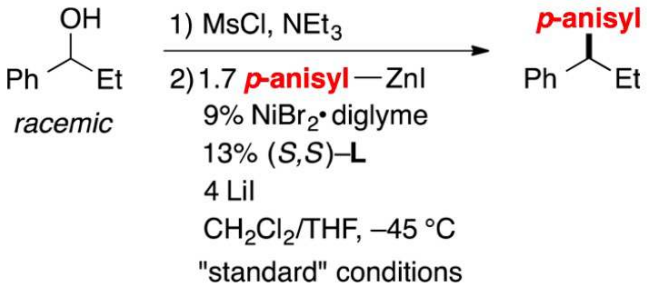

entry	variation from the "standard" conditions	ee (%)	yield (%)[b]
1	none	94	93

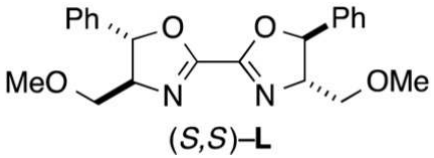

(*S*,*S*)–**L**

Do, H.-Q.; Chandrashekar, E. R. R.; Fu, G. C. *J. Am. Chem. Soc.* **2013**, *135*, 16288–16291.

Nickel Catalysis

Topics in nickel cross-coupling:

Directions in Precatalyst Synthesis

"Inert"/"Nonclassical" C(sp^2)–X Electrophiles Ni(0)/Ni(II)

Benzylic C(sp^3)–X Electrophiles Ni(0)/Ni(II)

X = OR, NR_3X

"Unactivated" C(sp^3)–X Electrophiles Ni(I)/Ni(III)

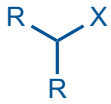

Cross-Electrophile Coupling Ni(0)/Ni(I)/Ni(II)/Ni(III)

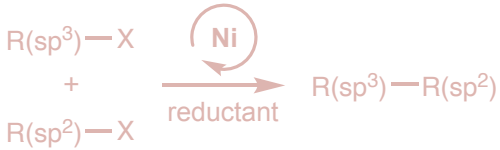

Conjunctive Cross-Coupling (Short)

Nickel Catalysis

Knochel (1995): One of the first nickel-catalyzed C(sp^3)–X cross-coupling reactions

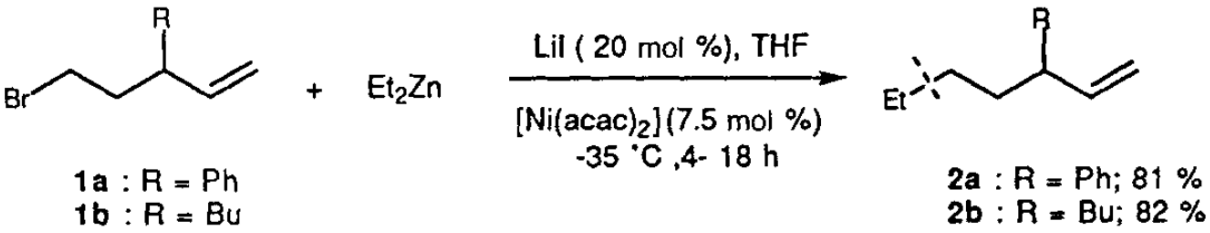

discovery: nickel-catalyzed cross-coupling in presence of alkene

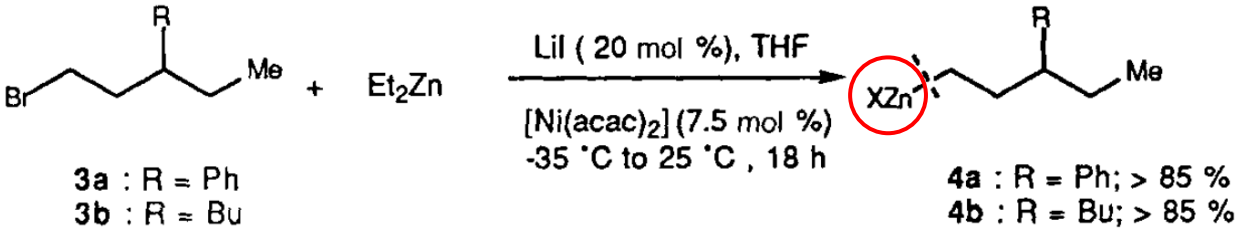

In absence of alkene: only Br–Zn exchange observed

Devasagayaraj, A.; Stüdemann, T.; Knochel, P. *Angew. Chem. Int. Ed. Engl.* **1995**, *34*, 2723–2725.

Nickel Catalysis

Knochel (1995): One of the first nickel-catalyzed C(sp^3)–X cross-coupling reactions

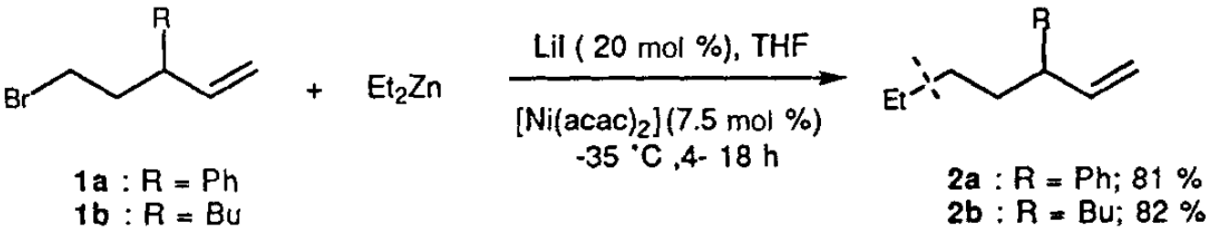

1a : R = Ph
1b : R = Bu

2a : R = Ph; 81 %
2b : R = Bu; 82 %

Proposal:

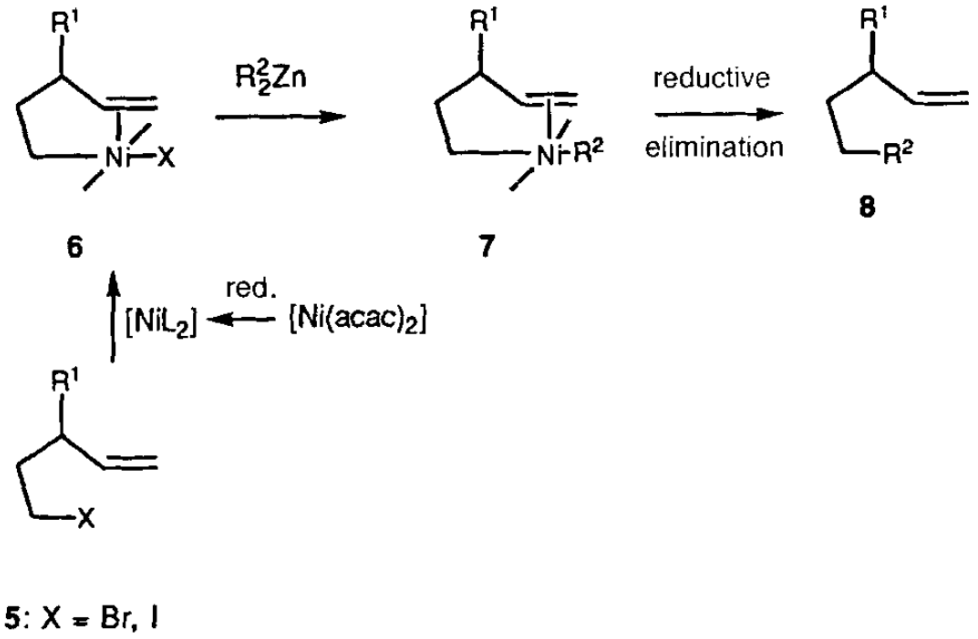

5: X = Br, I

Devasagayaraj, A.; Stüdemann, T.; Knochel, P. *Angew. Chem. Int. Ed. Engl.* **1995**, *34*, 2723–2725.

Nickel Catalysis

Knochel (1995): One of the first nickel-catalyzed C(sp^3)–X cross-coupling reactions

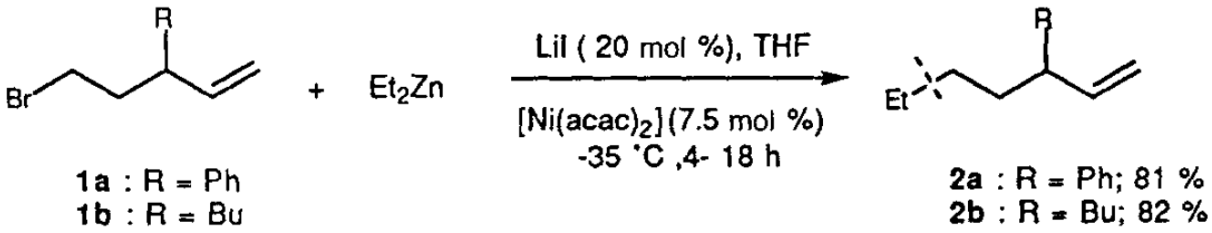

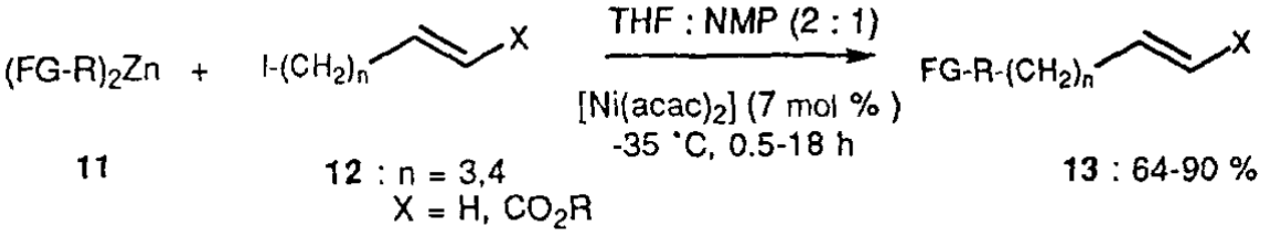

Scheme 3. FG-R = functionalized alkyl group, NMP = *N*-methylpyrrolidinone.

Devasagayaraj, A.; Stüdemann, T.; Knochel, P. *Angew. Chem. Int. Ed. Engl.* **1995**, *34*, 2723–2725.

Nickel Catalysis

Knochel (1998): Use of exogenous alkene as ligand

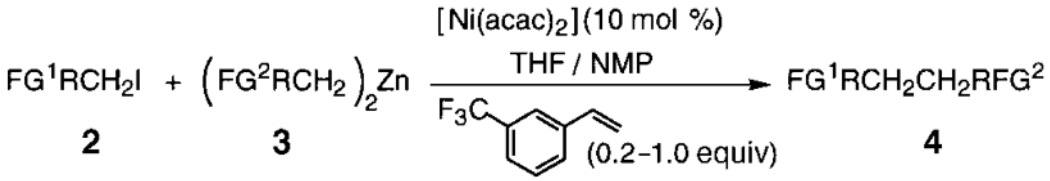

Scheme 1. Cross-coupling between sp^3 carbon centers in the presence of cocatalysts **1a**. FG = functional group; NMP = *N*-methylpyrrolidone.

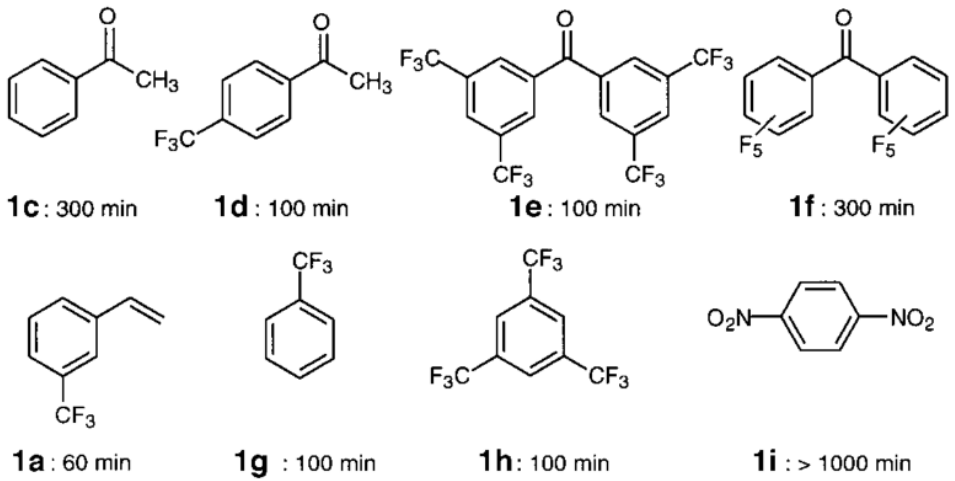

Scheme 5. Different cocatalysts and their influence of the cross-coupling of **2d** with **3a**.

Giovannini, R.; Stüdemann, T.; Dussin, G.; Knochel, P. *Angew. Chem. Int. Ed.* **1998**, *110*, 2449–2502.

Nickel Catalysis

Yamamoto (1997): Reductive elimination promoted by electron-deficient substrate

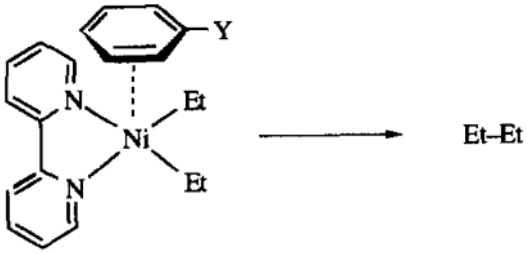

$NiEt_2(bpy)$ is stable in various non-aromatic solvents (e.g. acetone, THF, DMF, CH_3CN, and n-C_6F_{14}) and aromatic solvents without an electron-withdrawing group (e.g. benzene and toluene) at room temperature under N_2. On the other hand, addition of an aromatic compound with the electron-withdrawing group (e.g. C_6H_5CN and $C_6F_5CF_3$) into a solution (e.g. THF solution) of $NiEt_2(bpy)$ leads to the reductive elimination of Et–Et, butane (0.71–0.96 mol/mol $NiEt_2(bpy)$ as determined by gas chromatography). These results suggest

Yamamoto, T.; Abla, M. *J. Organomet. Chem.* **1997**, *535*, 209–211.

Nickel Catalysis

Yamamoto (1997): Reductive elimination promoted by electron-deficient substrate

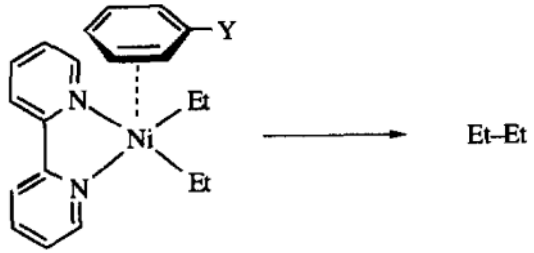

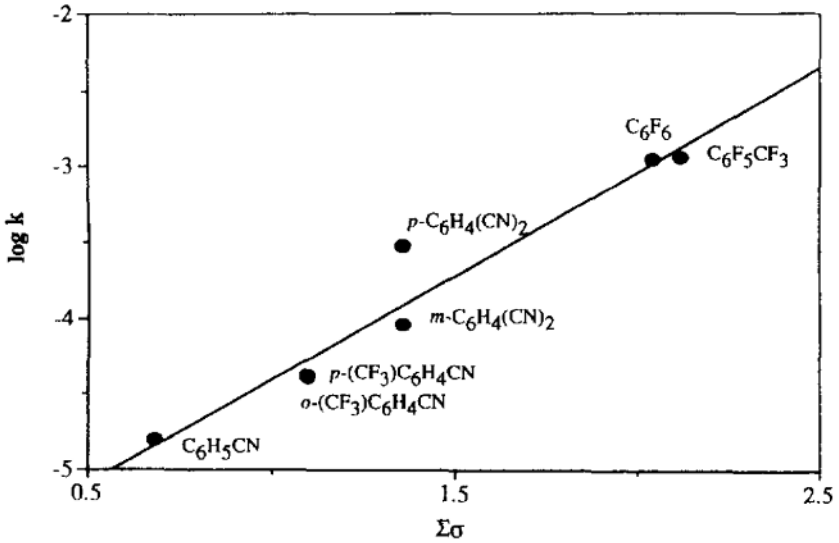

Fig. 3. Plot of $\log k$ (k in $M^{-1}\,s^{-1}$) against $\Sigma\sigma$ at 25°C; σ = Hammett's σ. p-$(CF_3)C_6H_4CN$ and o-$(CF_3)C_6H_4CN$ give almost the same k value.

Yamamoto, T.; Abla, M. *J. Organomet. Chem.* **1997**, *535*, 209–211.

Nickel Catalysis

Fu (2003): Alkyl–alkyl cross-coupling using pybox ligands

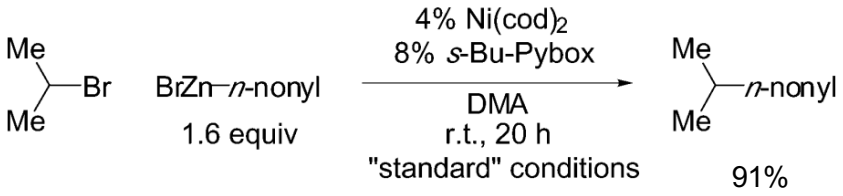

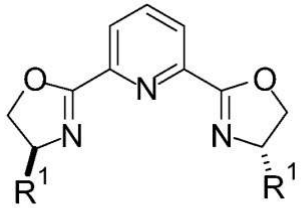

R^1-Pybox

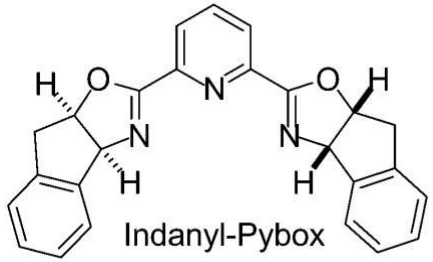

Indanyl-Pybox

Zhou, J.; Fu, G. C. *J. Am. Chem. Soc.* **2003**, *125*, 14726–14727.

Nickel Catalysis

Nickel-catalyzed C(sp^3)–X cross-coupling (Fu)

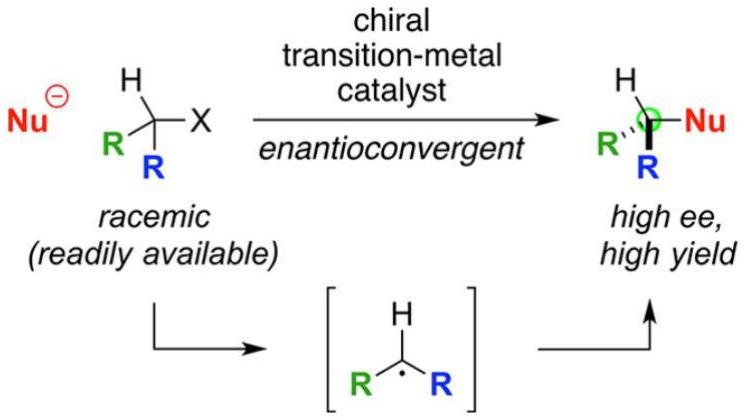

Fu, G. C. *ACS Cent. Sci.* **2017**, *3*, 692–700.

Nickel Catalysis

Examples of nickel-catalyzed C(sp^3)–X cross-coupling

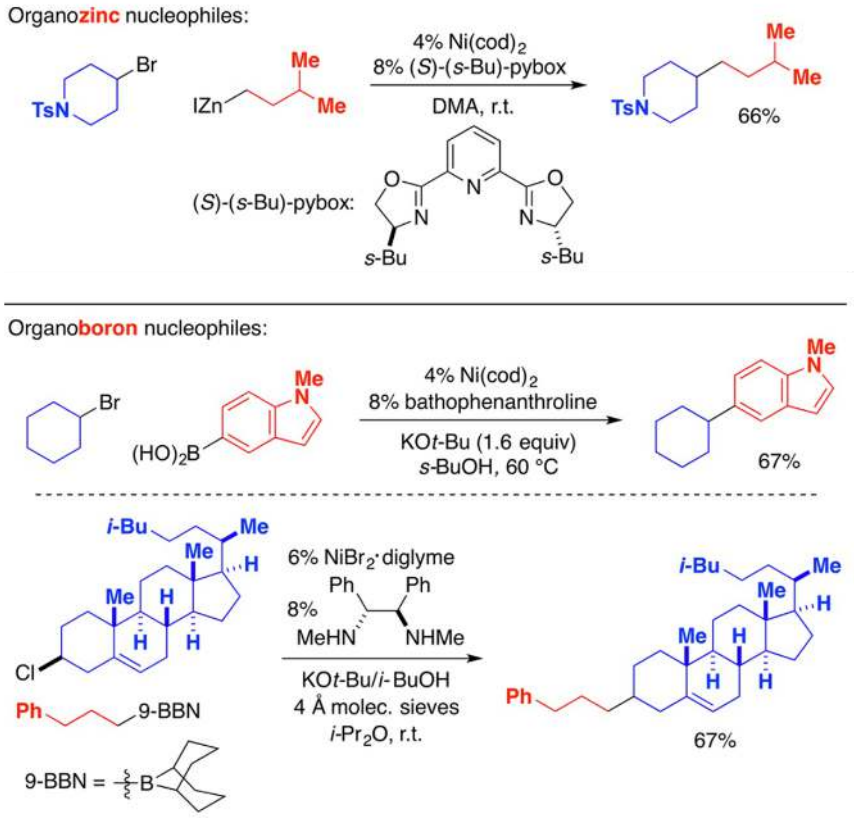

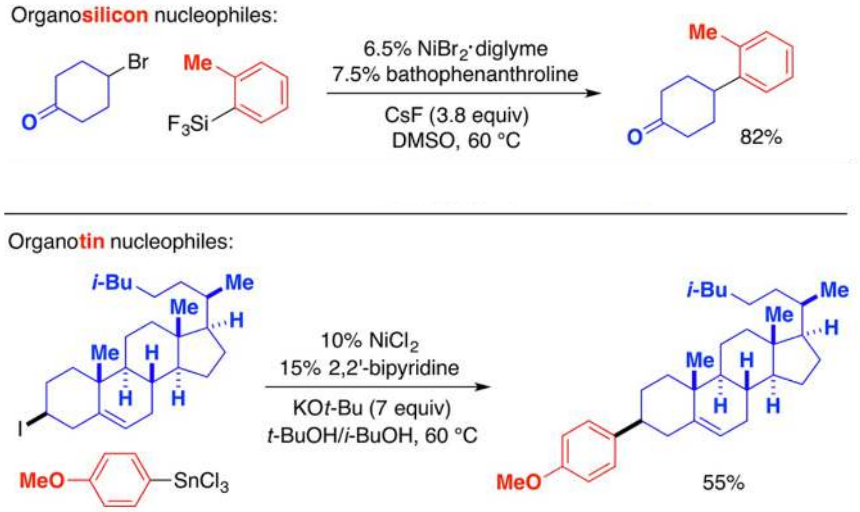

Fu, G. C. *ACS Cent. Sci.* **2017**, *3*, 692–700.

Nickel Catalysis

Examples of enantioconvergent nickel-catalyzed C(sp^3)–X cross-coupling

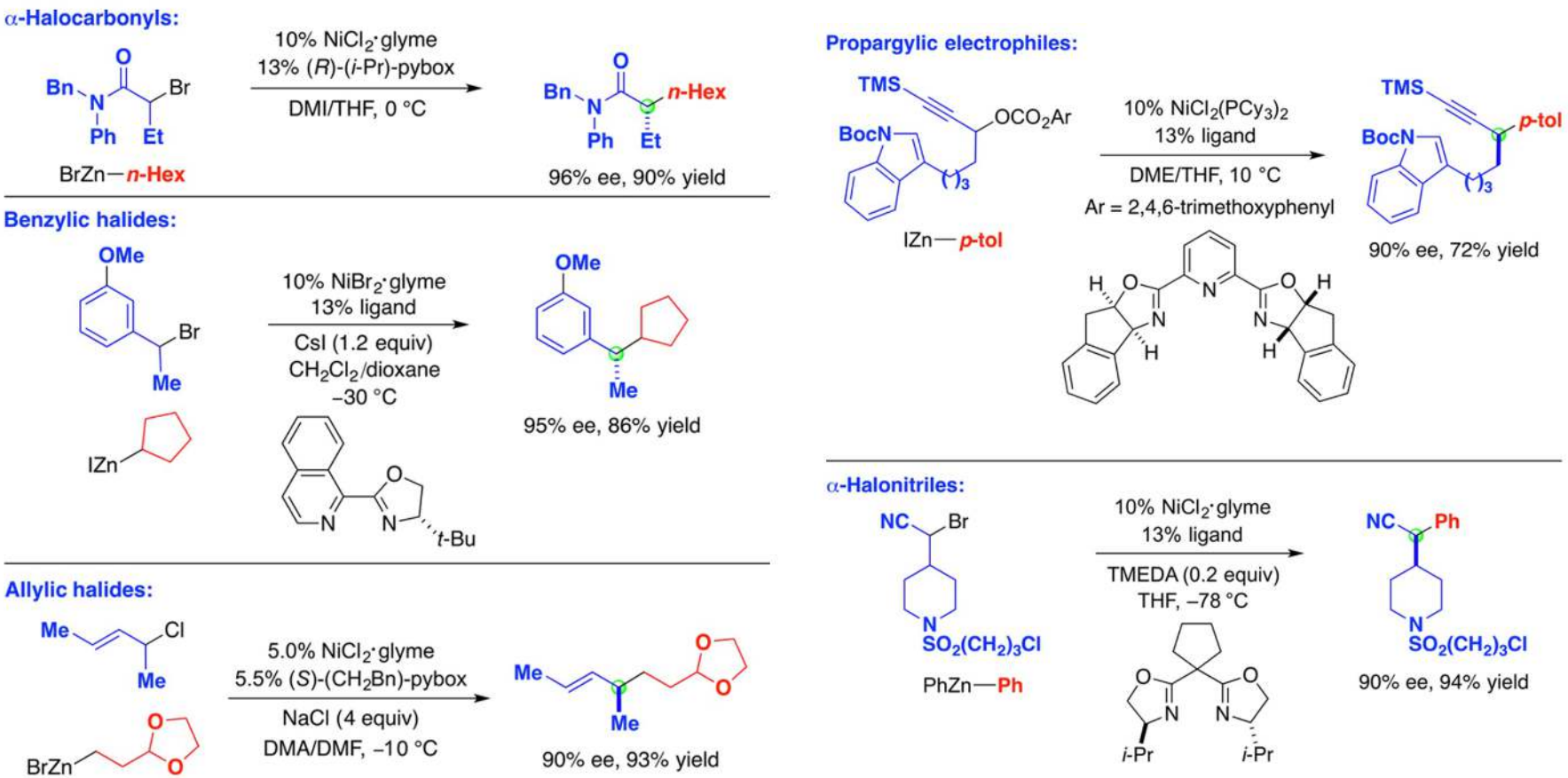

Fu, G. C. *ACS Cent. Sci.* **2017**, *3*, 692–700.

Nickel Catalysis

Vicic, (terpy)Ni–Me (*JACS*, 2004):

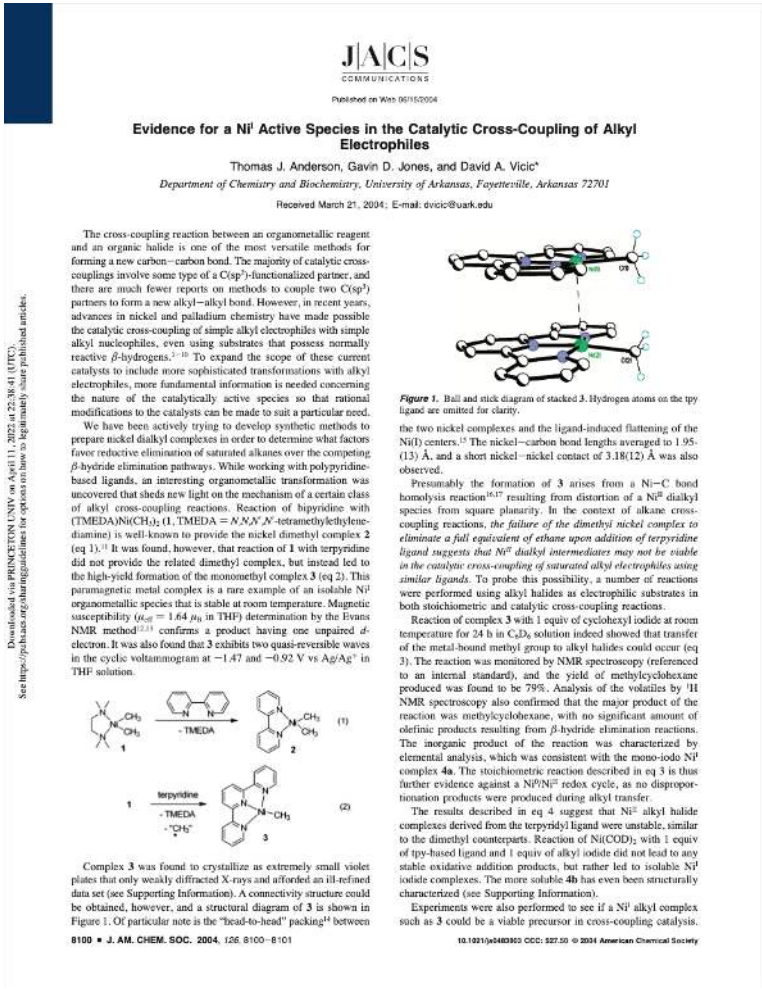

J|A|C|S COMMUNICATIONS

Published on Web 06/15/2004

Evidence for a Ni^{I} Active Species in the Catalytic Cross-Coupling of Alkyl Electrophiles

Thomas J. Anderson, Gavin D. Jones, and David A. Vicic*

Department of Chemistry and Biochemistry, University of Arkansas, Fayetteville, Arkansas 72701

Received March 21, 2004; E-mail: dvicic@uark.edu

Downloaded via PRINCETON UNIV on April 11, 2022 at 22:36:41 (UTC).
See https://pubs.acs.org/sharingguidelines for options on how to legitimately share published articles.

The cross-coupling reaction between an organometallic reagent and an organic halide is one of the most versatile methods for forming a new carbon−carbon bond. The majority of catalytic cross-couplings involve some type of a C(sp^2)-functionalized partner, and there are much fewer reports on methods to couple two C(sp^3) partners to form a new alkyl−alkyl bond. However, in recent years, advances in nickel and palladium chemistry have made possible the catalytic cross-coupling of simple alkyl electrophiles with simple alkyl nucleophiles, even using substrates that possess normally reactive β-hydrogens.[1-10] To expand the scope of these current catalysts to include more sophisticated transformations with alkyl electrophiles, more fundamental information is needed concerning the nature of the catalytically active species so that rational modifications to the catalysts can be made to suit a particular need.

We have been actively trying to develop synthetic methods to prepare nickel dialkyl complexes in order to determine what factors favor reductive elimination of saturated alkanes over the competing β-hydride elimination pathways. While working with polypyridine-based ligands, an interesting organometallic transformation was uncovered that sheds new light on the mechanism of a certain class of alkyl cross-coupling reactions. Reaction of bipyridine with (TMEDA)Ni(CH_3)$_2$ (**1**, TMEDA = *N,N,N′,N′*-tetramethylethylenediamine) is well-known to provide the nickel dimethyl complex **2** (eq 1).[11] It was found, however, that reaction of **1** with terpyridine did not provide the related dimethyl complex, but instead led to the high-yield formation of the monomethyl complex **3** (eq 2). This paramagnetic metal complex is a rare example of an isolable Ni^{I} organometallic species that is stable at room temperature. Magnetic susceptibility (χ_{corr} = 1.64 μ_B in THF) determination by the Evans NMR method[12,13] confirms a product having one unpaired *d*-electron. It was also found that **3** exhibits two quasi-reversible waves in the cyclic voltammogram at −1.47 and −0.92 V vs Ag/Ag^+ in THF solution.

Complex **3** was found to crystallize as extremely small violet plates that only weakly diffracted X-rays and afforded an ill-refined data set (see Supporting Information). A connectivity structure could be obtained, however, and a structural diagram of **3** is shown in Figure 1. Of particular note is the "head-to-head" packing[14] between

Figure 1. Ball and stick diagram of stacked **3**. Hydrogen atoms on the tpy ligand are omitted for clarity.

the two nickel complexes and the ligand-induced flattening of the Ni(I) centers.[15] The nickel−carbon bond lengths averaged to 1.95(13) Å, and a short nickel−nickel contact of 3.18(12) Å was also observed.

Presumably the formation of **3** arises from a Ni−C bond homolysis reaction[16,17] resulting from distortion of a Ni^{II} dialkyl species from square planarity. In the context of alkane cross-coupling reactions, *the failure of the dimethyl nickel complex to eliminate a full equivalent of ethane upon addition of terpyridine ligand suggests that Ni^{II} dialkyl intermediates may not be viable in the catalytic cross-coupling of saturated alkyl electrophiles using similar ligands*. To probe this possibility, a number of reactions were performed using alkyl halides as electrophilic substrates in both stoichiometric and catalytic cross-coupling reactions.

Reaction of complex **3** with 1 equiv of cyclohexyl iodide at room temperature for 24 h in C_6D_6 solution indeed showed that transfer of the metal-bound methyl group to alkyl halides could occur (eq 3). The reaction was monitored by NMR spectroscopy (referenced to an internal standard), and the yield of methylcyclohexane produced was found to be 79%. Analysis of the volatiles by ^{1}H NMR spectroscopy also confirmed that the major product of the reaction was methylcyclohexane, with no significant amount of olefinic products resulting from β-hydride elimination reactions. The inorganic product of the reaction was characterized by elemental analysis, which was consistent with the mono-iodo Ni^{I} complex **4a**. The stoichiometric reaction described in eq 3 is thus further evidence against a Ni^{0}/Ni^{II} redox cycle, as no disproportionation products were produced during alkyl transfer.

The results described in eq 4 suggest that Ni^{II} alkyl halide complexes derived from the terpyridyl ligand were unstable, similar to the dimethyl counterparts. Reaction of Ni(COD)$_2$ with 1 equiv of tpy-based ligand and 1 equiv of alkyl iodide did not lead to any stable oxidative addition products, but rather led to isolable Ni^{I} iodide complexes. The more soluble **4b** has even been structurally characterized (see Supporting Information).

Experiments were also performed to see if a Ni^{I} alkyl complex such as **3** could be a viable precursor in cross-coupling catalysis.

10.1021/ja0483903 CCC: $27.50 © 2004 American Chemical Society

Table 1. Catalytic Alkyl Cross-Coupling Reactions

R-X + *n*-pentylzinc bromide —(3 (5 mol %), THF, 23 h, room temperature)→ R-(CH_2)$_4$-CH_3

entry	alkyl halide	product	yield (%)[a]
1	hexyl-Br	undecane	15
2	Ph(CH_2)$_3$-Br	Ph(CH_2)$_7$-CH_3	13
3	Ph(CH_2)$_3$-I	Ph(CH_2)$_7$-CH_3	60
4	iodocyclohexane	pentylcyclohexane	64
5[b]	iodocyclohexane	pentylcyclohexane	65

[a] Yields based on GC relative to a calibrated internal standard. [b] Catalyst employed was Ni(COD)$_2$ and tpy (both 5 mol %).

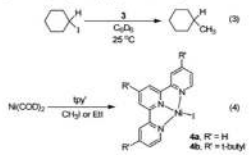

The results of this study are provided in Table 1, and show that, in the presence of a transmetallating agent such as alkylzinc halides, moderate yield formation of cross-coupled alkane could be achieved without any overwhelming formation of β-hydride elimination products. Of note is the greater efficiency of the cross-coupling reaction using alkyl iodides over alkyl bromides. High yields of a product containing a relatively bulky tertiary C(sp^2) center could even be achieved using secondary alkyl halides such as iodocyclohexane as the electrophile. Use of the commercially available starting materials Ni(COD)$_2$ and tpy yielded results (entry 4 vs 5) similar to those seen with **3**. The minor products in the catalysis of alkyl iodides suggest the presence of a radical pathway, as Ph-(CH_2)$_3$Ph and dicyclohexyl were detected for entries 3 and 4, respectively. Additionally, reaction of **3** with the radical clock iodomethylcyclopropane afforded substantial formation of olefinic products as detected by ^{1}H NMR spectroscopy.

In light of the fact that both the Ni^{I} alkyl halide and dialkyl complexes were found to be unstable with respect to their Ni^{I} decomposition products, and the fact that **3** can both transfer its methyl group to alkyl halides to form a Ni^{I} halide complex and to serve as an initiator for catalytic alkyl cross-coupling, we speculate that a radical mechanism of the type shown in Scheme 1 may be operative under catalytic conditions. There are two noteworthy features of the proposed mechanism which we find attractive. First, the 17-electron nickel alkyl complex is thermodynamically capable of reducing alkyl iodides in THF solution. In fact, the reduction potential of **3** is close to that of samarium diiodide, which is a well-known catalyst for alkyl iodide reductions.[18] Second, formation of **4a** after the cross-coupling event allows for the cycle to begin anew in the presence of alkylzinc halide reagents, as transmetalation will provide a new (tpy)NiR complex. A related electron-transfer mechanism has been proposed by Eisenberg and co-workers for

Scheme 1. Possible Mechanism for the Cross-Coupling of Saturated Alkyl Electrophiles Mediated by **3**

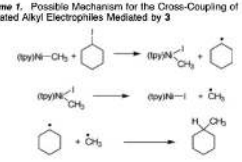

the reduction of alkyl halides by odd-electron rhodium complexes.[19] To our knowledge, this is the first time a Ni^{I} species has been proposed as the *catalytically* active species in the cross-coupling of saturated alkyl groups, and these results build upon the seminal work by Espenson and Kochi, who also observed electron-transfer reactions between organic halides and nickel complexes.[22,23] The results presented here may also be relevant to the cross-coupling chemistry involving other ligands such as those derived from pybox,[4] which are also tricoordinating in nature. A survey of new ligands which may be able to support a similar odd-electron redox shuttle and provide higher yields for catalytic cross-coupling of alkanes is currently being undertaken.

Acknowledgment. D.A.V. thanks the University of Arkansas, the Arkansas Biosciences Institute, and NIH (RR-15569) for support of this work.

Supporting Information Available: General methods and X-ray data for all relevant compounds (PDF, CIF). This material is available free of charge via the Internet at http://pubs.acs.org.

References

(1) Zhou, J.; Fu, G. C. *J. Am. Chem. Soc.* **2003**, *125*, 12527−12530.
(2) Terao, J.; Watanabe, H.; Ikumi, A.; Kuniyasu, H.; Kambe, N. *J. Am. Chem. Soc.* **2002**, *124*, 4222−4223.
(3) Cardenas, D. J. *Angew. Chem., Int. Ed.* **2003**, *42*, 384−387.
(4) Netherton, M. R.; Dai, C.; Neuschuetz, K.; Fu, G. C. *J. Am. Chem. Soc.* **2001**, *123*, 10099−10100.
(5) Kirchhoff, J. H.; Netherton, M. R.; Hills, I. D.; Fu, G. C. *J. Am. Chem. Soc.* **2002**, *124*, 13662−13663.
(6) Giovannini, R.; Studemann, T.; Dussin, G.; Knochel, P. *Angew. Chem., Int. Ed.* **1998**, *37*, 2387−2390.
(7) Giovannini, R.; Studemann, T.; Devasagayaraj, A.; Dussin, G.; Knochel, P. *J. Org. Chem.* **1999**, *64*, 3544−3553.
(8) Jensen, A. E.; Knochel, P. *J. Org. Chem.* **2002**, *67*, 79−85.
(9) Zhou, J.; Fu, G. C. *J. Am. Chem. Soc.* **2003**, *125*, 14726−14727.
(10) Zhou, J.; Fu, G. C. *J. Am. Chem. Soc.* **2004**, *126*, 1340−1341.
(11) Yamamoto, T.; Yamamoto, A.; Ikeda, S. *J. Am. Chem. Soc.* **1971**, *93*, 3350−9.
(12) Evans, D. F. *J. Chem. Soc.* **1959**, 2003−2005.
(13) Sur, S. K. *J. Magn. Reson.* **1989**, *82*, 169−73.
(14) Wong, Y.-S.; Lippard, S. J. *J. Chem. Soc., Chem. Commun.* **1977**, 824−825.
(15) Brunner, H.; Dormeier, S.; Grau, I.; Zabel, M. *Eur. J. Inorg. Chem.* **2002**, 2603−2613.
(16) Schofield, M. H.; Halpern, J. *Inorg. Chim. Acta* **2003**, *345*, 353−358.
(17) Holland, P. L.; Cundari, T. R.; Perez, L. L.; Eckert, N. A.; Lachicotte, R. J. *J. Am. Chem. Soc.* **2002**, *124*, 14416−14424.
(18) Prasad, E.; Flowers, R. A. *J. Am. Chem. Soc.* **2002**, *124*, 6895−6899.
(19) Sofranko, J. A.; Eisenberg, R.; Kampmeier, J. A. *J. Am. Chem. Soc.* **1979**, *101*, 1042−1044.
(20) Bakac, A.; Espenson, J. H. *J. Am. Chem. Soc.* **1986**, *108*, 719−723.
(21) Morrell, D. G.; Kochi, J. K. *J. Am. Chem. Soc.* **1975**, *97*, 7262−7270.

JA0483903

Anderson, T. J.; Jones, G. D.; Vicic, D. A. *J. Am. Chem. Soc.* **2004**, *126*, 8100–8101.

Nickel Catalysis

Vicic, (terpy)Ni–Me (2004)

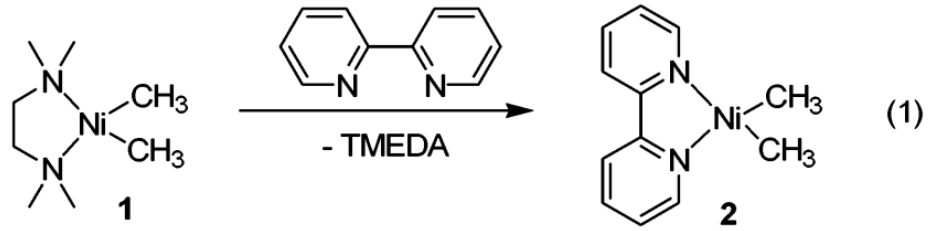

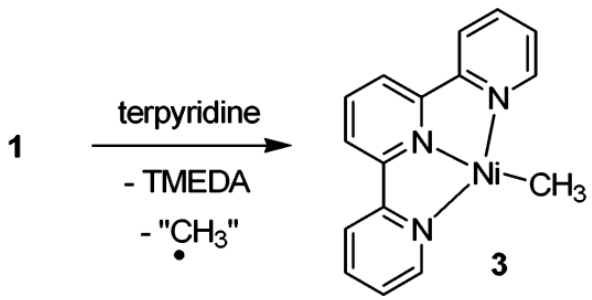

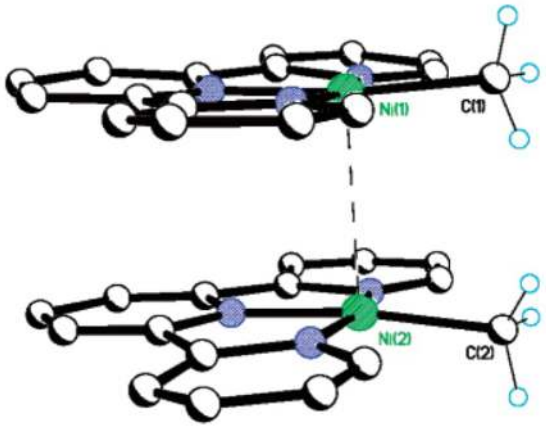

Anderson, T. J.; Jones, G. D.; Vicic, D. A. *J. Am. Chem. Soc.* **2004**, *126*, 8100–8101.

Nickel Catalysis

Vicic, (terpy)Ni–Me (2004)

Chart 1. Representations of **2a** as a Ni(I)−Methyl Complex (left) and the Charge-Transfer State Comprising a Ni(II)−Alkyl Cation (right)

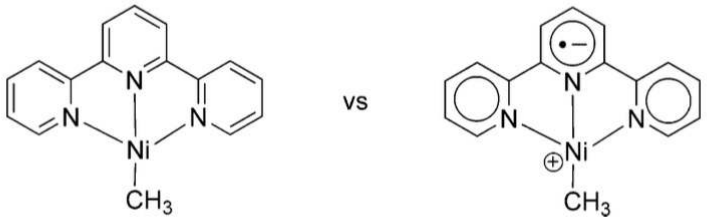

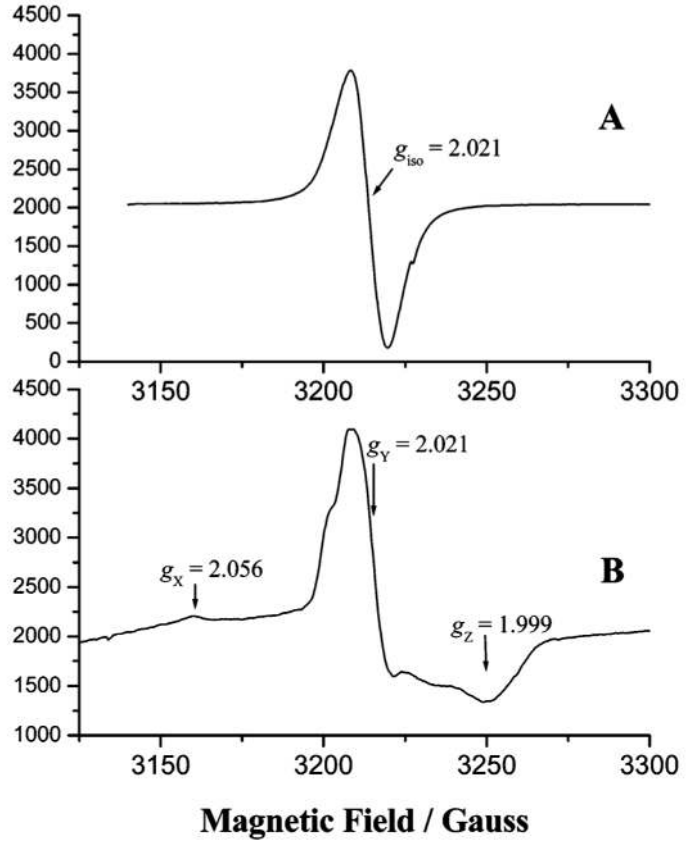

Figure 1. X-band EPR spectra of **2a** in THF (a) in fluid solution at room temperature, (b) in frozen glass at 77 K. Parameters: microwave frequency 9.095 GHz; microwave power 5 mW; modulation amplitude 1 G; gain 2×10^3.

Radical in extended π-system: g = 2.003–2.005
4-coordinate Ni(I): g = 2.18

Jones, G. D.; Martin, J. L.; McFarland, C.; Allen, O. R.; Hall, R. E.; Haley, A. D.; Brandon, R. J.; Konovalova, T.; Desrochers, P. J.; Pulay, P.; Vicic, D. A. *J. Am. Chem. Soc.* **2006**, *128*, 13175–13183.

Nickel Catalysis

Vicic, (terpy)Ni–Me (2004)

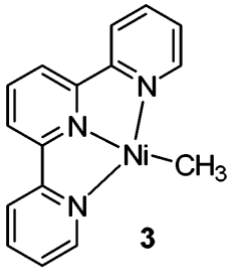

3

Table 1. Catalytic Alkyl Cross-Coupling Reactions

R-X + *n*-pentylzinc bromide —(**3** (5 mol %); THF, 23 h; room temperature)→ R-$(CH_2)_4$-CH_3

entry	alkyl halide	product	yield (%)[a]
1	hexyl-Br	undecane	15
2	$Ph(CH_2)_3Br$	$Ph(CH_2)_7CH_3$	13
3	$Ph(CH_2)_3I$	$Ph(CH_2)_7CH_3$	60
4	iodocyclohexane	pentylcyclohexane	64
5[b]	iodocyclohexane	pentylcyclohexane	65

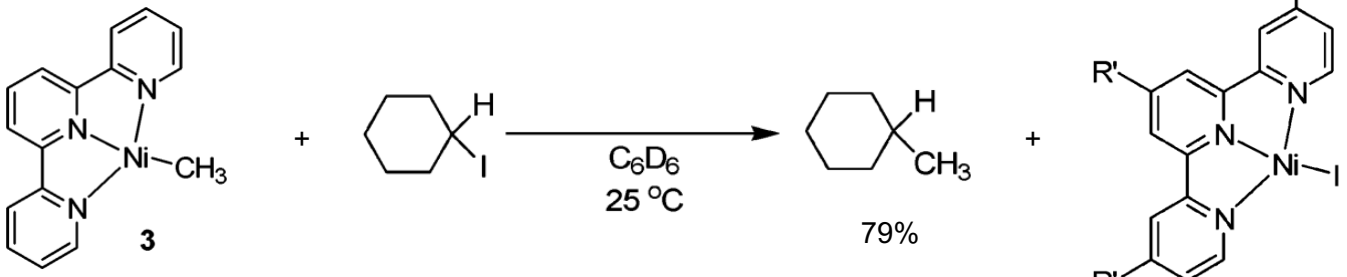

major inorganic product (R' = H)

Anderson, T. J.; Jones, G. D.; Vicic, D. A. *J. Am. Chem. Soc.* **2004**, *126*, 8100–8101; Jones, G. D.; McFarland, C.; Anderson, T. J.; Vicic, D. A. *Chem. Commun.* **2005**, 4211–4213.

Nickel Catalysis

Fu: Mechanistic study of C(sp^3)–Br Negishi cross-coupling

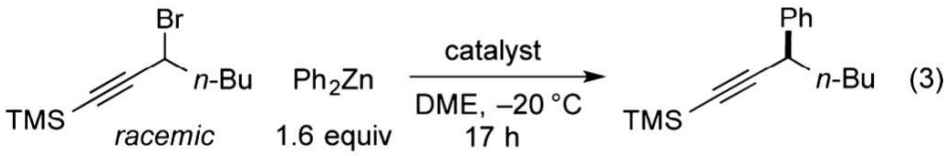

catalyst	
3.0% $NiBr_2$ • DME/3.9% (–)-indanyl-pybox	*76% yield, 85% ee*
3.0% $NiBr_2$ • DME/3.9% (–)-*i*-Pr-pybox	*77% yield, 82% ee*
3.0% ((–)-*i*-Pr-pybox)$NiBr_2$	*72% yield, 81% ee*

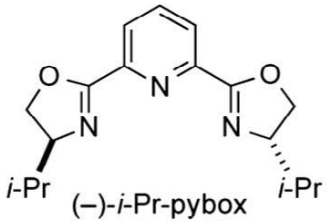

(–)-*i*-Pr-pybox

Schley, N. D.; Fu, G. C. *J. Am. Chem. Soc.* **2014**, *136*, 16588–16593.

Nickel Catalysis

Fu: Mechanistic study of C(sp^3)–Br Negishi cross-coupling

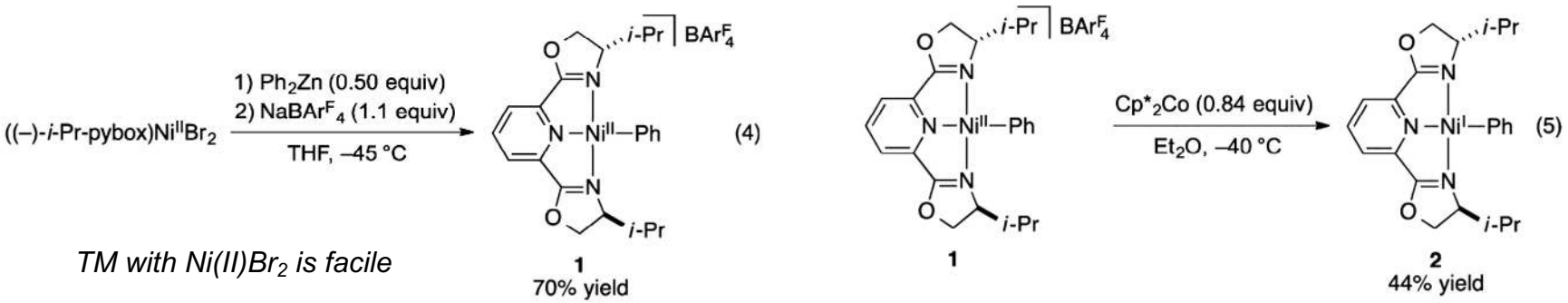

TM with Ni(II)Br_2 is facile

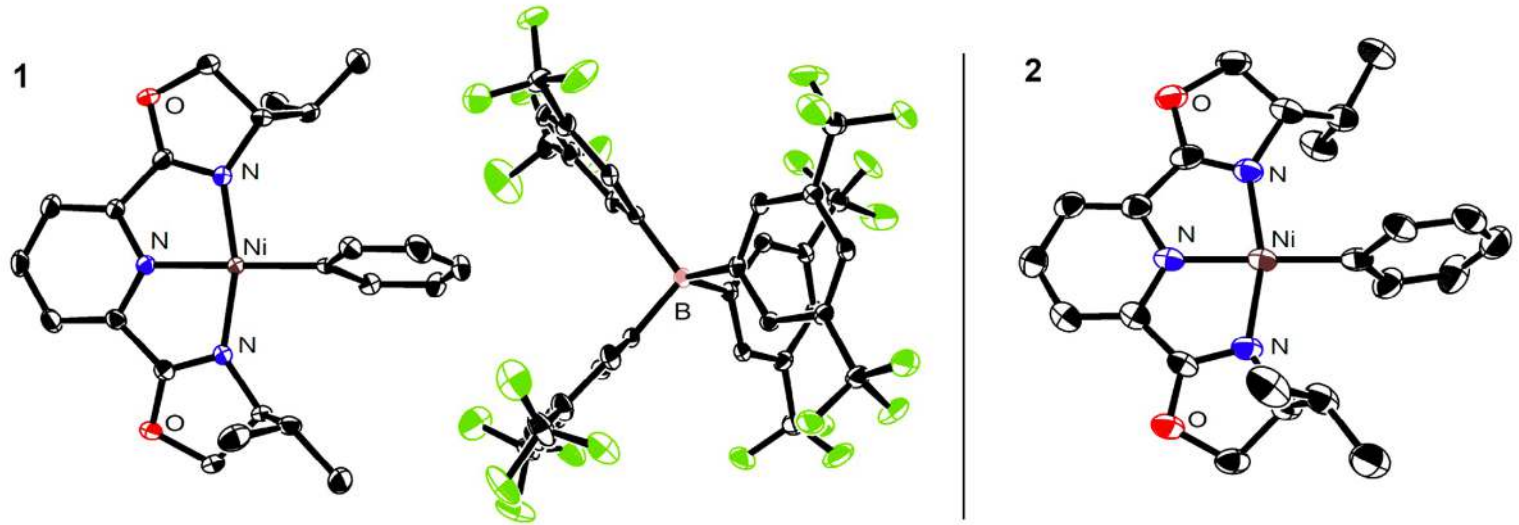

One of the first Ni(I)–aryl compounds!!

Schley, N. D.; Fu, G. C. *J. Am. Chem. Soc.* **2014**, *136*, 16588–16593.

Nickel Catalysis

Fu: Mechanistic study of C(sp^3)–Br Negishi cross-coupling

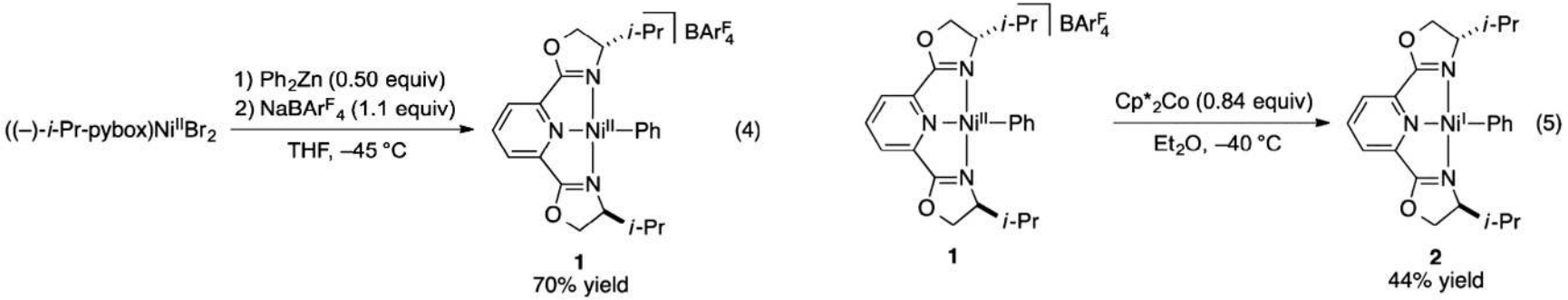

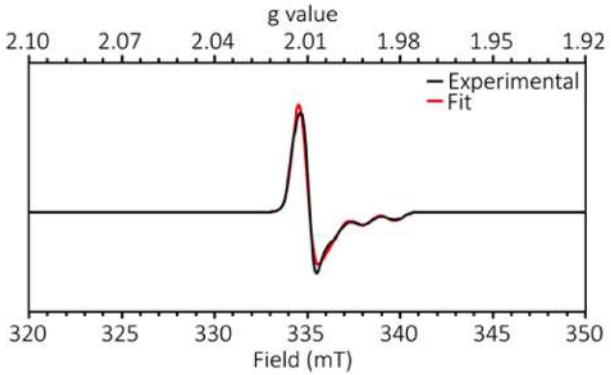

Figure 3. EPR spectrum of ((–)-*i*-Pr-pybox)Ni^{I}Ph (**2**; black) and corresponding fit (red). Fit parameters: g_1 = 2.0067, g_2 = 2.0075, g_3 = 1.9889, ^{14}N coupling (MHz) = 0.0205, 0.0124, 47.2047, line width = 0.9929. X-band EPR spectra were collected at 77 K in a toluene glass at υ = 9.411 GHz at 2 mW power and a modulation amplitude of 2 G.

One of the first Ni(I)–aryl compounds!!

Schley, N. D.; Fu, G. C. *J. Am. Chem. Soc.* **2014**, *136*, 16588–16593.

Nickel Catalysis

Fu: Mechanistic study of C(sp^3)–Br Negishi cross-coupling

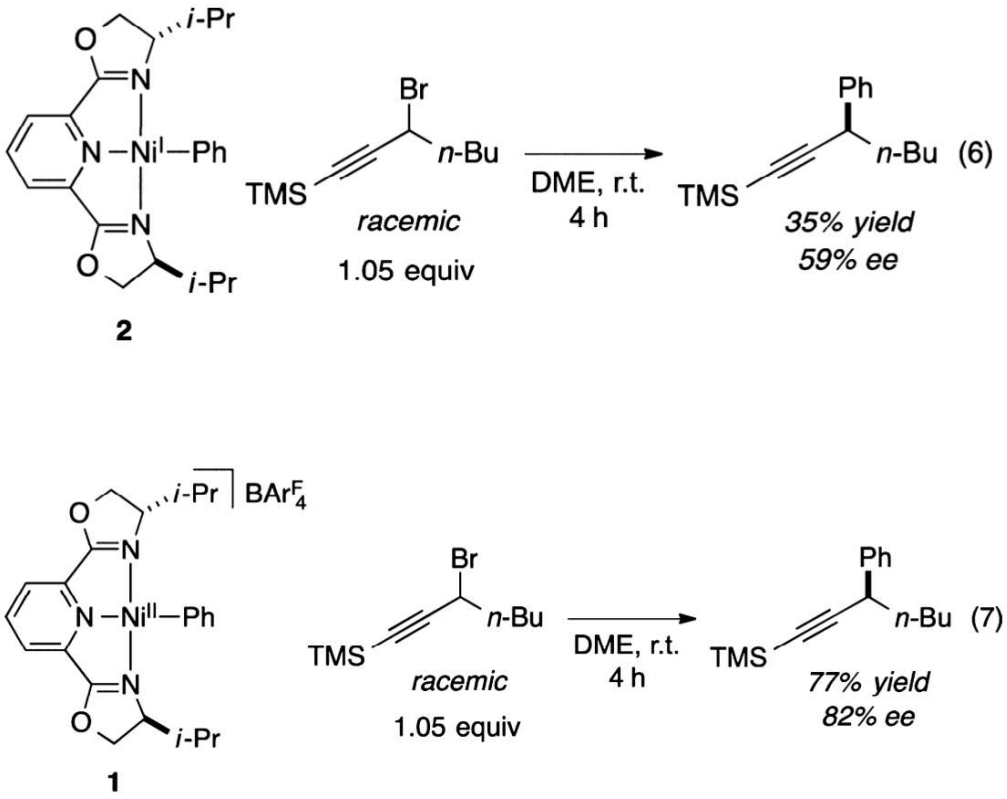

(pybox)Ni(I)–Ph seems less relevant to productive C–C bond formation

Schley, N. D.; Fu, G. C. *J. Am. Chem. Soc.* **2014**, *136*, 16588–16593.

Nickel Catalysis

Hazari: Synthesis, stability of Ni(I)–aryl compounds

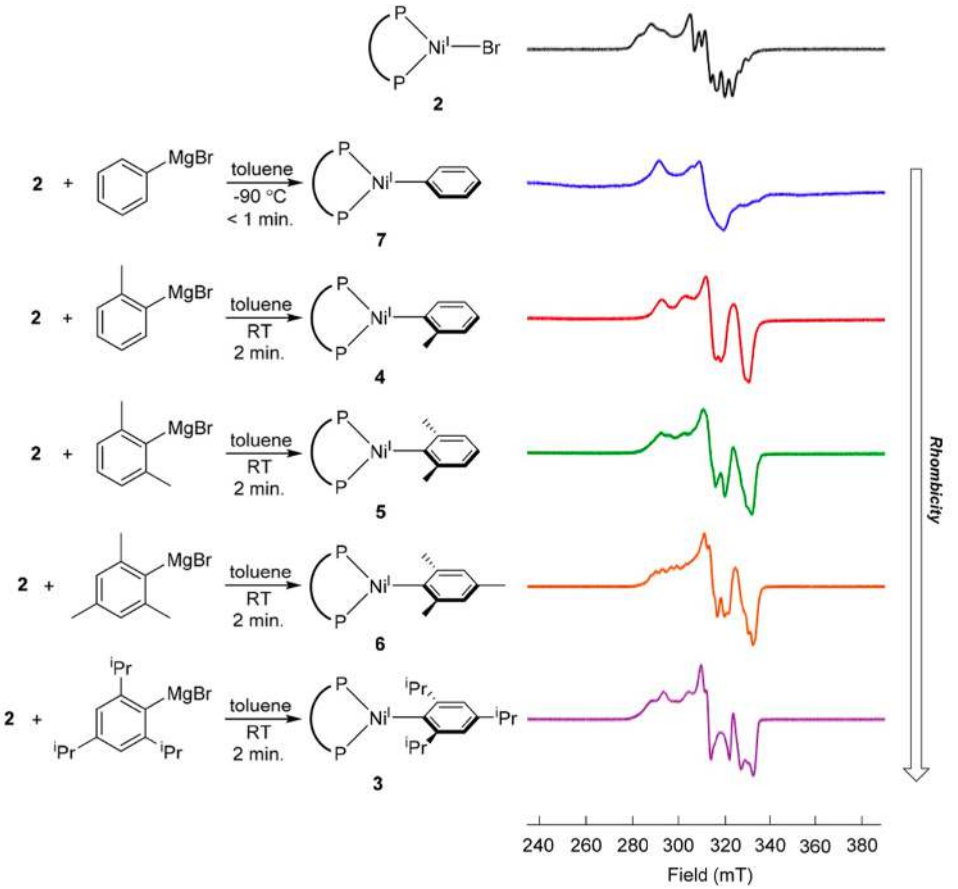

Ni^{I}(2,4,6-mesityl) (**6**). As the size of the aryl group decreases, the stability of the Ni(I) aryl species decreases significantly, with **4** decomposing completely in approximately 6 h at room temperature. The instability of these species prevented

Mohadjer Beromi, M.; Bannerjee, G.; Brudvig, G. W.; Hazari, N.; Mercado, B. Q. *ACS Catal.* **2018**, *8*, 2526–2533.

Nickel Catalysis

Fu: Mechanistic study of C(sp^3)–Br Negishi cross-coupling

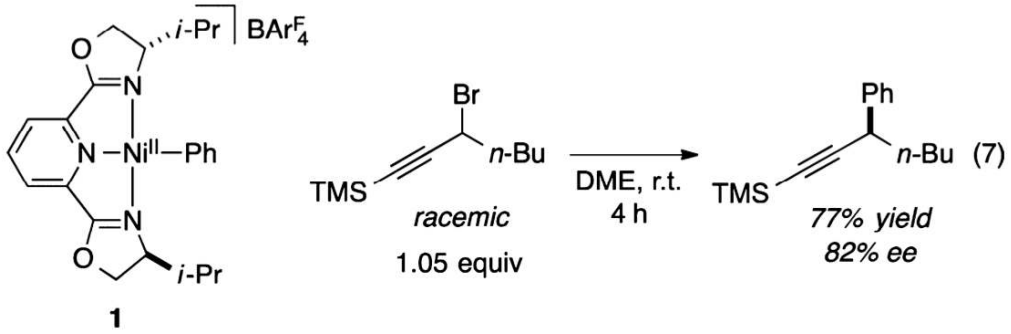

reaction takes 4 h

Compare with (pybox)NiBr:

Treatment of a solution of (*i*-Pr-pybox)Ni^{I}Br (3) with the propargylic bromide (1.0 equiv) leads to immediate bleaching (violet → colorless) and the formation of (*i*-Pr-pybox)Ni^{II}Br$_2$ (identified by UV–vis spectroscopy) and a mixture of racemic

yield, 82% ee; eq 9). Similarly, in the absence of TEMPO, the addition of (*i*-Pr-pybox)Ni^{I}Br to a solution of phenylnickel(II) complex (1) and the propargylic bromide leads to an enhanced rate of carbon–carbon bond formation.[23]

established that (*i*-Pr-pybox)Ni^{I}Br reacts much more rapidly with a propargylic bromide than with Ph_2Zn). The mechanism

1. *(pybox)NiBr likely activates Alk–Br (faster activation)*
2. *(pybox)Ni(II)Ph[X] captures radical (consistent with Alk–Br activation by Ni(I)Br)*

Schley, N. D.; Fu, G. C. *J. Am. Chem. Soc.* **2014**, *136*, 16588–16593.

Nickel Catalysis

Fu: Mechanistic study of C(sp^3)–Br Negishi cross-coupling

Proposal:

1. *(pybox)NiBr likely activates Alk–Br*
2. *(pybox)Ni(II)Ph[X] captures radical*

Cyclic Voltammagram of [(*i*-Pr-pybox)$Ni^{II}Ph]BAr^F_4$ overlaid with (*i*-Pr-pybox)Ni^IBr in THF (100 mV/s, 0.10 M $TBAPF_6$, arbitrary *y* scale).

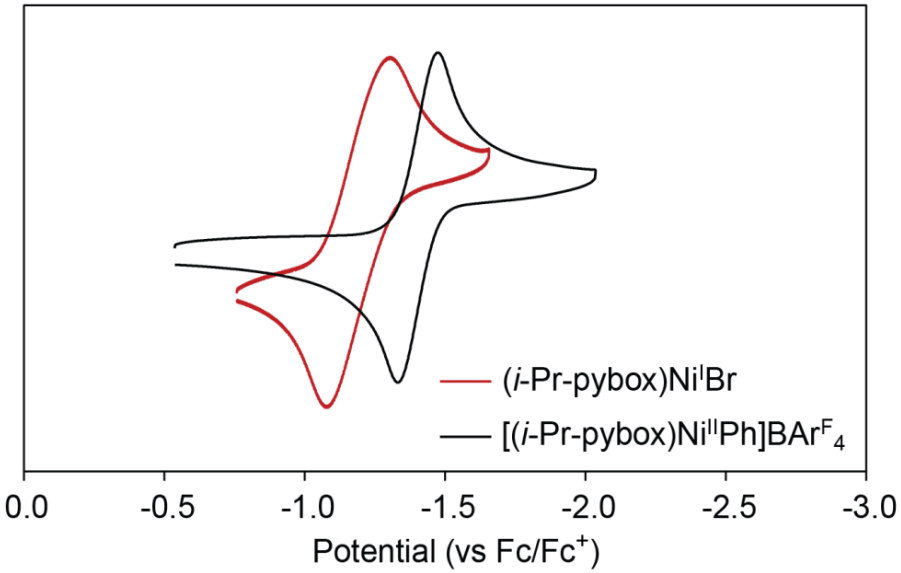

Kinetics of substrate activation are distinct from thermodynamics of electron transfer (likely not ET mechanism)

Schley, N. D.; Fu, G. C. *J. Am. Chem. Soc.* **2014**, *136*, 16588–16593.

Nickel Catalysis

Fu: Mechanistic study of C(sp^3)–Br Negishi cross-coupling

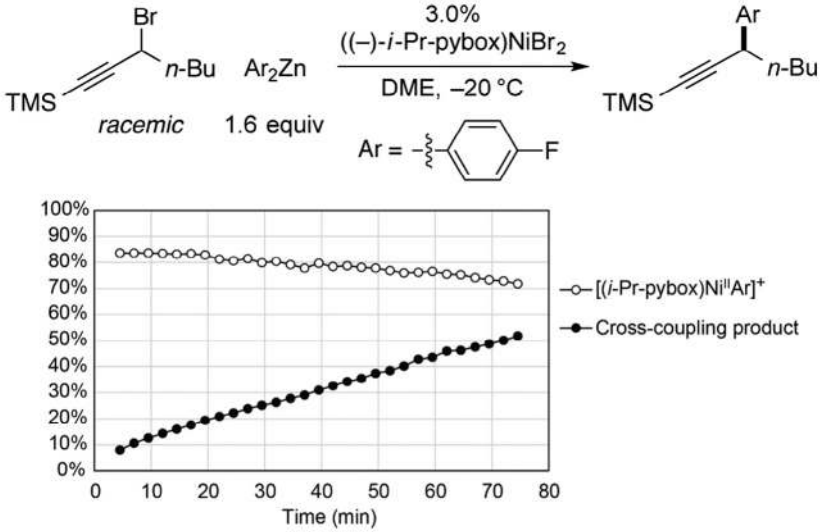

Figure 9. Analysis via ^{19}F NMR spectroscopy of a catalyzed Negishi reaction in progress: (○) $[(i\text{-Pr-pybox})Ni^{II}Ar]^+$ as a percentage of all nickel that is present; (●) yield of cross-coupling product.

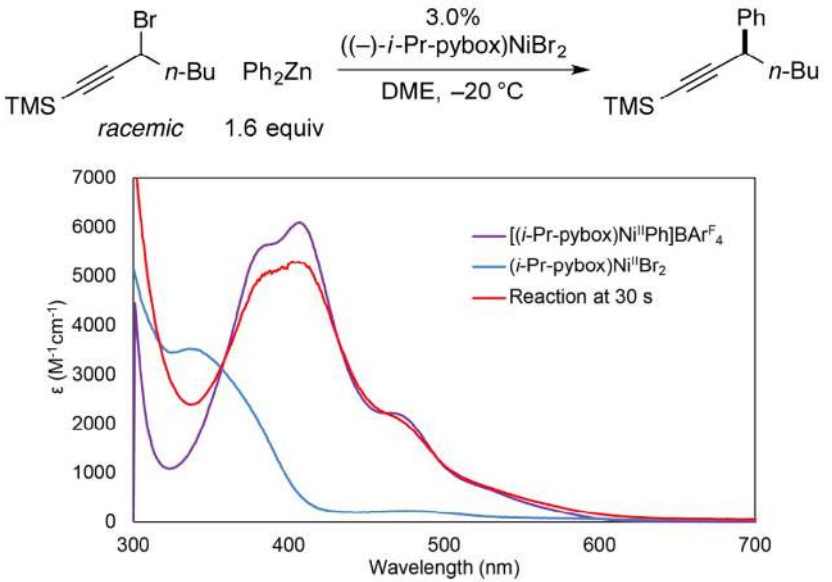

Figure 10. Analysis via UV–vis spectroscopy of a catalyzed Negishi reaction in progress: blue: $(i\text{-Pr-pybox})Ni^{II}Br_2$; red: cross-coupling reaction in progress; purple: $[(i\text{-Pr-pybox})Ni^{II}Ph]BAr^F{}_4$.

4-FPh by ^{19}F NMR (DME):
(pybox)$Ni^{II}Ar^+$: −62.33 ppm
Product: −116.97 ppm

Resting state established as Ni(II)–Ar by ^{19}F NMR and UV-vis spectroscopy

Schley, N. D.; Fu, G. C. *J. Am. Chem. Soc.* **2014**, *136*, 16588–16593.

Nickel Catalysis

Fu: Mechanistic study of C(sp^3)–Br Negishi cross-coupling

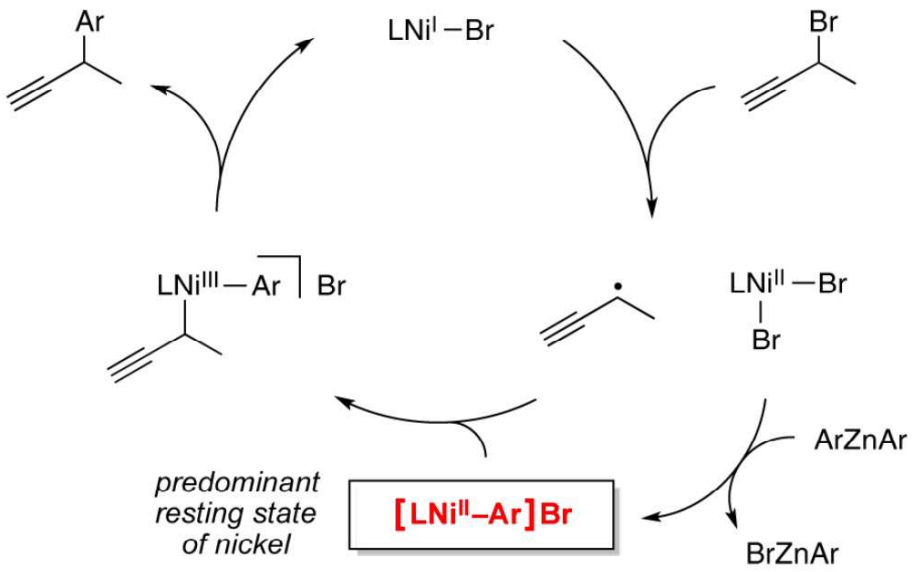

Figure 6. A possible catalytic cycle for the nickel/pybox-catalyzed Negishi arylation of a propargylic bromide. For the sake of simplicity, all elementary steps are illustrated as being irreversible.

Very small amount of nickel "activates" (i.e., turns to Ni(I))
Essentially a radical initiation/propagation mechanism

For related Kumada cross-coupling study: Yin, H.; Fu, G. C. *J. Am. Chem. Soc.* **2019**, *141*, 15433–15440.

Schley, N. D.; Fu, G. C. *J. Am. Chem. Soc.* **2014**, *136*, 16588–16593.

Nickel Catalysis

Beyond halides: Baran and Weix—Ni-catalyzed reactions of redox-active esters

Baran (2016):

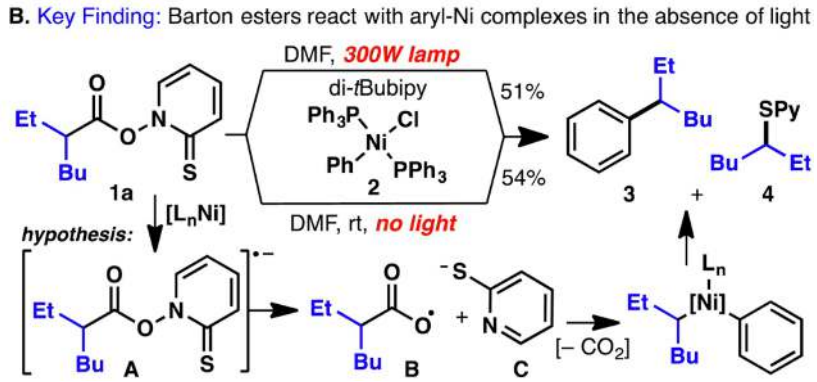

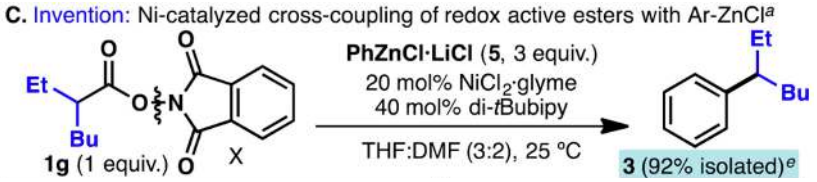

entry	deviation from above	yield (%)[b]
1	X = 2-pyridothione, **1a**	43
2	**1a** (150W Lamp)	43
3	X = Cl	<1[c]
4	X = OMe	<1[c]
5	X = OAt, **1b**	42[d]
6	X = OBt, **1c**	51[d]
7	**1d**	<1[c]
8	X = NHS, **1e**	<1[c]
9	**1f**	46
10	**1g** (w/o Ni catalyst)	<1[c]
11	**1g** (150W lamp)	82
12	**1g** (rigorously dark)	89
13	**1g** (w/ $NiCl_2 \cdot 6H_2O$)	93[e]

[a] 0.1 mmol. [b] Yield determined by ^1H NMR using CH_2Br_2 as an internal standard. [c] No product was observed by GC/MS. [d] Prepared *in situ* from HATU or HBTU, respectively (see SI for details). [e] 0.25 mmol scale, isolated

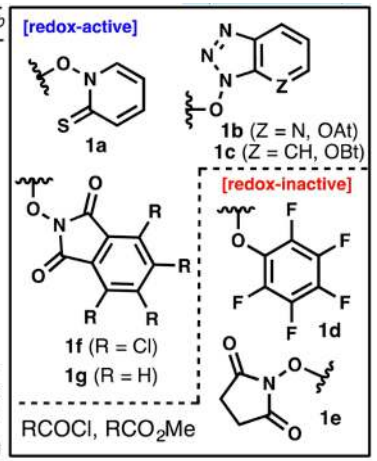

Weix (2016):

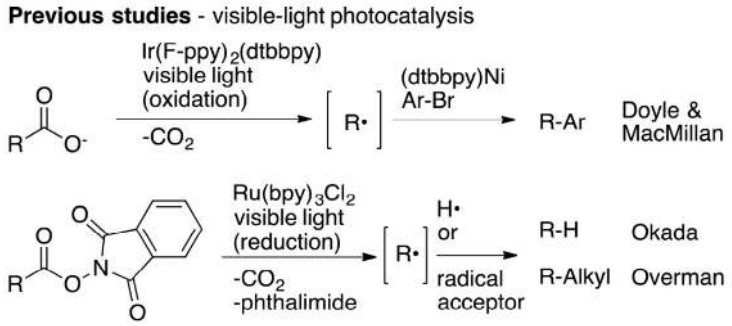

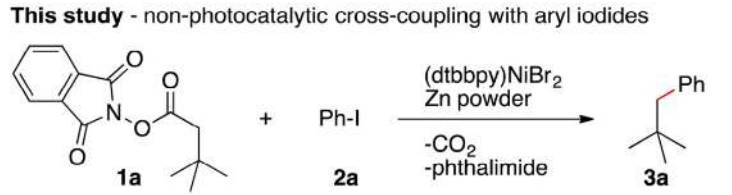

entry	change from standard conditions	**1a** (%)[b]	**3a** (%)[b]
1	none[a]	0	60
2	reaction run in the dark	0	62
3	$Ni(diglyme)Br_2$ as catalyst	0	0
4	no nickel or ligand	84	0
5	no zinc	85	0
6	NHS ester in place of NHP ester[c]	81	0

(a) Cornella, J.; Edwards, J. T.; Qin, T.; Kawamura, S.; Wang, J.; Pan, C.-M.; Gianatassio, R.; Schmidt, M.; Eastgate, M. D.; Baran, P. S. *J. Am. Chem. Soc.* **2016**, *138*, 2174–2177.

(b) Huihui, K. M. M.; Caputo, J. A.; Melchor, Z.; Olivares, A. M.; Spiewak, A. M.; Johnson, K. A.; DiBenedetto, T. A.; Kim, S.; Ackerman, L. K. G.; Weix, D. J. *J. Am. Chem. Soc.* **2016**, *138*, 5016–5019.

Nickel Catalysis

Baran: Ni-catalyzed reactions of redox-active esters

Table 1. Initial Scope of the Nickel-Catalyzed Cross-Coupling of Redox-Active *N*-Hydroxyphthalimide Esters with Aryl Zinc Reagents

- 28 examples
- cyclic and acyclic substrates
- Lewis-basic heteroatoms
- unactivated (non-heteroatom stabilized) acids
- simple setup, room temp

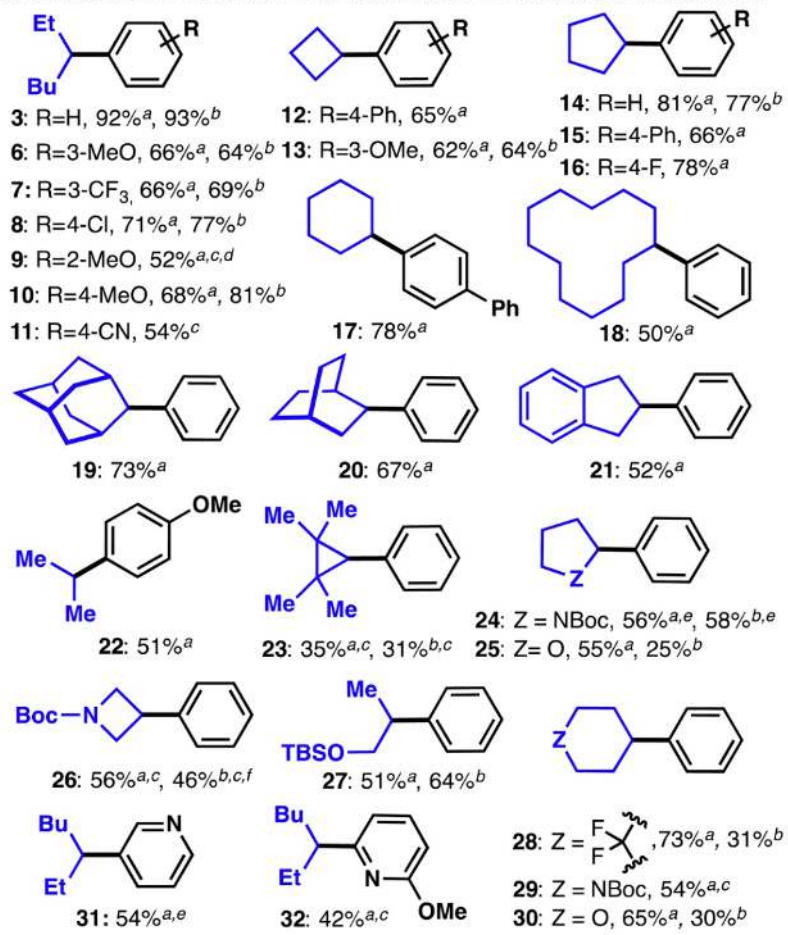

Cornella, J.; Edwards, J. T.; Qin, T.; Kawamura, S.; Wang, J.; Pan, C.-M.; Gianatassio, R.; Schmidt, M.; Eastgate, M. D.; Baran, P. S. *J. Am. Chem. Soc.* **2016**, *138*, 2174–2177.

Nickel Catalysis

Baran: Ni-catalyzed reactions of redox-active esters

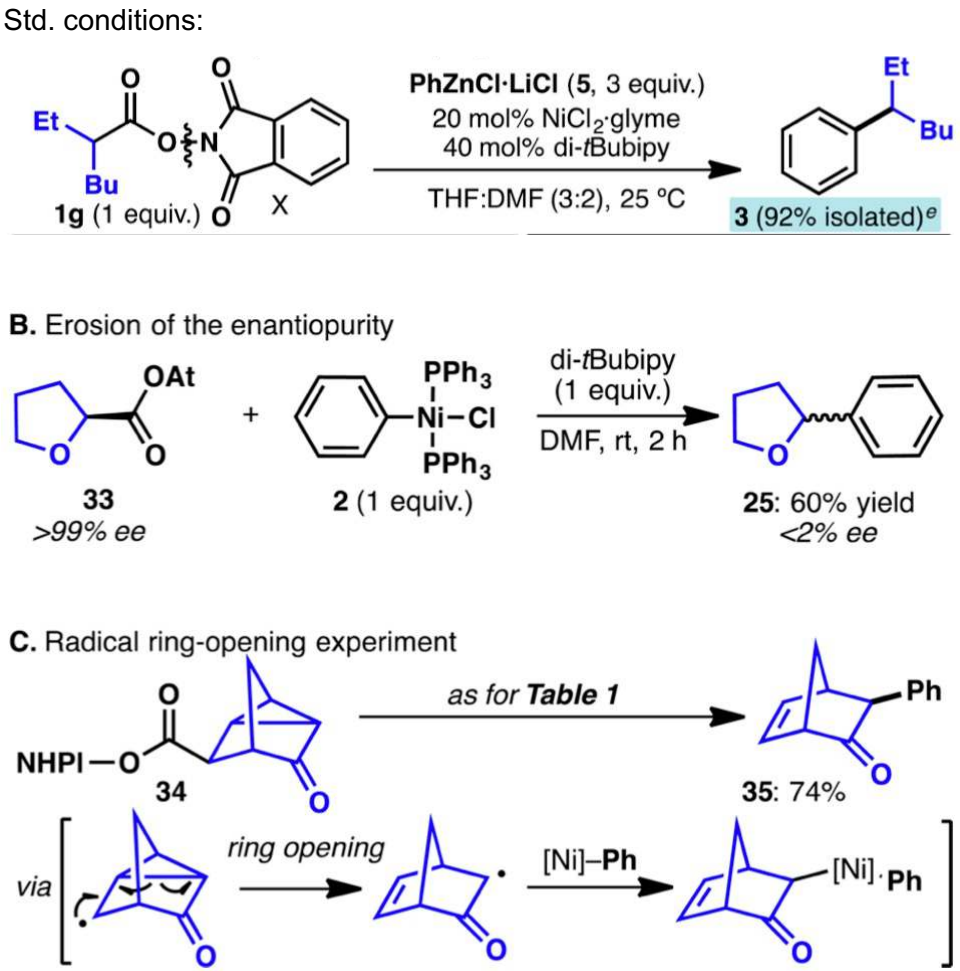

Cornella, J.; Edwards, J. T.; Qin, T.; Kawamura, S.; Wang, J.; Pan, C.-M.; Gianatassio, R.; Schmidt, M.; Eastgate, M. D.; Baran, P. S. *J. Am. Chem. Soc.* **2016**, *138*, 2174–2177.

Nickel Catalysis

Baran: Ni-catalyzed reactions of redox-active esters

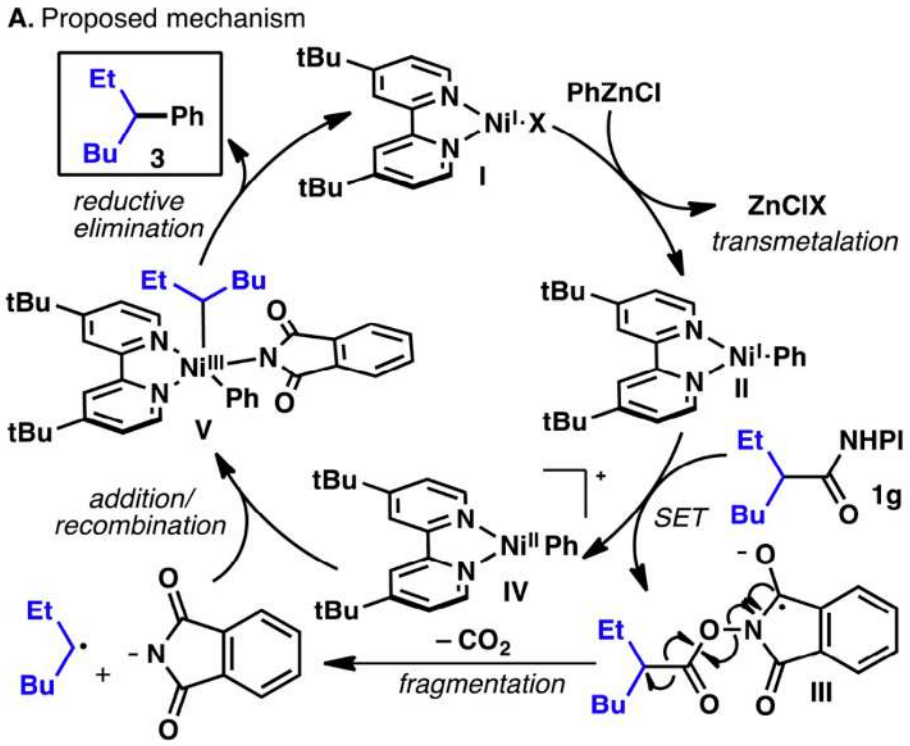

Cornella, J.; Edwards, J. T.; Qin, T.; Kawamura, S.; Wang, J.; Pan, C.-M.; Gianatassio, R.; Schmidt, M.; Eastgate, M. D.; Baran, P. S. *J. Am. Chem. Soc.* **2016**, *138*, 2174–2177.

Nickel Catalysis

Baran: Ni-catalyzed reactions of redox-active esters

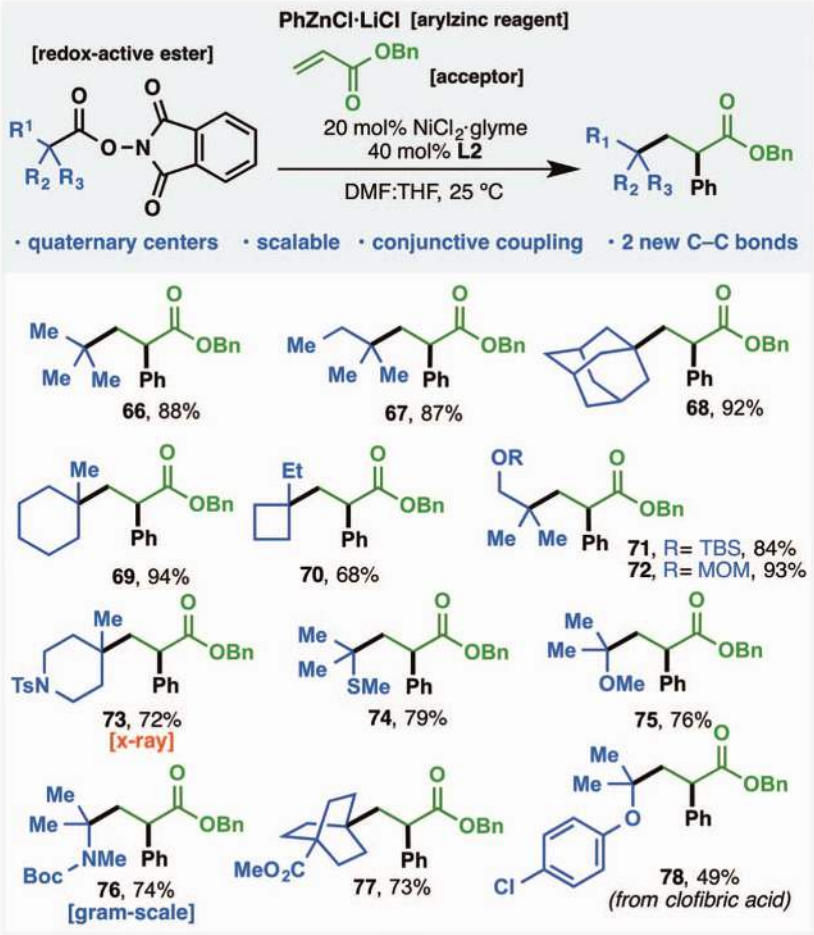

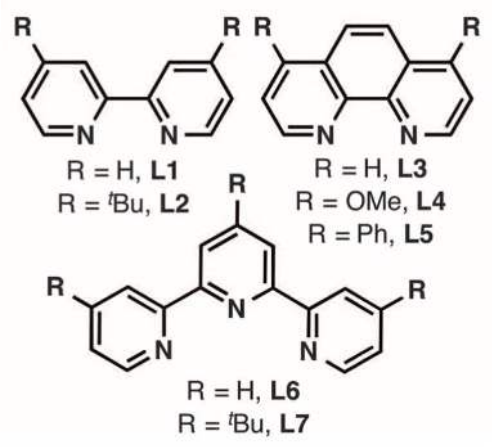

Fig. 4. Scope of the Ni-catalyzed three-component conjunctive cross-coupling. Standard conditions were redox-active ester (1 eq), acceptor (2.5 eq), PhZnCl·LiCl complex (3 eq), $NiCl_2$·glyme (20 mol %), **L2** (40 mol %), THF:DMF, 25°C, 8 hours. All the products shown were obtained in racemic form.

Qin, T.; Cornella, J.; Li, C.; Malins, L. R.; Edwards, J. T.; Kawamura, S.; Maxwell, B. D.; Eastgate, M. D.; Baran, P. S. *Science* **2016**, *352*, 801–805.

Nickel Catalysis

Ni-catalyzed reactions of redox-active esters

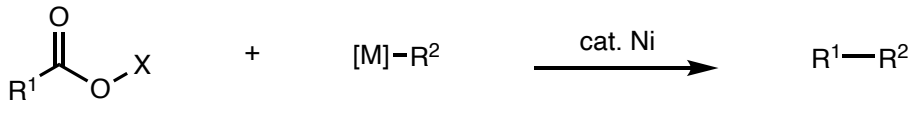

Redox-active esters:

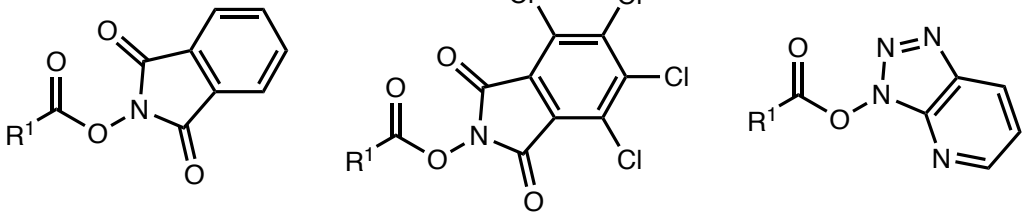

[M]–R^2 sources

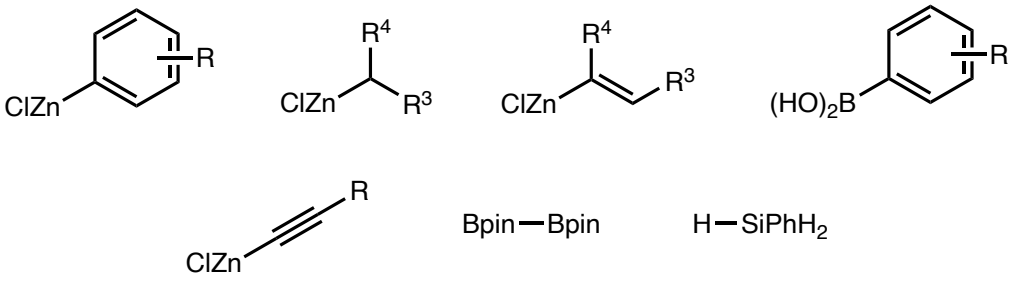

See: Murarka, S. *Adv. Synth. Catal.* **2018**, *360*, 1735–1753 and references therein.

Nickel Catalysis

Watson: Nickel-catalyzed activation of alkyl pyridiniums (Katritzky salts):

Table 1. Optimization[a]

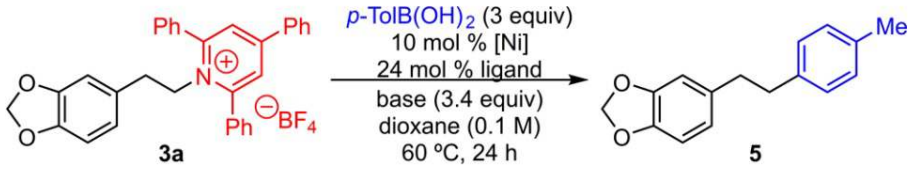

entry	[Ni]	ligand	base	yield (%)[b]
1	$Ni(cod)_2$	PPh_2Cy	K_3PO_4	6
2	$Ni(cod)_2$	BPhen	K_3PO_4	21
3	$Ni(cod)_2$	BPhen	KO^{t}Bu	24
4	$Ni(OAc)_2{\cdot}4H_2O$	BPhen	KO^{t}Bu	39
5[c]	$Ni(OAc)_2{\cdot}4H_2O$	BPhen	KO^{t}Bu	52
6[c,d]	$Ni(OAc)_2{\cdot}4H_2O$	BPhen	KO^{t}Bu	81
7[c,d]	$Ni(OAc)_2{\cdot}4H_2O$	BPhen	KOEt	68
8[c,d]	–	BPhen	KO^{t}Bu	0
9[c,d]	$Ni(OAc)_2{\cdot}4H_2O$	–	KO^{t}Bu	0
10[c,d]	$Ni(OAc)_2{\cdot}4H_2O$	bipy	KO^{t}Bu	54
11[c,d]	$Ni(OAc)_2{\cdot}4H_2O$	BPhen	–	0
12[c,d]	$Ni(OAc)_2{\cdot}4H_2O$	BPhen	K_3PO_4	3

[a]Conditions: pyridinium salt **3a** (0.1 mmol), [Ni] (10 mol %), ligand (24 mol %), *p*-TolB(OH)$_2$ (3.0 equiv), base (3.4 equiv), dioxane (0.1 M), 60 °C, 24 h. [b]Determined by ^{1}H NMR using 1,3,5-trimethoxybenzene as internal standard. [c]Two mixtures (Vial 1: [Ni], BPhen, dioxane. Vial 2: *p*-TolB(OH)$_2$, KO^{t}Bu, EtOH, dioxane. **3a** in either vial.) were stirred for 1 h before combining. [d]EtOH (5 equiv) added.

Katritzky, A. R.; De Ville, G.; Patel, R. C. *Tetrahedron* **1981**, *37*, 25–30; Basch, C. H.; Liao, J.; Xu, J.; Piane, J. J.; Watson, M. P. *J. Am. Chem. Soc*. **2017**, *139*, 5313–5316.

Nickel Catalysis

Watson: Nickel-catalyzed activation of alkyl pyridiniums (Katritzky salts):

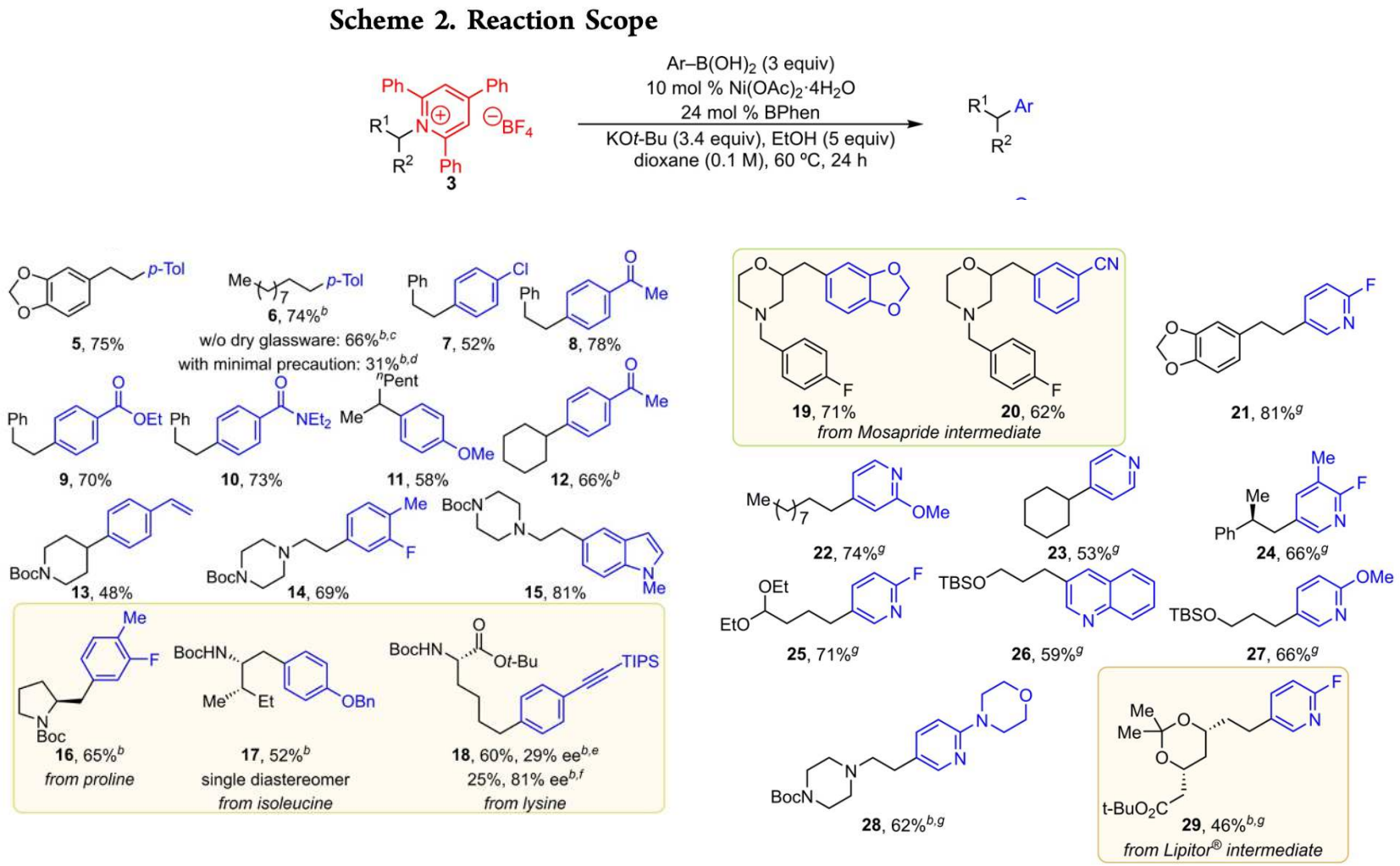

Katritzky, A. R.; De Ville, G.; Patel, R. C. *Tetrahedron* **1981**, *37*, 25–30; Basch, C. H.; Liao, J.; Xu, J.; Piane, J. J.; Watson, M. P. *J. Am. Chem. Soc*. **2017**, *139*, 5313–5316.

Nickel Catalysis

Watson: Nickel-catalyzed activation of alkyl pyridiniums (Katritzky salts):

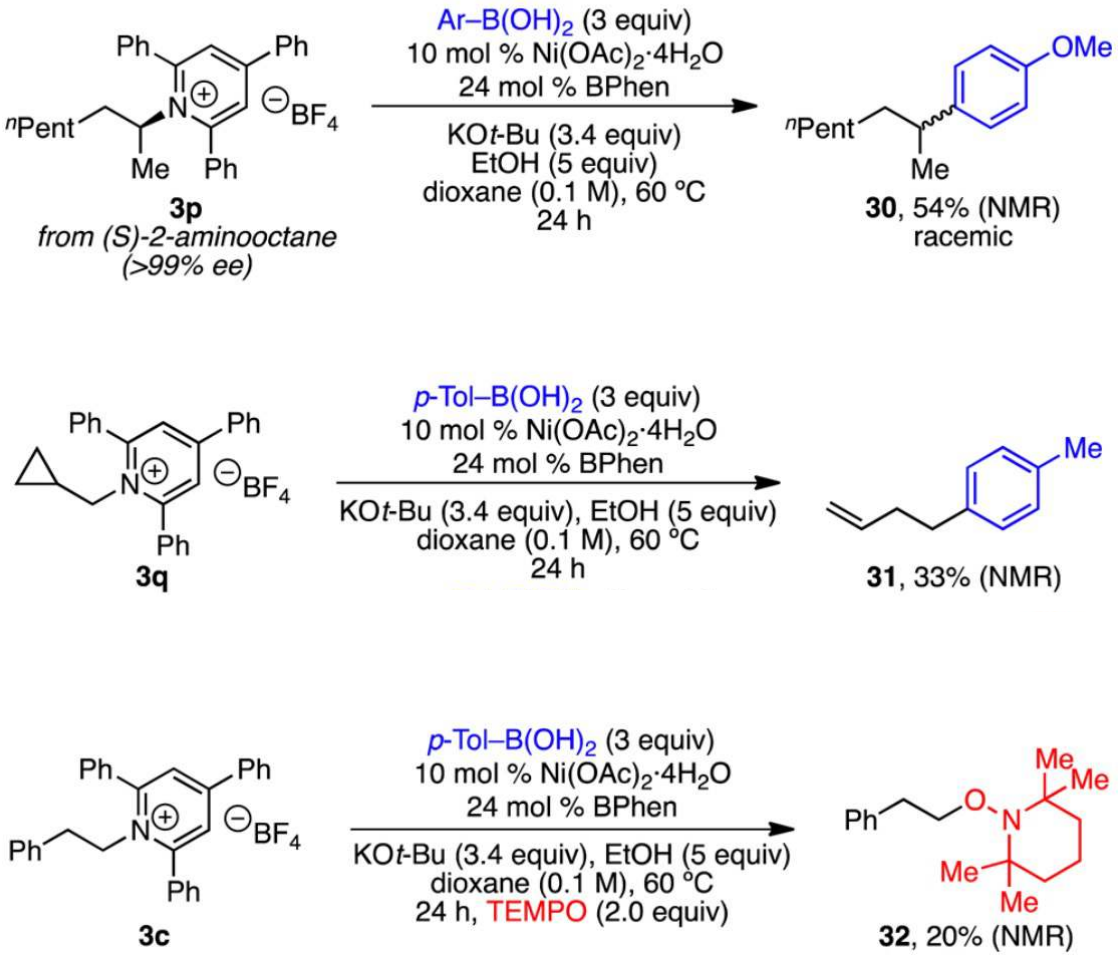

Katritzky, A. R.; De Ville, G.; Patel, R. C. *Tetrahedron* **1981**, *37*, 25–30; Basch, C. H.; Liao, J.; Xu, J.; Piane, J. J.; Watson, M. P. *J. Am. Chem. Soc*. **2017**, *139*, 5313–5316.

Nickel Catalysis

Watson: Nickel-catalyzed activation of alkyl pyridiniums (Katritzky salts):

Scheme 4. Mechanistic Proposal

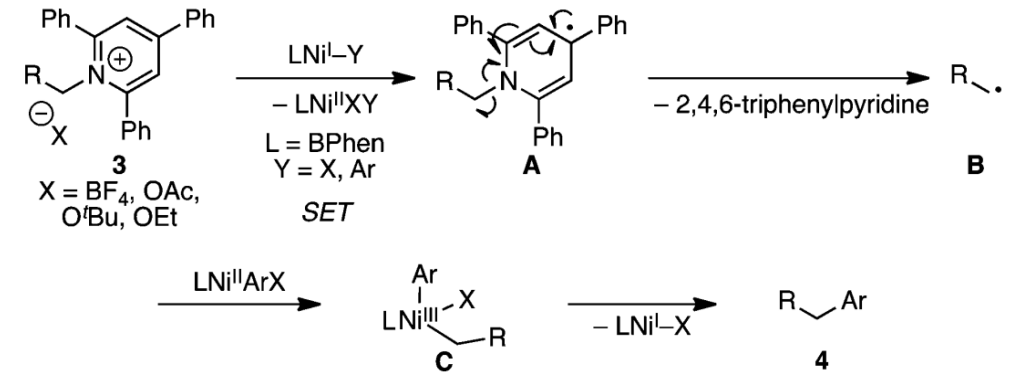

Katritzky, A. R.; De Ville, G.; Patel, R. C. *Tetrahedron* **1981**, *37*, 25–30; Basch, C. H.; Liao, J.; Xu, J.; Piane, J. J.; Watson, M. P. *J. Am. Chem. Soc*. **2017**, *139*, 5313–5316.

Nickel Catalysis

Baran: Nickel-catalyzed activation of alkyl sulfones (2018)

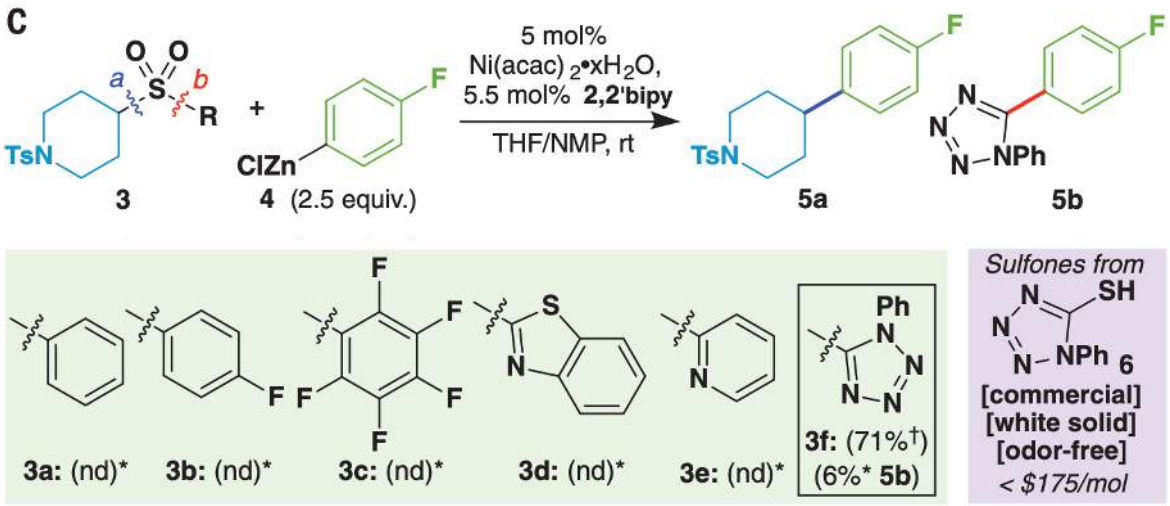

Inspiration for these leaving groups (Denmark 2013, iron chemistry):
Denmark, S. E.; Cresswell, A. J. *J. Org. Chem.* **2013**, *78*, 12593–12628.

Merchant, R. R.; Edwards, J. T.; Qin, T.; Fruszyk, M. M.; Bi, C.; Che, G.; Bao, D.-H.; Qiao, W.; Sun, L.; Collins, M. R.; Fadeyi, O. O.; Gallego, G. M.; Mousseau, J. J.; Nuhant, P.; Baran, P. S. *Science* **360**, *2018*, 75–80.

Nickel Catalysis

Baran: Nickel-catalyzed activation of alkyl sulfones (2018)

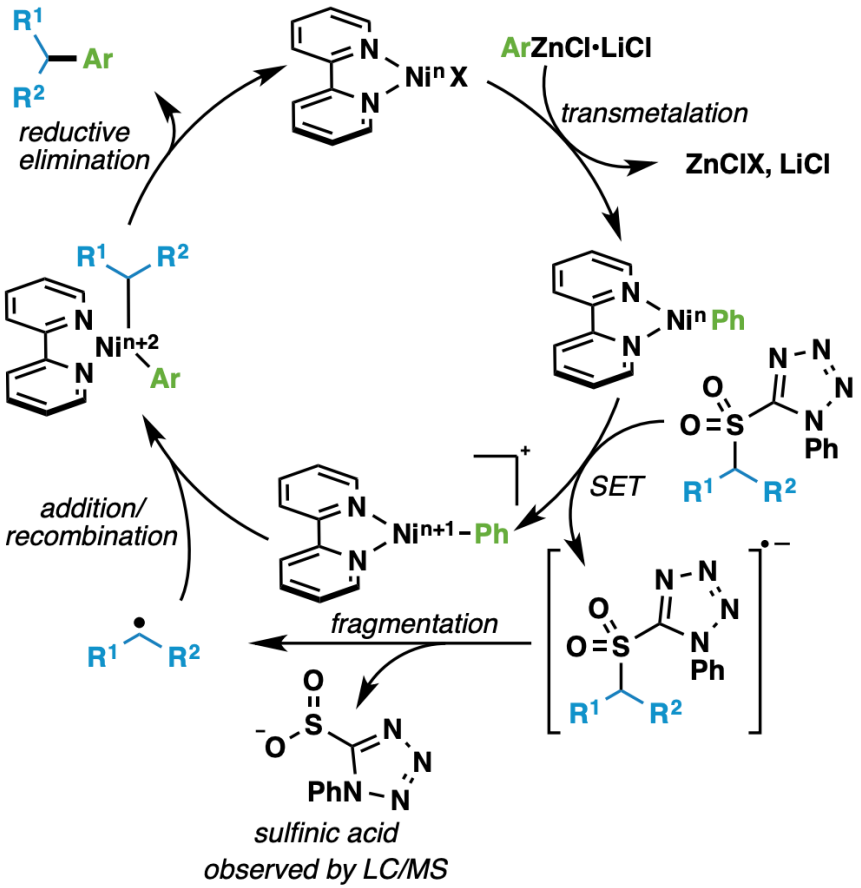

Figure S9: Possible catalytic cycle for the desulfonylative arylation. (*54-57*)

Merchant, R. R.; Edwards, J. T.; Qin, T.; Fruszyk, M. M.; Bi, C.; Che, G.; Bao, D.-H.; Qiao, W.; Sun, L.; Collins, M. R.; Fadeyi, O. O.; Gallego, G. M.; Mousseau, J. J.; Nuhant, P.; Baran, P. S. *Science* **360**, *2018*, 75–80.

Nickel Catalysis

Topics in nickel cross-coupling:

Directions in Precatalyst Synthesis

"Inert"/"Nonclassical" $C(sp^2)$–X Electrophiles Ni(0)/Ni(II)

Benzylic $C(sp^3)$–X Electrophiles Ni(0)/Ni(II)

X = OR, NR_3X

"Unactivated" $C(sp^3)$–X Electrophiles Ni(I)/Ni(III)

Cross-Electrophile Coupling Ni(0)/Ni(I)/Ni(II)/Ni(III)

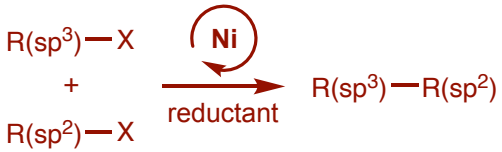

Conjunctive Cross-Coupling (Short)

Nickel Catalysis

Prototypical cross-electrophile coupling (Weix, 2010)

Table 1. Optimized Reaction Conditions[a]

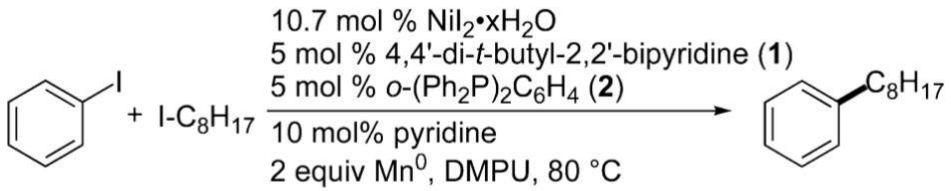

Entry	Deviation from Standard Conditions	Yield (%)[b]
1	none	88

Everson, D. A.; Shrestha, R.; Weix, D. J. *J. Am. Chem. Soc.* **2010**, *132*, 920–921.

Nickel Catalysis

Typical reactivity trends (important for discriminating between coupling partners in cross-electrophile coupling)

Reactivity with C(sp^2)–X electrophiles

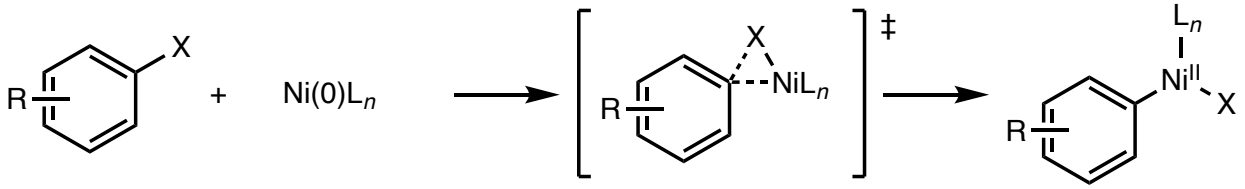

Reactivity with C(sp^3)–X electrophiles

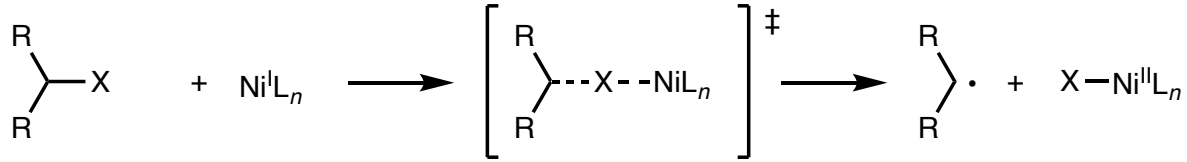

(a) Everson, D. A.; Weix, D. J. *J. Org. Chem.* **2014**, *79*, 4793–4798; (b) Hartwig, J. Organotransition Metal Chemistry: From Bonding to Catalysis. University Science Books: Sausalito, 2010.

Nickel Catalysis

Prevailing mechanism: “Radical chain” mechanism

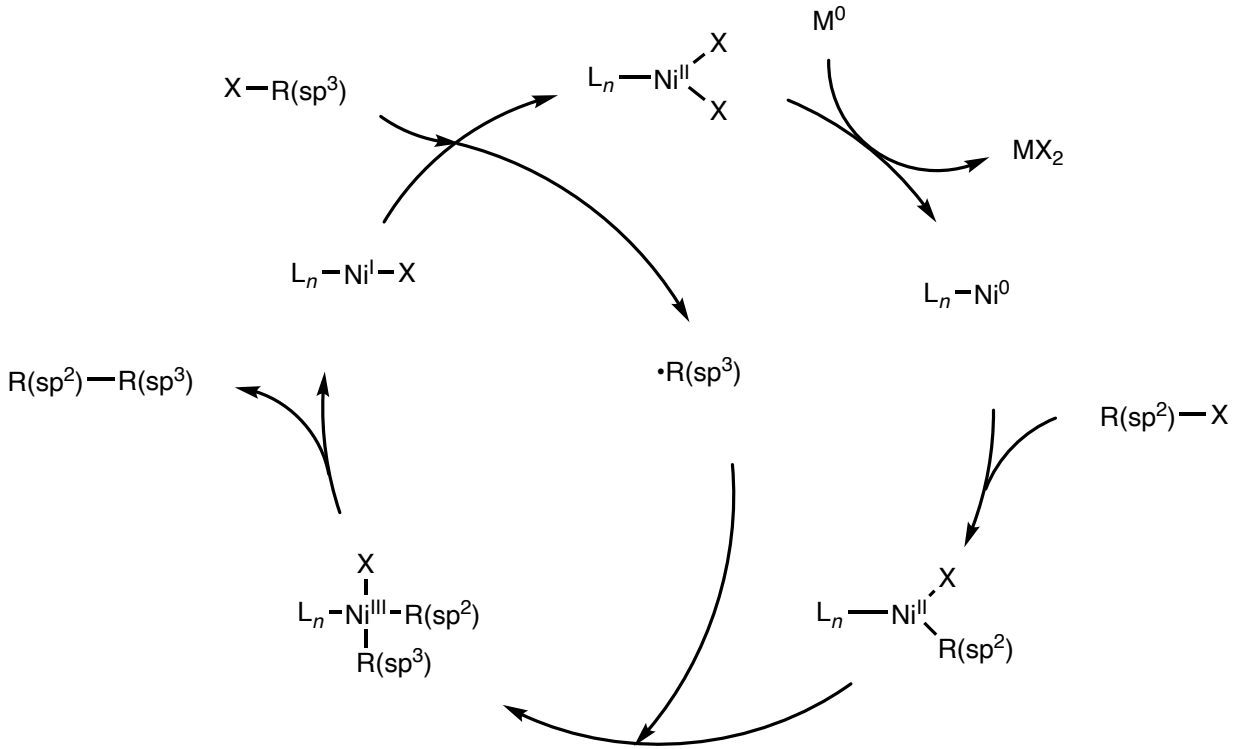

Biswas, S.; Weix, D. J. *J. Am. Chem. Soc.* **2013**, *135*, 16192–16197.

Nickel Catalysis

Weix, 2013: Reactivity of Ni(0) with electrophiles

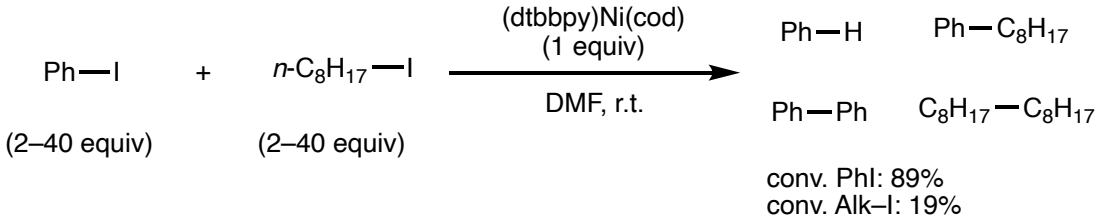

Table 2. Selectivity in Oxidative Addition to (L)Ni^0(cod)^a

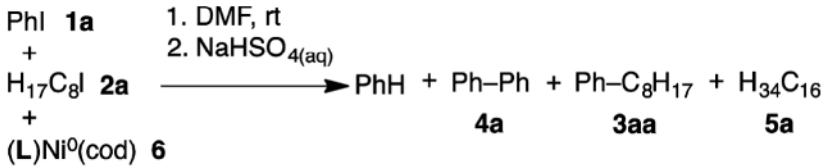

		yield (%)^c			
substrate	total conv (%)^b	alkyl-H or Ph-H	4a	3aa	5a
Ph-I	89	49	21	13	NA
$H_{17}C_8$-I	19	0	NA	51	45

^{a}A 1:1 mixture of **1a**:**2a** was added to a DMF solution of **6**. Samples were analyzed by GC. Reported values are an average of data using between 2 and 40 equiv each of **1a** and **2a** to **6**. See Supporting Information for full experimental details. ^{b}Conversion with respect to amount of **6**. ^{c}Yield with respect to amount of **6**. NA = not applicable.

Biswas, S.; Weix, D. J. *J. Am. Chem. Soc.* **2013**, *135*, 16192–16197.

Nickel Catalysis

Gong: Reactivity with C(sp^2)–X and C(sp^3)–X electrophiles

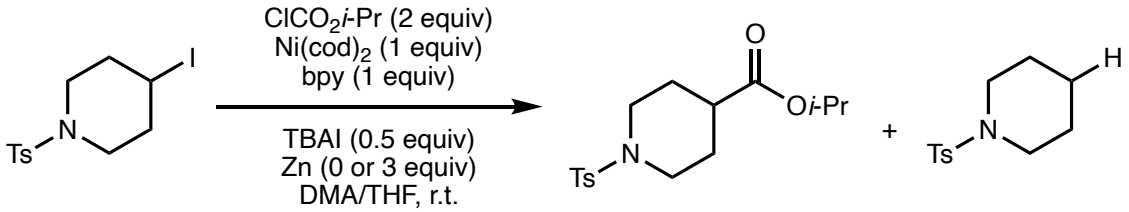

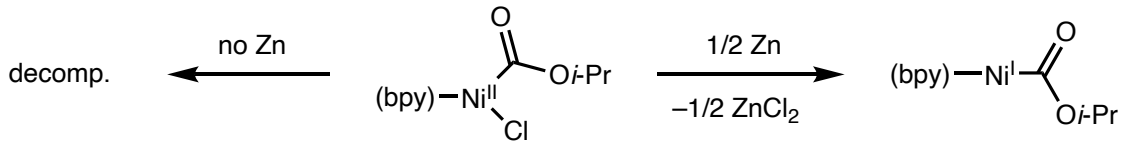

Zheng, M.; Xue, W.; Xue, T.; Gong, H. *Org. Lett.* **2016**, *18*, 6152–6155.

Nickel Catalysis

Diao: Reactivity of Ni(I)–Aryl compounds

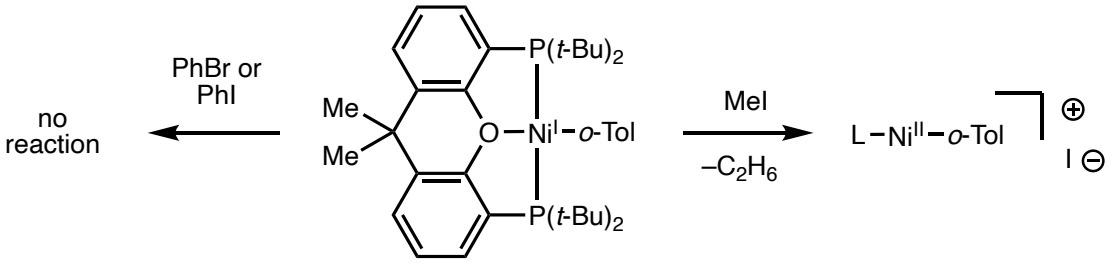

Scheme 5. Ni(I) Complex 6-Mediated Activation of Alkyl and Aryl Halides

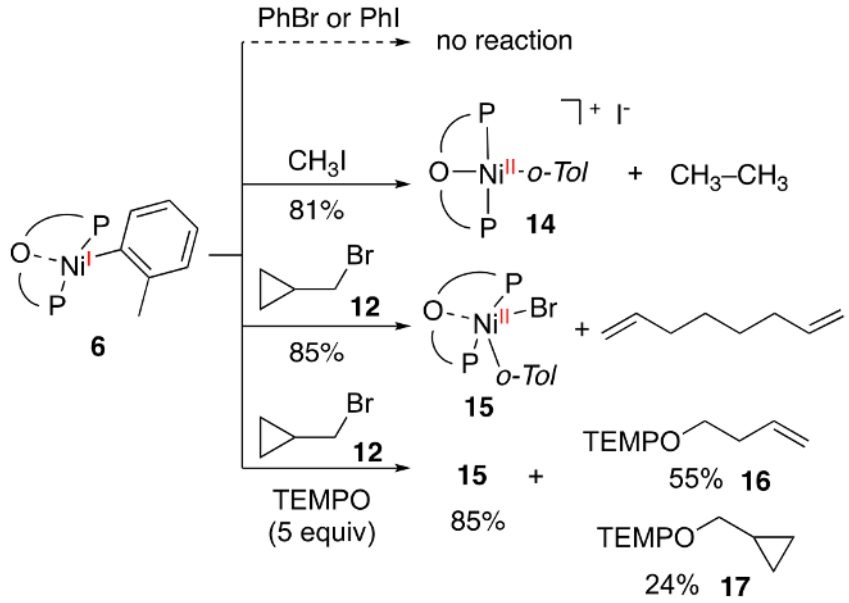

Diccianni, J. B.; Katigbak, J.; Hu, C.; Diao, T. *J. Am. Chem. Soc.* **2019**, *141*, 1788–1796.

Nickel Catalysis

Weix, 2013: Mechanism of cross-electrophile coupling

Scheme 3. Radical Clock Experiments[a]

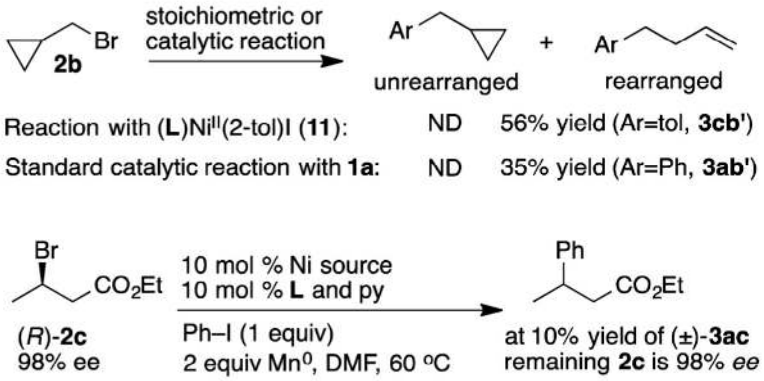

[a]ND = none detected. Catalytic reaction as in Table 1, entry 1.

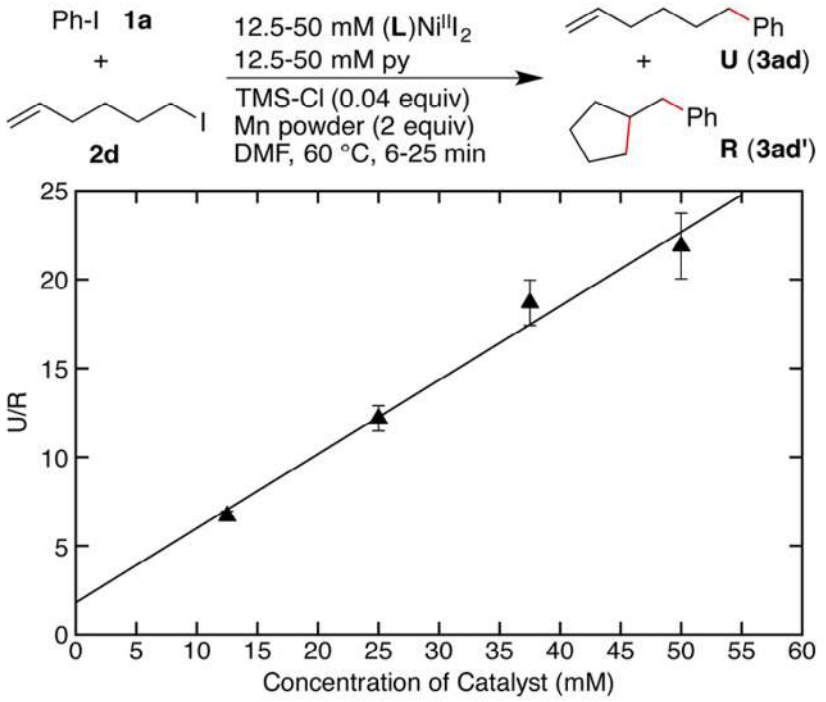

Figure 4. Ratio of **U** (**3ad**, includes olefin isomers) to **R** (**3ad′**) formed in reactions at different catalyst concentrations, showing that the degree of rearrangement, a measure of the radical lifetime, depends upon nickel concentration. The data shown are for 50–100% conversion to avoid fluctuations in active catalyst concentration at the beginning of the reaction. Error bars are the standard deviation of the data used for the plot. Linear fit: $f(x) = 0.417x + 1.83$; $R^2 = 0.984$.

steep slope consistent with catalyst resting state being
(L)Ni(II)(Ar)(X)
(or another productive intermediate)

Biswas, S.; Weix, D. J. *J. Am. Chem. Soc.* **2013**, *135*, 16192–16197.

Nickel Catalysis

Weix, 2013: Mechanism of cross-electrophile coupling

Scheme 4. Proposed Mechanism for Cross-Electrophile Coupling of Aryl Halides with Alkyl Halides

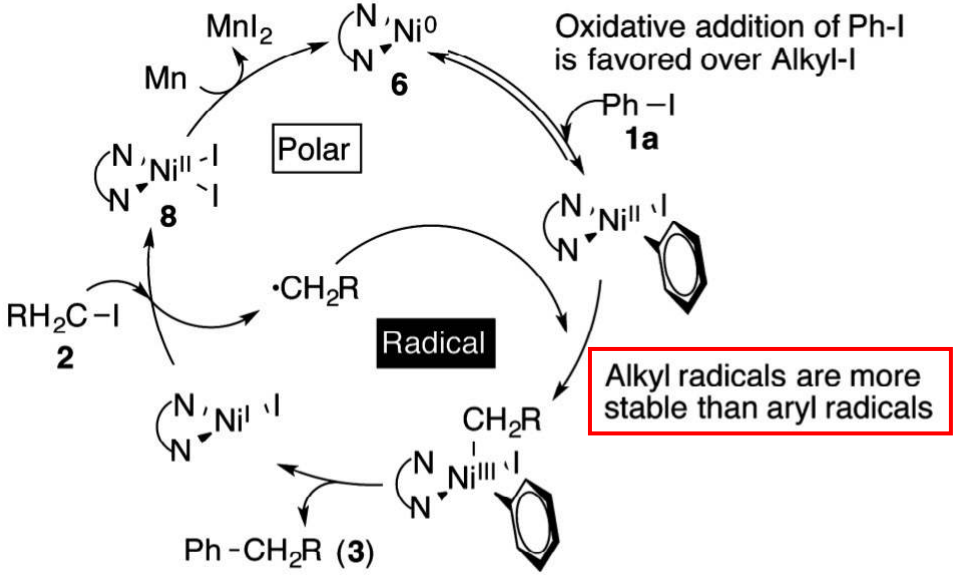

Biswas, S.; Weix, D. J. *J. Am. Chem. Soc.* **2013**, *135*, 16192–16197.

Nickel Catalysis

Weix: Dual ligand system for selective activation of electrophiles (2022)

Table 1. Optimization and Control Studies[a]

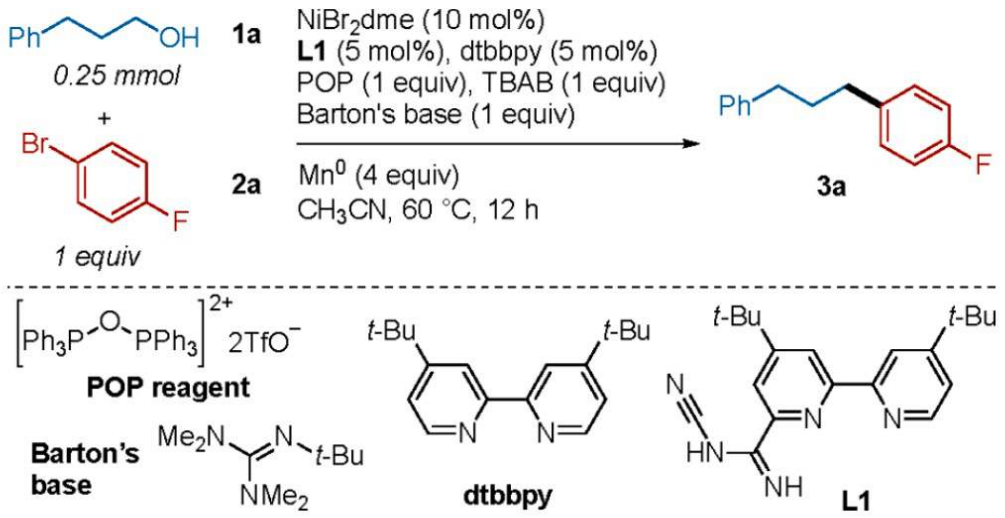

entry	deviations from above conditions	3a[b] (%)
1	none	89 (79)

and dtbbpy had complementary reactivity: dtbbpy-ligated Ni primarily consumed the aryl bromide, whereas L1-ligated Ni favored alkyl bromide consumption. The synergistic effect of

Chi, B. K.; Widness, J. K.; Gilbert, M. M.; Salgueiro, D. C.; Garcia, K. J.; Weix, D. J. *ACS Catal.* **2022**, *12*, 580–586.

Nickel Catalysis

Overview: Reductive cross-electrophile coupling

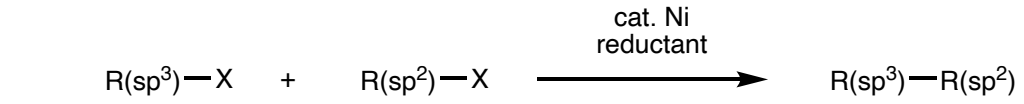

Representative R(sp^3)–X coupling partners

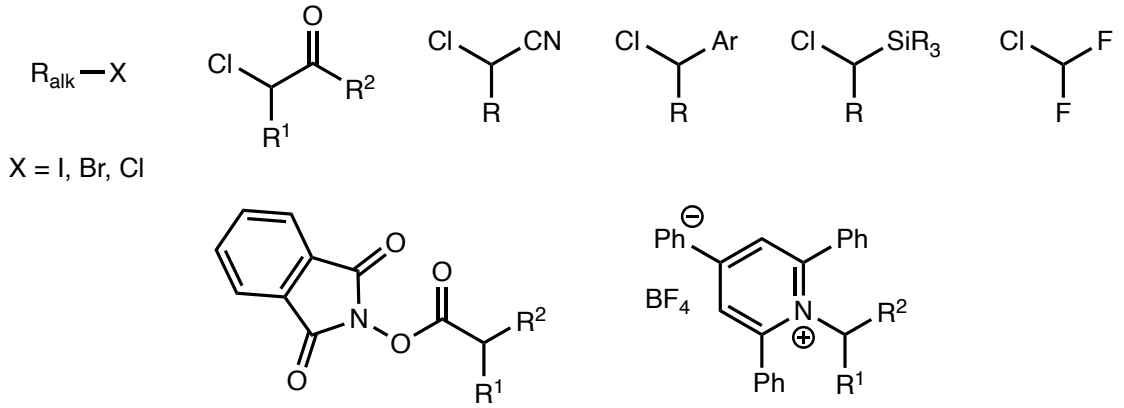

Representative R(sp^2)–X coupling partners

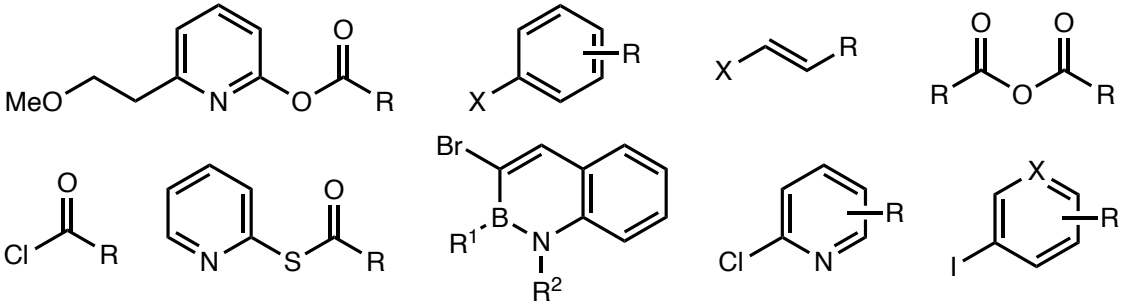

For reviews: Knappke, C. E. I.; Grupe, S.; Gärtner, D.; Corpet, M.; Gosmini, C.; von Wangelin, A. J. *Chem. Eur. J*. **2014**, *20*, 6828–6842; Everson, D. A.; Weix, D. J. *J. Org. Chem*. **2014**, *79*, 4793–4798; Weix, D. J. *Acc. Chem. Res*. **2015**, *48*, 1767–1775; Goldfogel, M. J.; Huang, L.; Weix, D. J. Cross-Electrophile Coupling: Principles and New Reactions, pp. 183– 222, in *Nickel Catalysis in Organic Synthesis*. Wiley-VCH, 2020; Gu, J.; Wang, X.; Xue, W.; Gong, H. *Org. Chem. Front*. **2015**, *2*, 1411–1421; Wang, X.; Dai, Y.; Gong, H. *Top. Curr. Chem*. **2016**, *374*, 43; Lucas, E. L.; Jarvo, E. R. *Nat. Chem. Rev*. **2017**, *1*, 0065; Richmond, E.; Moran, J. *Synthesis* **2018**, *50*, 499–513; Diccianni, J. B.; Diao, T. *Trends Chem*. **2019**, *1*, 830–844; Diccianni, J.; Lin, Q.; Diao, T. *Acc. Chem. Res*. **2020**, *53*, 906–919.

Nickel Catalysis

Cross-electrophile coupling with π-electrophiles (CO_2) (Tsuji, 2012)

Table 1. Nickel-Catalyzed Carboxylation of 1a Employing Carbon Dioxide[a]

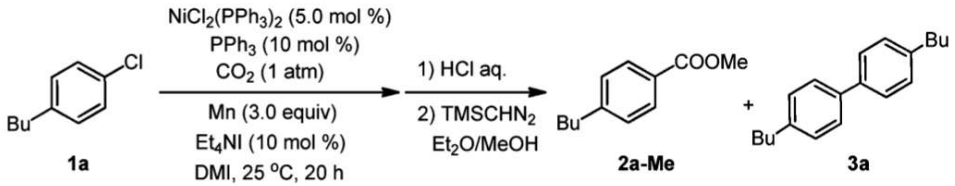

entry	catalyst system: change from standard conditions	yield (%)[b] 2a-Me	3a
1	standard conditions	95 (84)[c]	0

Fujihara, T.; Nogi, K.; Xu, T.; Terao, J.; Tsuji, Y. *J. Am. Chem. Soc.* **2012**, *134*, 9106–9109.

Nickel Catalysis

Cross-electrophile coupling with π-electrophiles (CO_2) (Tsuji, 2012)

Scheme 3. Plausible Reaction Mechanism

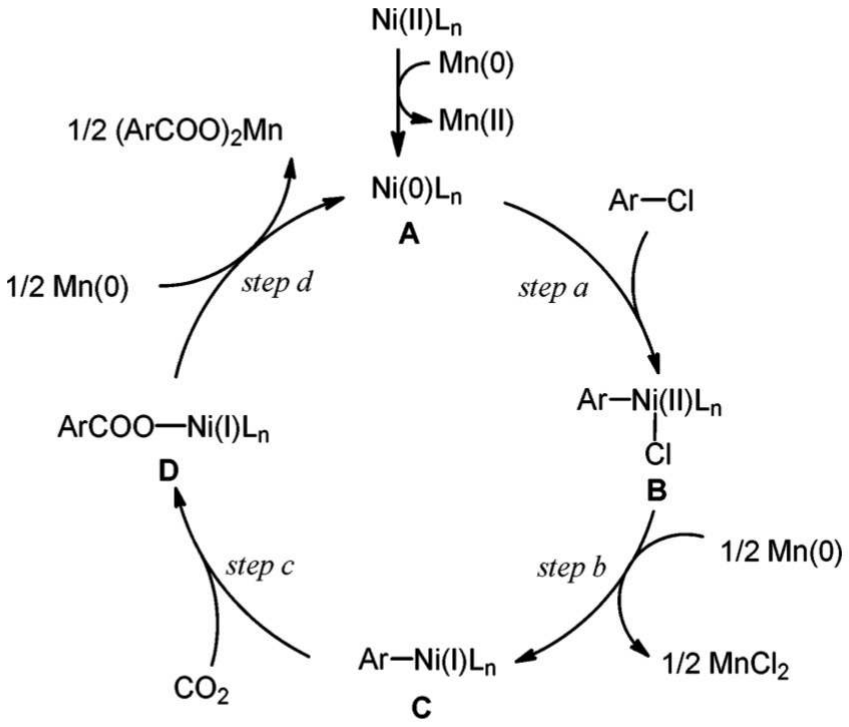

Fujihara, T.; Nogi, K.; Xu, T.; Terao, J.; Tsuji, Y. *J. Am. Chem. Soc.* **2012**, *134*, 9106–9109.

Nickel Catalysis

Cross-electrophile coupling with π-electrophiles (CO_2) (Tsuji, 2012)

Scheme 2. Stoichiometric Reactions Relevant to Mechanism

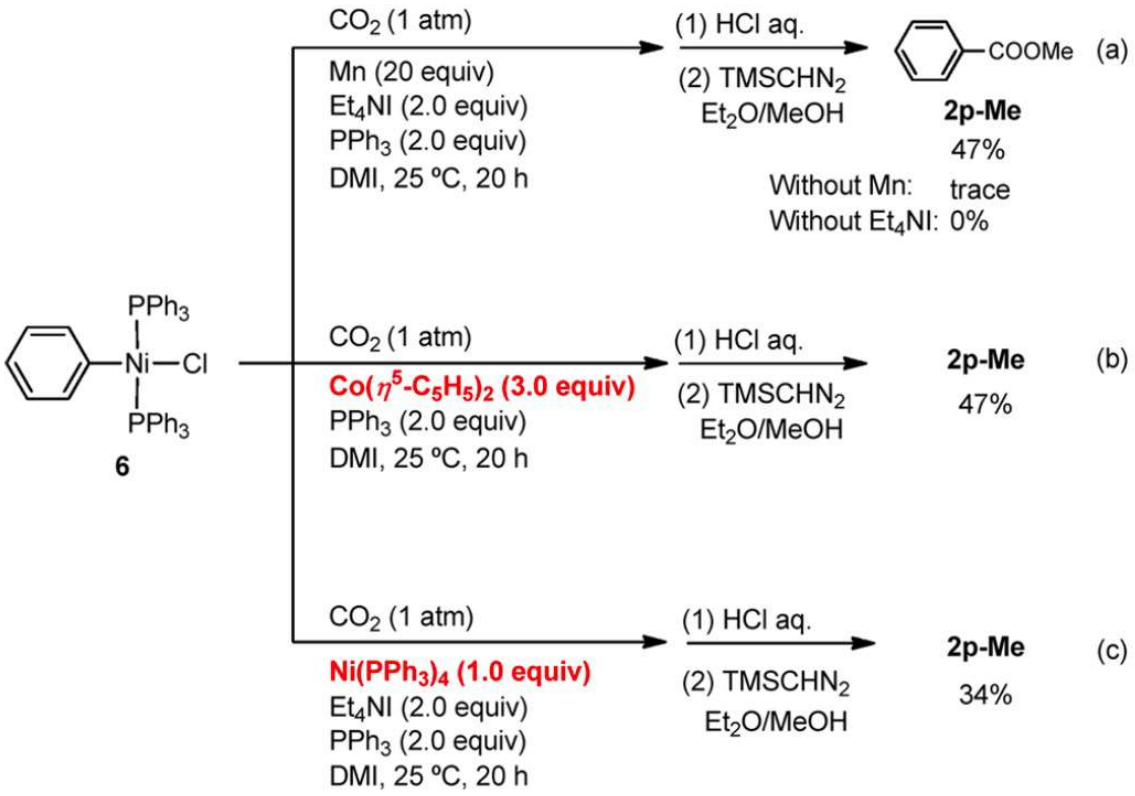

Fujihara, T.; Nogi, K.; Xu, T.; Terao, J.; Tsuji, Y. *J. Am. Chem. Soc.* **2012**, *134*, 9106–9109.

Nickel Catalysis

Reductive carboxylation using CO_2 (Martin)

Table 1. Ni-Catalyzed Carboxylation of 1a with CO_2[a]

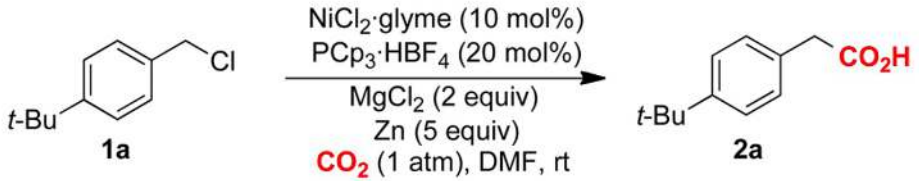

entry	change from standard conditions	yield of **2a** (%)[b]
1	none	74 (70[c])

León, T.; Correa, A.; Martin, R. *J. Am. Chem. Soc.* **2013**, *135*, 1221–1224.

Nickel Catalysis

Reductive carboxylation using CO_2 (Martin)

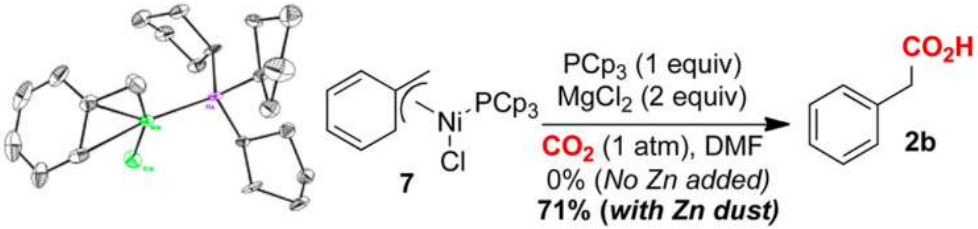

Scheme 3. Proposed Catalytic Cycle

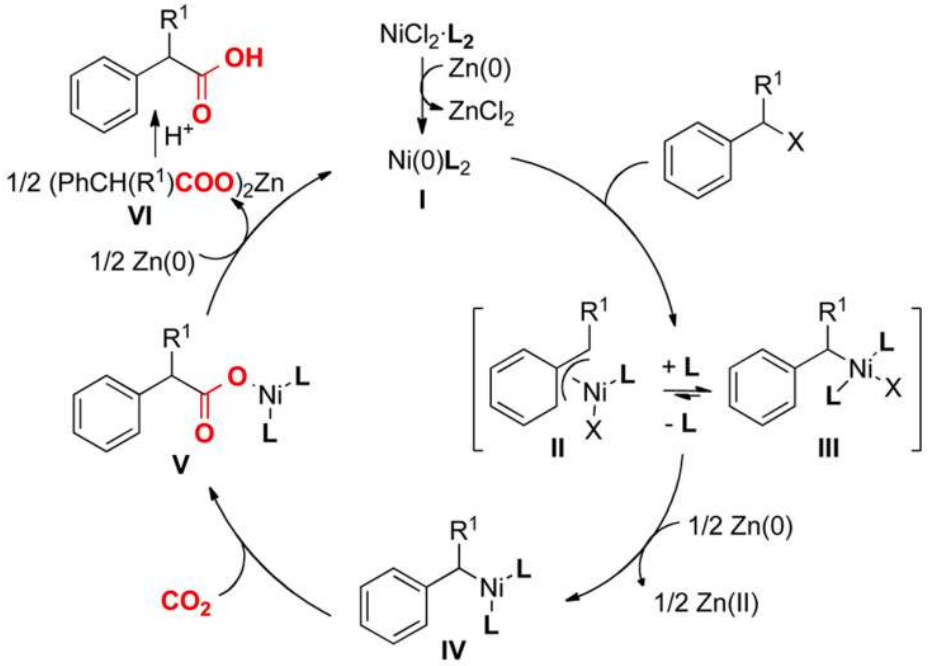

León, T.; Correa, A.; Martin, R. *J. Am. Chem. Soc.* **2013**, *135*, 1221–1224.

Nickel Catalysis

Diao: Migratory insertion into CO_2

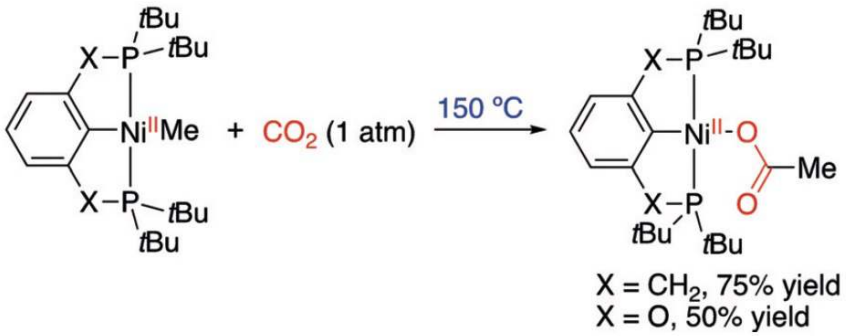

Ni(II): requires forcing conditions

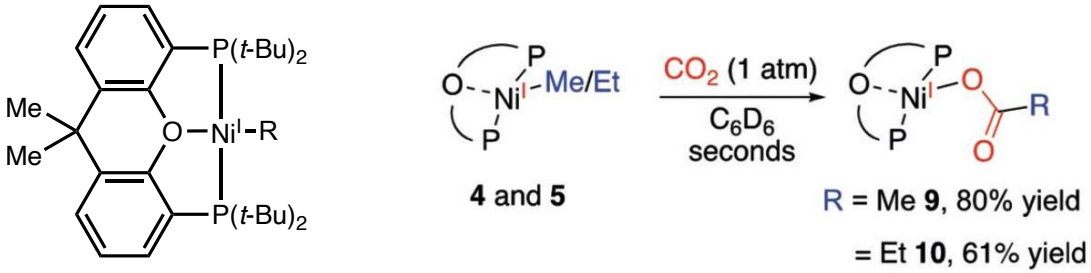

Diccianni, J. B.; Hu, C. T.; Diao, T. *Angew. Chem. Int. Ed.* **2019**, *58*, 13865–13868.

Nickel Catalysis

Hopmann and Martin, 2020: Insertion into CO_2

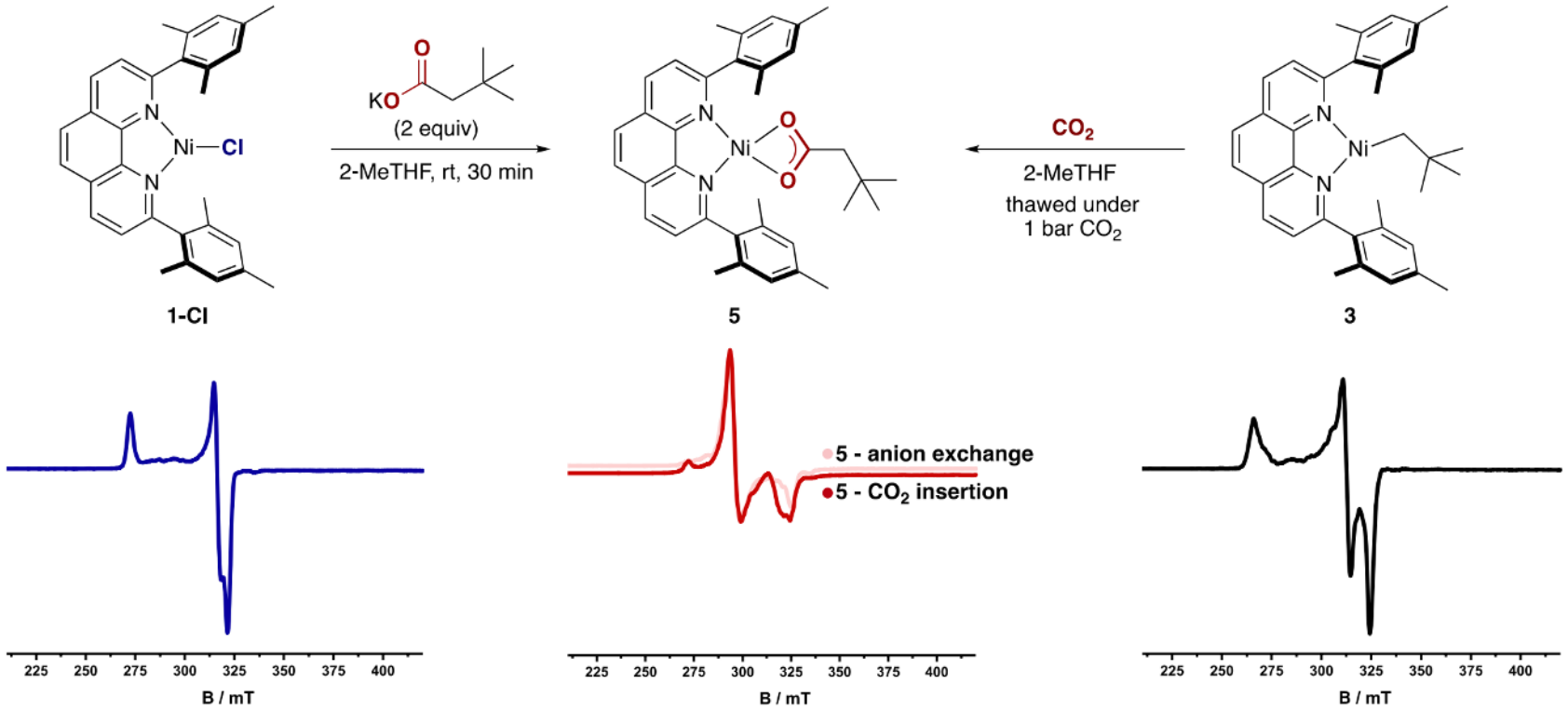

Figure 2. CO_2 insertion at Ni(I). (top) Anion metathesis reaction (left) and CO_2 insertion into **3** (right). (bottom) Changes in the 77 K X-band EPR spectra of **1-Cl** (left, $g_x = 2.084$, $g_y = 2.119$, $g_z = 2.461$) after anion metathesis and after CO_2 insertion at **3** (right, $g_x = 2.065$, $g_y = 2.145$, $g_z = 2.519$) to form **5** (center, $g_x = 2.299$, $g_y = 2.272$, $g_z = 2.064$).

Somerville, R. J.; Odena, C.; Obst, M. F.; Hazari, N.; Hopmann, K. H.; Martin, R. *J. Am. Chem. Soc.* **2020**, *142*, 10936–10941.

Nickel Catalysis

Hopmann and Martin, 2020: Insertion into CO_2

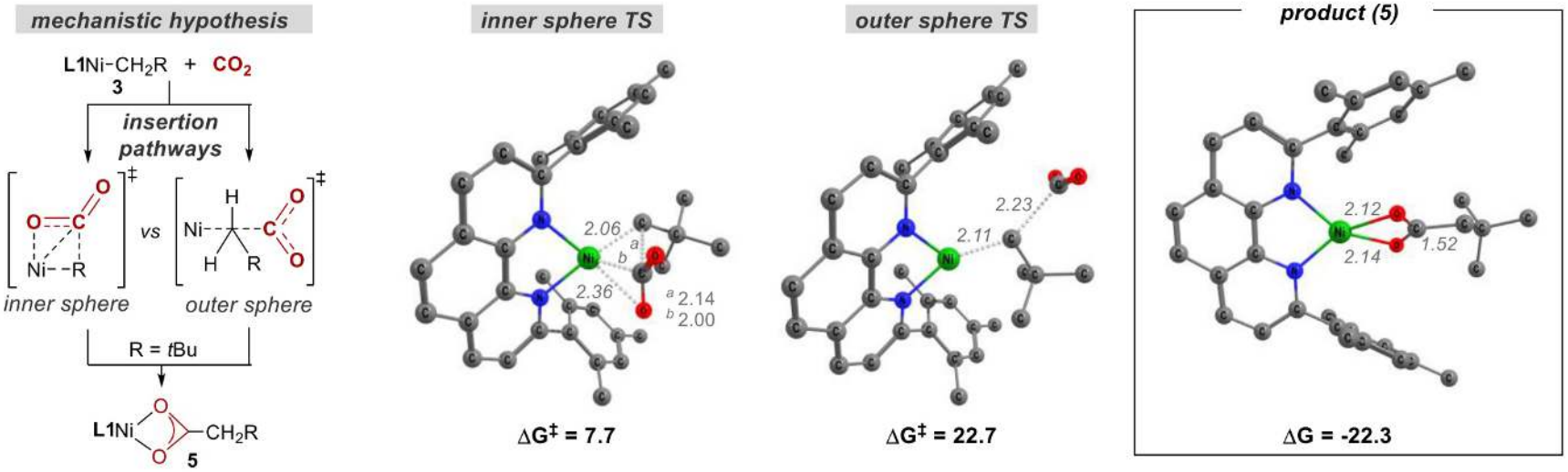

Figure 3. Optimized TS geometries for inner-sphere vs outer-sphere CO_2 insertion and the optimized geometry of **5** (PBE-D3BJ/def2-TZVP/IEFPCM, H atoms omitted, distances in Å, energies in kcal mol^{-1} relative to **3** + free CO_2, 298.15 K).

Somerville, R. J.; Odena, C.; Obst, M. F.; Hazari, N.; Hopmann, K. H.; Martin, R. *J. Am. Chem. Soc.* **2020**, *142*, 10936–10941.

Nickel Catalysis

Reductive coupling with C(sp^2) π-electrophiles:

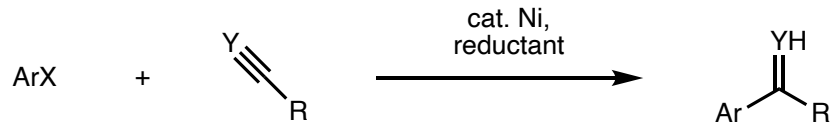

Representative aryl electrophiles

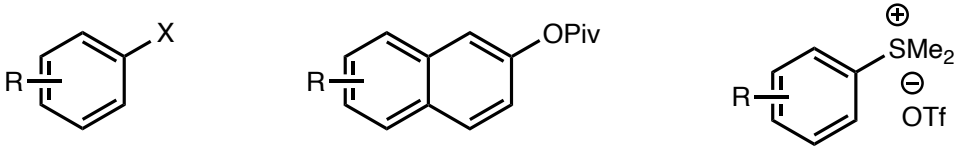

X = I, Cl, OTf

Representative π-electrophiles

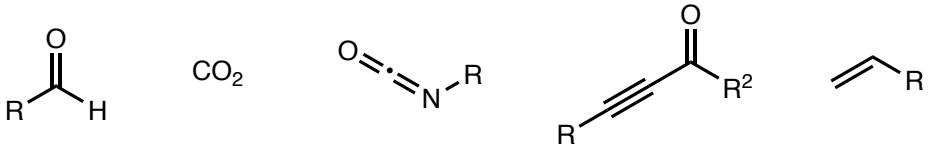

Huang, Y.-C.; Majumdar, K.; Cheng, C.-H. *J. Org. Chem.* **2002**, *67*, 1682–1684; Nogi, K.; Fujihara, T.; Terao, J.; Tsuji, Y. *J. Org. Chem.* **2015**, *80*, 11618–11623; Correa, A.; León, T.; Martin, R. *J. Am. Chem. Soc.* **2014**, *136*, 1062–1069; Yanagi, T.; Somerville, R. J.; Nogi, K.; Martin, R.; Yorimitsu, H. *ACS Catal.* **2020**, *10*, 2117–2123; Vandavasi, J. K.; Hua, X.; Halima, H. B.; Newman, S. G. *Angew. Chem. Int. Ed.* **2017**, *56*, 15441–15445; Garcia, K. J.; Gilbert, M. M.; Weix, D. J. *J. Am. Chem. Soc.* **2019**, *14*, 1823–1827; (a) Meng, Q.-Y.; Wang, S.; König, B. *Angew. Chem. Int. Ed.* **2017**, *56*, 13426–13430; Wang, S.; Xi, C. *Org. Lett.* **2018**, *20*, 4131–4134; Ma, C.; Zhao, C.-Q.; Xu, X.-T.; Li, Z.-M.; Wang, X.-Y.; Zhang, K.; Mei, T.-S. *Org. Lett.* **2019**, *21*, 2464–2467; Correa, A.; Martin, R. *J. Am. Chem. Soc.* **2014**, *136*, 7253–7256; Wang, X.; Nakajima, M.; Serrano, E.; Martin, R. *J. Am. Chem. Soc.* **2016**, *138*, 15531–15534; Dorn, S. C. M.; Olsen, A. K.; Kelemen, R. E.; Shrestha, R.; Weix, D. *Tetrahedron Lett.* **2015**, *56*, 3365– 3367; Ninokata, R.; Yamahira, T.; Onodera, G.; Kimura, M. *Angew. Chem. Int. Ed.* **2017**, *56*, 208–211; Xiao, J.; Wang, Y.-W.; Peng, Y. *Synthesis* **2017**, *49*, 3576–3581; Anthony, D.; Lin, Q.; Baudet, J.; Diao, T. *Angew. Chem. Int. Ed.* **2019**, *58*, 3198–3202; Walker, B. R.; Sevov, C. S. *ACS Catal.* **2019**, *9*, 7197–7203; Lin, T.; Mi, J.; Song, L.; Gan, J.; Luo, P.; Mao, J.; Walsh, P. J. *Org. Lett.* **2018**, *20*, 1191–1194.

Nickel Catalysis

Topics in nickel cross-coupling:

Directions in Precatalyst Synthesis

"Inert"/"Nonclassical" $C(sp^2)$–X Electrophiles Ni(0)/Ni(II)

Benzylic $C(sp^3)$–X Electrophiles Ni(0)/Ni(II)

X = OR, NR_3X

"Unactivated" $C(sp^3)$–X Electrophiles Ni(I)/Ni(III)

Cross-Electrophile Coupling Ni(0)/Ni(I)/Ni(II)/Ni(III)

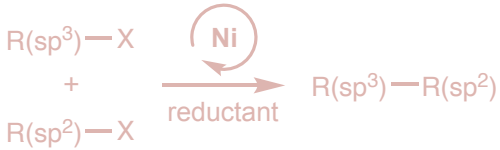

Conjunctive Cross-Coupling (Short)

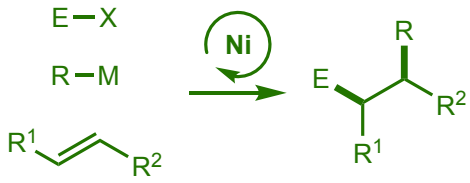

Nickel Catalysis

Advances in conjunctive cross-coupling (Engle):

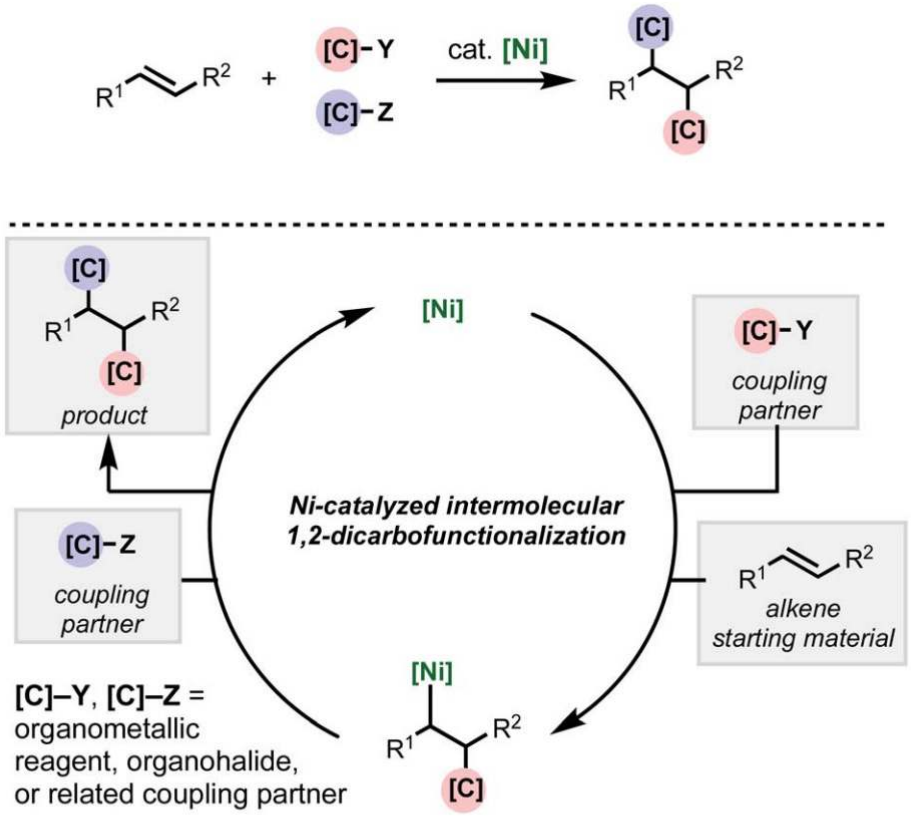

Regimes:

1. Radical 1,2 addition chemistry
2. Coordination-insertion chemistry

Derosa, J.; Apolinar, O.; Kang, T.; Tran, V. T.; Engle, K. M. *Chem. Sci.* **2020**, *11*, 4287–4296.

Nickel Catalysis

Nickel-catalyzed, directed conjunctive cross-coupling (Engle, 2017):

Table 2. Aryl/Vinyl Electrophile and Alkyl/Aryl Nucleophile Scope[a]

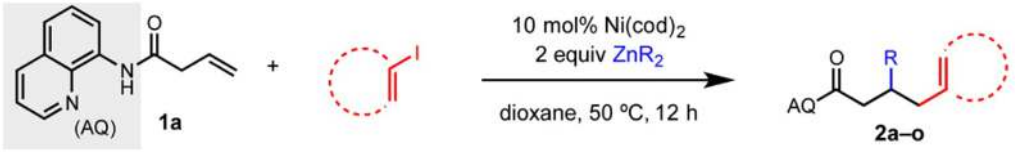

Scheme 3. Proposed Catalytic Cycle

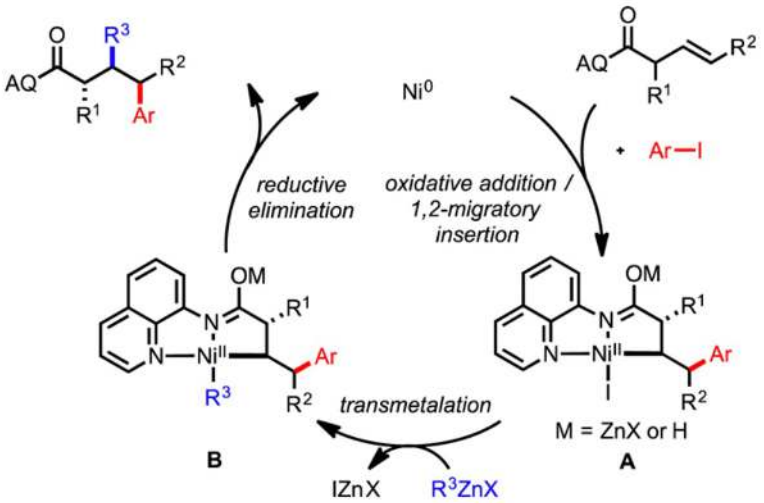

Derosa, J.; Tran, V. T.; Boulous, M. N.; Chen, J. S.; Engle, K. M. *J. Am. Chem. Soc.* **2017**, *139*, 10657–10660.

Nickel Catalysis

Radical conjunctive cross-coupling regime (Nevado, 2017):

Table 1. Optimization of the Reaction Conditions[a]

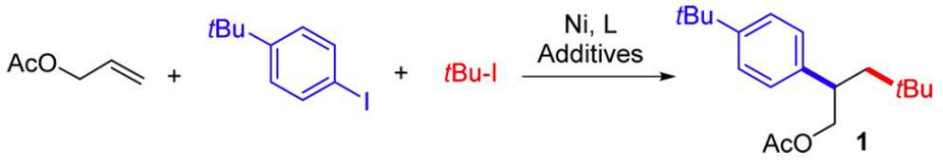

entry	Ni	ligand	additive	yield of 1 (%)[b]
1	$NiCl_2$·DME	L1	Zn	0
2	$NiCl_2$·DME	L1	Mn	0
3	$NiCl_2$·DME	L1	B_2pin_2/KO*t*Bu	0
4	$NiCl_2$·DME	L1	TDAE[c]	17
5	$NiCl_2$·DME	L2	TDAE[c]	1
6	$NiCl_2$·DME	L3	TDAE[c]	2
7	$NiCl_2$·DME	L4	TDAE[c]	0
8	$NiBr_2$·DME	L1	TDAE[c]	54
9	$Ni(acac)_2$	L1	TDAE[c]	27
10	$NiCl_2(Py)_4$	L1	TDAE[c]	82 (83)
11	–	L1	–	0
12	$NiCl_2(Py)_4$	–	TDAE[c]	0

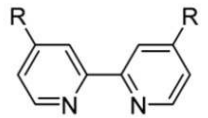

L1: dtbbpy (R = *t*Bu)
L2: bpy (R = H)

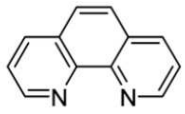

L3: phen

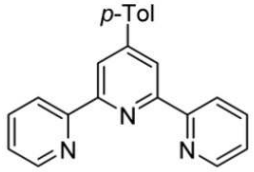

L4: tolterpy

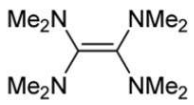

TDAE

García-Domínguez, A.; Li, Z.; Nevado, C. *J. Am. Chem. Soc.* **2017**, *139*, 6835–6838.

Nickel Catalysis

Radical conjunctive cross-coupling regime (Nevado, 2017):

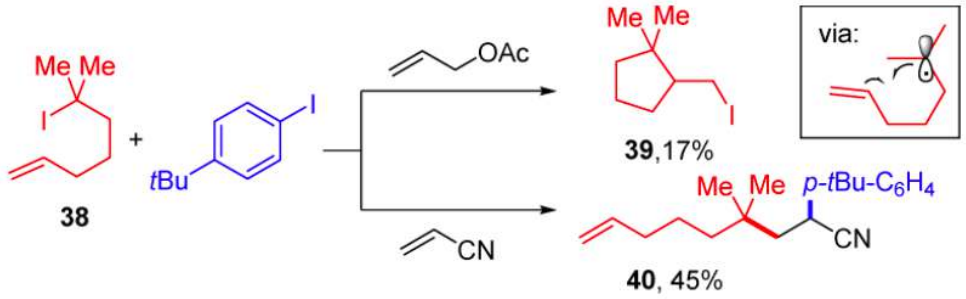

5-exo-trig radical cyclization observed (cage-escaped radical)

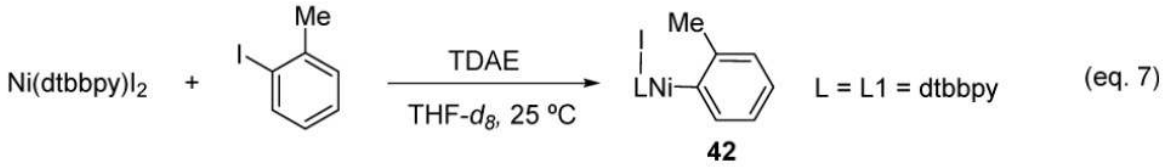

Reaction with ArI leads to (dtbbpy)Ni(II)(aryl)(I)

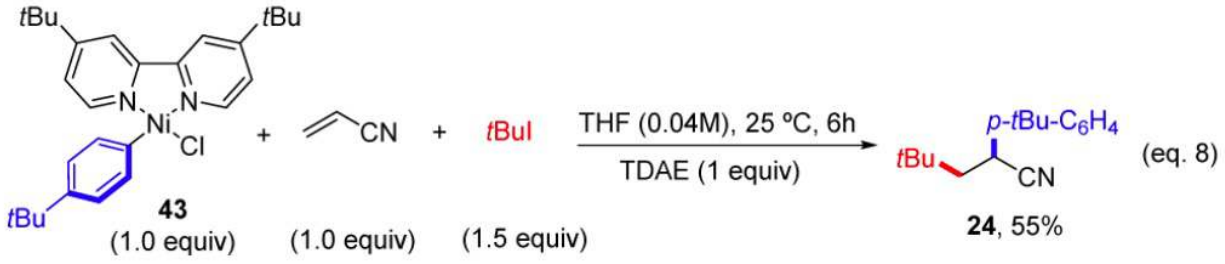

Oxidative addition intermediate is competent in stoichiometric reaction

García-Domínguez, A.; Li, Z.; Nevado, C. *J. Am. Chem. Soc.* **2017**, *139*, 6835–6838.

Nickel Catalysis

Radical conjunctive cross-coupling regime (Nevado, 2017):

Scheme 4. Proposed Reaction Mechanism

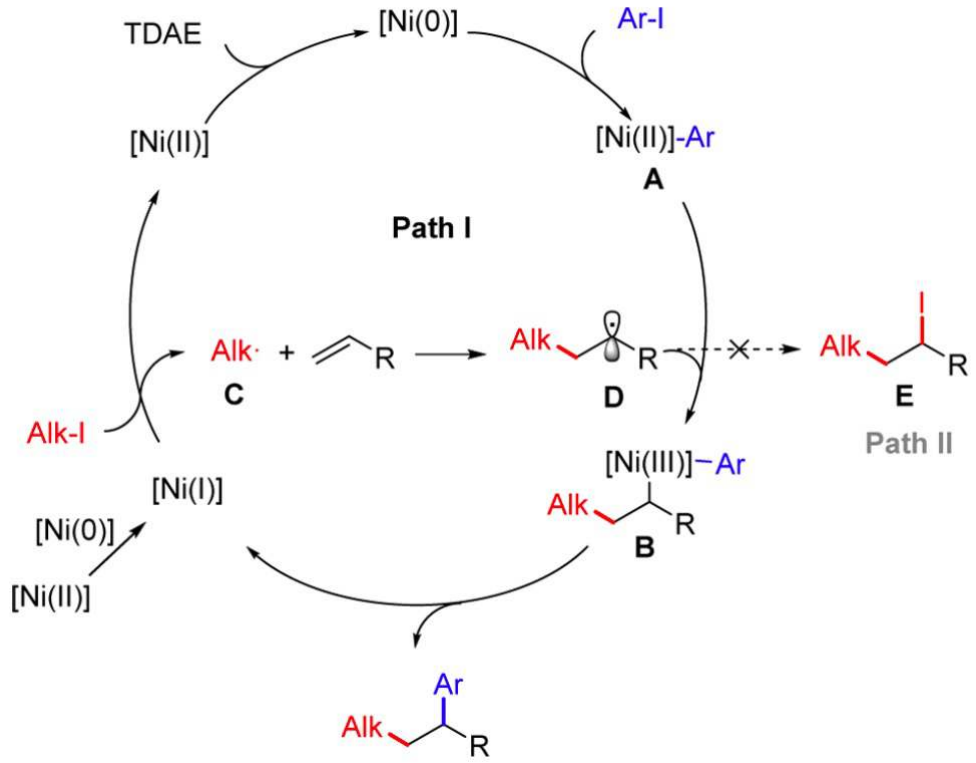

For a relevant mechanistic study, see:
Lin, Q.; Diao, T. *J. Am. Chem. Soc.* **2019**, *141*, 17937–17948.

García-Domínguez, A.; Li, Z.; Nevado, C. *J. Am. Chem. Soc.* **2017**, *139*, 6835–6838.

Nickel Catalysis

Topics in nickel cross-coupling:

Directions in Precatalyst Synthesis

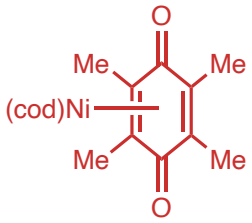

"Inert"/"Nonclassical" $C(sp^2)$–X Electrophiles Ni(0)/Ni(II)

Benzylic $C(sp^3)$–X Electrophiles Ni(0)/Ni(II)

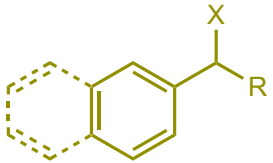

X = OR, NR_3X

"Unactivated" $C(sp^3)$–X Electrophiles Ni(I)/Ni(III)

Cross-Electrophile Coupling Ni(0)/Ni(I)/Ni(II)/Ni(III)

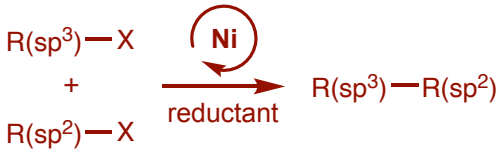

Conjunctive Cross-Coupling (Short)